



Changes in Optical Properties of Spacecraft Materials Due to Combined Effects of Aging Factors in a Space Environment

***Dr. Sergei A. Khatipov**

***Dr. Oleg Viktorovich**

***(1) National Research Nuclear University (MEPhI), 31, Kashirskoye Shosse, Moscow, 115409, Russia**

(2) OAO Kompozit , 4, Pionerskaya St., Korolyev, 141070, Russia

(3) Research Institute of Nuclear Physics of Moscow State University (INP MSU), Building of Experimental Installations, Vorobyovy Gory, Moscow, 119899, Russia

ISTC 07-7005/Project #3806p

Report Date: July 2013

Final Report for 01 November 2007 to 31 October 2012

Distribution Statement A: Approved for public release distribution is unlimited.

**Air Force Research Laboratory
Air Force Office of Scientific Research
European Office of Aerospace Research and Development
Unit 4515 Box 14, APO AE 09421**

REPORT DOCUMENTATION PAGE				Form Approved OMB No. 0704-0188	
Public reporting burden for this collection of information is estimated to average 1 hour per response, including the time for reviewing instructions, searching existing data sources, gathering and maintaining the data needed, and completing and reviewing the collection of information. Send comments regarding this burden estimate or any other aspect of this collection of information, including suggestions for reducing the burden, to Department of Defense, Washington Headquarters Services, Directorate for Information Operations and Reports (0704-0188), 1215 Jefferson Davis Highway, Suite 1204, Arlington, VA 22202-4302. Respondents should be aware that notwithstanding any other provision of law, no person shall be subject to any penalty for failing to comply with a collection of information if it does not display a currently valid OMB control number. PLEASE DO NOT RETURN YOUR FORM TO THE ABOVE ADDRESS.					
1. REPORT DATE (DD-MM-YYYY) 16-07-2013		2. REPORT TYPE Final Report		3. DATES COVERED (From – To) 01 November 2007 – 31 October 2012	
4. TITLE AND SUBTITLE Changes in Optical Properties of Spacecraft Materials Due to Combined Effects of Aging Factors in a Space Environment				5a. CONTRACT NUMBER FA8655-07-7005 (ISTC Project #3806p)	
				5b. GRANT NUMBER ISTC 07-7005	
				5c. PROGRAM ELEMENT NUMBER 3004EF	
				5d. PROJECT NUMBER	
6. AUTHOR(S) *Dr. Sergei A. Khatipov *Dr. Oleg Viktorovich				5d. TASK NUMBER	
				5e. WORK UNIT NUMBER	
7. PERFORMING ORGANIZATION NAME(S) AND ADDRESS(ES) *(1) National Research Nuclear University (MEPhI), 31, Kashirskoye Shosse, Moscow, 115409, Russia (2) OAO Kompozit , 4, Pionerskaya St., Korolyev, 141070, Russia (3) Research Institute of Nuclear Physics of Moscow State University (INP MSU) Building of Experimental Installations, Vorobyovy Gory, Moscow, 119899, Russia				8. PERFORMING ORGANIZATION REPORT NUMBER N/A	
9. SPONSORING/MONITORING AGENCY NAME(S) AND ADDRESS(ES) EOARD Unit 4515 APO AE 09421-4515				10. SPONSOR/MONITOR'S ACRONYM(S) AFRL/AFOSR/IOE (EOARD)	
				11. SPONSOR/MONITOR'S REPORT NUMBER(S) AFRL-AFOSR-UK-TR-2013-0036	
12. DISTRIBUTION/AVAILABILITY STATEMENT Distribution A: Approved for public release; distribution is unlimited.					
13. SUPPLEMENTARY NOTES					
14. ABSTRACT This project conducted experimental investigations on the degradation of the optical properties of materials used on the external surfaces of spacecraft in conditions of the space environment. What started as an International Science and Technology project (#2342p) titled "Development of a Database on the Changes in the Optical Properties of Materials Used on the External Surfaces of Spacecraft under the Action of the Space Environment Factors," this project continued for five years to investigate and formulate a comprehensive database of spacecraft material aging properties. The following has been achieved during the course of this effort: 1) Tests were conducted on the Sheldahl films, MAP paints and the Russian materials EKOM-4 and the arimide fabric TTKA-S 56420 under the separate action of protons with the energies 50, 150 и 500 keV, electrons with the energies 50, 100 and 200 keV and UV radiation; 2) Tests were conducted in simulating the combined effects of space environment factors, such as electromagnetic solar radiation (visible, ultraviolet, vacuum ultraviolet and soft X-rays) and charged particles (electrons and protons), at GEO altitudes (conducted on the Russian materials, Sheldahl films, and MAP paints); 3) Laboratory tests were performed in simulating the combined effects of space environment factors, such as atomic oxygen, electromagnetic solar radiation (visible, ultraviolet, vacuum ultraviolet and soft X-ray radiation) at an altitude of 400 km; 4) Bidirectional scattering distribution function (BSDF) and Bidirectional reflectance distribution function (BRDF) measurements were conducted for the wavelengths 532 and 1063 nm; and 5) Measurements were conducted on the Directed Hemispherical Reflectance (DHR) in the range 2.5—10 µm. The results of the experimental studies from the complex impact of the space environment factors on the optical properties of spacecraft materials have been entered into a materials database in both digital and graphical forms. The resulting database is in Microsoft Access 2000 format and contains about 3,500 records.					
15. SUBJECT TERMS EOARD, space environment factors; electrons; protons; atomic oxygen; UV radiation; optical characteristics; thermal control coatings; solar arrays					
16. SECURITY CLASSIFICATION OF:			17. LIMITATION OF ABSTRACT SAR	18. NUMBER OF PAGES 106	19a. NAME OF RESPONSIBLE PERSON Kevin Bollino
a. REPORT UNCLAS	b. ABSTRACT UNCLAS	c. THIS PAGE UNCLAS			19b. TELEPHONE NUMBER (Include area code) +44 (0)1895 616163

Project # 3806p

Final Project Technical Report

Page 1 / 100

ISTC Project #3806p**Changes in Optical Properties of Spacecraft Materials
Due to Combined Effects of Aging Factors
in a Space Environment****Final Project Technical Report****of the work performed from November 1, 2007, to October 31, 2012****National Research Nuclear University (MEPhI)****Project Manager****Sergei Amerzyanovich
KHATIPOV
Doctor of Physical and
Mathematical Sciences****Pro-Rector****Oleg Viktorovich
NAGORNOV
Doctor of Physical and
Mathematical Sciences**

2013

This work was supported financially by the European Office of Aerospace Research and Development (EOARD, London) and performed under a contract to the International Science and Technology Center (ISTC, Moscow).

This work was supported financially by the European Office of Aerospace Research and Development (EOARD, London) and performed under a contract to the International Science and Technology Center (ISTC, Moscow).

Distribution A: Approved for public release; distribution is unlimited.

Title of the Project: Changes in Optical Properties of Spacecraft Materials Due to Combined Effects of Aging Factors in a Space Environment

Commencement Date: November 1, 2007

Duration: 5 years

Project Manager: Sergei Amerzyanovich KHATIPOV

phone number: +7(495)916-67-94

fax number: +7(495)916-67-94

e-mail address: khatipov@nifhi.ru

Leading Institution: National Research Nuclear University (MEPhI)
31, Kashirskoye Shosse
Moscow, 115409, Russia
+7(495)324-45-41
OVNagornov@mephi.ru

Participating Institutions:: OAO Kompozit
4, Pionerskaya St.
Korolyev, 141070, Russia
+7(495)513-22-80
info@kompozit-mv.ru

Research Institute of Nuclear Physics of Moscow State
University (INP MSU)
Building of Experimental Installations (Building #19, Rooms 1-
51, 2P-01, 2P-02.), Vorobyovy Gory
Moscow, 119899, Russia
+7(495)939-18-18
panasyuk@srdlan.npi.msu.su

Foreign Collaborators: None

Keywords: *space environment factors; electrons; protons; atomic oxygen; UV radiation; optical characteristics; thermal control coatings; solar arrays*

Summary

The present Project is a complex of experimental investigations on the degradation of the optical properties of materials used on the external surfaces of spacecraft in conditions of the space environment.

The present Project is a continuation of ISTC Project #2342p “Development of a Database on the Changes in the Optical Properties of Materials Used on the External Surfaces of Spacecraft under the Action of the Space Environment Factors.”

The following has been achieved during the course of the Project:

- 1) Tests have been conducted of the Sheldahl films, MAP paints and the Russian materials EKOM-4 and the arimide fabric TTKA-S 56420 under the separate action of protons with the energies 50, 150 и 500 keV, electrons with the energies 50, 100 and 200 keV and UV radiation
- 2) Tests have been conducted in simulating the combined effects of space environment factors, such as electromagnetic solar radiation (visible, ultraviolet, vacuum ultraviolet and soft X-rays) and charged particles (electrons and protons), at GEO altitudes. These tests have been conducted on the Russian materials, Sheldahl films, and MAP paints.
- 3) Laboratory tests have been performed in simulating the combined effects of space environment factors, such as atomic oxygen, electromagnetic solar radiation (visible, ultraviolet, vacuum ultraviolet and soft X-ray radiation) at an altitude of 400 km
- 4) BSDF/BRDF measurements have been conducted for the wavelengths 532 and 1063 nm.
- 5) Measurements have been conducted of the Directed Hemispherical Reflectance (DHR) in the range 2.5—10 μm .

The results of the experimental studies conducted of the complex impact of the space environment factors on the optical properties of spacecraft materials have been entered into the Database in digital and graphic forms. The resulting Database is in Microsoft Access 2000 format and contains about 3,500 records.

Contents

List of Figures	5
List of Tables	6
List of Symbols, Abbreviations, and Acronyms	6
1. Introduction. Brief description of the Work Plan	7
1.1. Project goals	7
1.2. Expected results of the Project	9
1.3. Technical approach and methodology	10
2. Techniques of conducting the tests and measurements	22
2.1. Technique of conducting tests of materials under combined exposure	22
2.2. Technique of conducting tests under separate exposure to electrons and protons	27
2.3. Testing materials in a plasma flux of atomic oxygen	37
2.4. Measuring the spectral and integral optical parameters	43
2.5. Technique of measuring the BRDF (BSDF)	45
3. Results of performing work under the Project	47
4. Conclusion	49
5. References	51
 Appendix 1. Examples of the Database structure and interface	 52
Appendix 2. Characteristic test results obtained in the course of realizing the tasks stipulated under the Project	 75
Appendix 3. Database in MS Access 2000 format	

List of Figures

Figure 1. Diagram of the automated test bench UV-1/2	23
Figure 2. Device scheme of the electronic injector	28
Figure 3. Target for irradiation of the samples	28
Figure 4. Appearance of the device (upper photo), the whole view of the device (lower photo), electron source with the system of beam transportation	29
Figure 5. Control panel	30
Figure 6. High-voltage pulse	31
Figure 7. Current pulses from the target	31
Figure 8. Multiple-collector Faraday cylinder	32
Figure 9. Photograph of the electromagnets	33
Figure 10. Distribution of the current	34
Figure 11. Diagram of the installation for increasing energy	34
Figure 12. Diagram of the experimental installation	36
Figure 13. Characteristics of the flux of oxygen plasma	37
Figure 14. Diagram of the plasma-beam test bench at INP MSU	39
Figure 15. Optical diagram of measuring the solar radiation reflectance R_s	44
Appendix 1.	
Figures 1-23. Examples of the Database structure and interface	52-74
Appendix 2.	
Figure 1. Spectrum of reference samples of Russian materials	75
Figure 2. Dependence of solar absorbance A_s of samples of Russian materials on the fluence proton irradiation of a complex irradiation	76
Figure 3. Dependence of solar absorbance A_s of samples of Arimide frame fabric (article 56420) on time of a complex irradiation (electrons + protons + UV Sun radiation)	77
Figure 4. Dependence of solar absorbance A_s of samples of PM-1EU-OA on time of a complex irradiation (electrons + protons + UV Sun radiation)	77
Figure 5. Dependence of solar absorbance A_s of samples of NIIKLAM-RAM-2 on time of a complex irradiation (electrons + protons + UV Sun radiation)	78
Figure 6. Dependence of solar absorbance A_s of samples of SOT-1-S-100 films on time of a complex irradiation (electrons + protons + UV Sun radiation)	78
Figure 7. Spectrum of reference samples of Sheldahl films	79
Figures 8-11. Dependence of solar absorbance A_s of samples of Sheldahl films on time of a complex irradiation (electrons + protons + UV Sun radiation)	82-87
Figures 12-15. Dependence of the solar radiation absorptance A_s of the MAP samples on the fluence of proton irradiation	90-95
Figures 16-17. Dependence of solar absorbance A_s for samples of Sheldahl films on electron radiation fluence with energy of 50 keV	97-100

List of Tables

Table 1. List of materials provided by the Project partners for testing	11
Table 2. List of the Russian materials most important from the point of view of their use in spacecraft that were selected for testing	12
Table 3. The principal technical parameters of the UV-1/2 test bench	25
Table 4. Parameters of the installation	32
Table 5. Parameters of the modernized electron injector	35
Table 6. Relative erosion factors of polymer materials	42
Appendix 2.	
Table 1. Values of the solar radiation reflectance of MAP paints before and after exposure to protons	89
Table 2. Influence of factors of the space environment on the integral emission ability for different materials	103

List of Symbols, Abbreviations, and Acronyms

LEO – Low Earth orbit
GEO – Geostationary Earth Orbit
BRDF – Bidirectional reflectance distribution function
BSDF – Bidirectional scattering distribution function
DHR – Directed Hemispherical Reflectance

1. Introduction. Brief description of the Work Plan: objective, expected results, technical approach

1.1. Project goals.

Increasing requirements to the stability of materials, as well as the creation of new equipment, against the background of the general trend towards the extension of the active lifetimes of spacecraft, call for developing the methods of radiation testing, of predicting radiation stability and a deeper insight into the peculiarities of the operation conditions of polymers in space.

The project is devoted to the theoretical and experimental study of the degradation of the optical properties of materials used on the external surfaces of spacecraft, such as solar array cells, thermal control and thermal insulation materials, in conditions of the space environment on both LEO and GEO. From the viewpoint of radiation effects, the fundamental distinctive features of operating polymers in near-Earth space are: the presence of ionizing radiations of different nature; the wide distribution of the ionizing particles in energy; the composite nature of the impact of particles on the materials; and the wide range of temperature changes in the latter.

On the external surfaces of spacecraft, polymer materials are directly exposed to the entire spectrum of the ionizing radiations of the space environment: to protons (with energies 20 — 1,000 MeV), electrons (0.05 MeV), bremsstrahlung (0.05 MeV), solar X-rays (1 — 10 nm) and vacuum UV radiation; and, for orbits crossing the radiation belts of the Earth, to protons (0.01 — 60 MeV), electrons (0.02 — 5 MeV) and bremsstrahlung (0.02 — 5 MeV). Large amount of data about physical and chemical processes interaction of different kinds of radiation with substances including polymers is contained in [1-11].

The existence of a distribution of space radiation particles in energy results in an inhomogeneous distribution of the absorbed dose in the depth of the material. Estimates show that the total surface dose on GEO is extremely high (approx. 10^7 Gy/year); however, the depth-averaged dose turns out to be significantly lower, since a considerable share in the total spectrum of radiation is that of the low-energy part of ionizing radiations (X-rays, vacuum UV radiation, electrons and protons with energies less than 0.05 and 1 MeV respectively). At a depth of 10 micrometers, the value of the absorbed dose decreases by more than an order of magnitude.

The bulk of the experimental data on the radiation stability of polymers contained in reference books and monographs (e. g. [12, 13]) has been obtained under the action of monoenergetic fluxes of ionizing particles (electrons, gamma-quanta) in conditions of an ionization of the material that is macroscopically homogenous in volume. In such conditions, the values of the absorbed dose very seldom cross an upper limit that may be defined at 0.5×10^7 Gy, which corresponds to a dose absorbed

on GEO over a period of ten years behind a protective layer of $\sim 0.01\text{g/cm}^2$ (approx. 25 μm in aluminum). At the same time, the value of the dose absorbed in a single year by the material's surface layer on this orbit is several times higher. The nature of the influence of such high surface doses on the macroscopic properties of polymers over a long period of operation in a space environment has not so far been sufficiently investigated and the corresponding requirements for laboratory testing have not been formulated. In conducting laboratory testing, the most difficult — and not yet finally solved — questions remain those connected with simulating (or imitating) the distribution of particles in energy and with the combined (or simultaneous) impact of ionizing particles of different nature.

One of the solutions to the problem of simulating the energy spectrum of ionizing radiation is the use of several monoenergetic beams, creating an absorbed dose profile in the depth of the material, which is close to that in actual operating conditions. The necessity for performing this kind of tests follows from the dependence of the material properties on the form of the dose distribution in depth and not on the averaged dose. Thus, e. g., it is quite obvious that the changes of the parameters will be considerably different depending on whether the energy absorption took place in the thin surface layer or homogeneously in the volume of the material. Using depth-averaged dose values, without taking into consideration the distribution of the dose in depth, to assess the radiation stability of materials is not correct. It is the approach outlined above that has been utilized in this project. For simulating the energy spectrum of ionizing radiation of the space environment, electrons and protons were used with different energies in the range 50 — 500 keV. For estimating and predicting the aging effects in space, tests were conducted with the combined action of simulated electromagnetic solar radiation, electrons and protons (for GEO), as well as with that of electromagnetic solar radiation and atomic oxygen (for LEO).

The present Project is a complex of theoretical and experimental investigations on the degradation of the optical properties of materials used on the external surfaces of spacecraft in conditions of the space environment. The Project has been realized by employees of three institutions: MEPhI, OAO Kompozit and INP MSU.

The Project has a duration of 60 months. The list of the tasks is given below:

Task 1. Testing materials under the separate action of electrons and protons.

Task 2. Testing materials under the combined action of electrons, protons and UV radiation.

Task 3. Testing materials under the combined action of atomic oxygen and UV radiation.

Task 4. Performing measurements of the optical parameters of the samples after exposure to different space environment factors.

Task 5. Modernization of the experimental equipment for performing measurements of the optical properties.

1.2. Expected results of the Project:

1. results of the laboratory tests of Sheldahl films and MAP paints, as well as the Russian materials EKOM-4 and the arimide fabric TTKA-S 56420, under the separate action of protons (50, 150, 300 and 500 keV), electrons (100 and 200 keV) and UV radiation (all tests to be conducted with exposures equivalent to one year on GEO);
2. results of the laboratory tests of the Russian materials, Sheldahl films and MAP paints under the combined action of different types of space radiation ($e + p + UV$) with an acceleration factor of three to four for UV radiation and an equivalent fluence corresponding to 3 years at GEO altitudes;
3. results of the laboratory tests of a limited set of materials (to be agreed upon with the Partner) under the combined action of atomic oxygen and UV radiation ($AO + UV$) with an acceleration factor of one for UV radiation and an equivalent fluence corresponding to 3 years at LEO altitudes (400 km);
4. results of the measurement of the spectral and integral coefficients of reflectance, transmittance and absorptance in the wavelength range $0.3 - 10 \mu m$ for the Russian materials, Sheldahl films and MAP paints, before and after exposure to different space environment factors;
5. results of BSDF/BRDF measurements on the wavelengths 532 and 1063 nm for the Russian materials, Sheldahl films and MAP paints, before and after exposure to different space environment factors;

The Project falls under the category of applied research. Its results will be used for determining the endurance of materials used on the external surfaces of spacecraft and having thermal control, thermal insulation and protective functions, in conditions of their long-term operation in open space.

The results of the theoretical and experimental research carried out under the Project must be presented in the form of a Database in Microsoft Access 2000 (or later) format.

Experimental research is to be carried out for Russian materials, such as thermal control enamels: EKOM-1 (white), KO-5191 (white), TR-SO-TsM (white), EKOM-4 (white), EKOM-2 (black); fabrics: the arimide fabric TTKA-S 56420, the metallized glass fabric TSON-SOT-M(bts); metallized films: the thermal control covering SOT-1S-100, the thermal control covering PM-1EU-OA; the fabric and film composite material NIIKAM-RAM-2; solar cells: FP-200 and FP-100 (both with bifacial sensitivity), FP-BSFR-100 and FP-BSFR-200 (both with a reflecting rear surface). The following foreign materials are also to be tested: US Sheldahl Kapton films (8 brands) and Teflon FEP films (6 brands), as well as French MAP paints (4 brands).

Most of the Russian materials included in this Project were previously studied under ISTC Project #2342p under separate exposures to electromagnetic solar radiation, electrons and protons that were equivalent to one year of operation on GEO. In the present Project, which is a continuation of ISTC Project #2342p, tests of all the declared materials are to be carried out under a simultaneous exposure to electromagnetic solar radiation, electrons with the energy 50 keV and protons with the energy 50 keV that is equivalent to three years on GEO with an acceleration factor of three to four, as well as under a simultaneous exposure to electromagnetic solar radiation and atomic oxygen (20 keV) that is equivalent to three years on LEO. The Sheldahl and MAP films and paints, as well as two Russian materials: EKOM-4 and the TTKA-S 56420 brand arimide fabric, are to be investigated under both simultaneous and separate action of the space environment factors. In the latter case, the testing conditions are to be identical to those under the previous project. Investigation under the simultaneous action of electromagnetic solar radiation and atomic oxygen is scheduled for a limited set of materials.

The optical parameters to be investigated are the spectral and integral coefficients of reflectance, transmittance and heat emission in the wavelength range 0.3—10 μm , optical density, as well as the angular distribution function of reflected light (BSDF/BRDF) on two wavelengths: 532 and 1063 nm.

In order to be able to perform measurements of the entire set of optical parameters required by the Partner, modernization is to be carried out of the installation for measuring reflectance spectra in the infrared region and of the installation for measuring the angular distribution function of reflected light. In the first case, the capability is to be created for automatically recording reflectance spectra in the wavelength range 2.5—10 μm with the step 100 nm and the spectral resolution of the probing beam ± 20 nm; in the second case, for BSDF/BRDF measurements on the wavelengths 532 nm and 1063 nm with the angular resolution $0.2 \div 0.5^\circ$ (for samples with a mixed, specular and diffuse, type of reflectance) and 2° (for samples with a diffuse type of reflectance), with the possibility of conducting measurements outside the plane of incidence of the beam.

As the end result of the Project, a Database is to be created, containing data on the degradation of the optical properties of materials of the external surfaces of spacecraft, including literature data and results of the optical properties research conducted under the Project.

1.3. Technical approach and methodology

In all cases, the procedures used for conducting the tests are based on well-known experimental and calculated values of the factors acting upon the materials on LEOs and GEOs. An exposure to solar radiation has been investigated, equivalent to 3 years of 1-sun at air mass zero; the same can be said of exposure to electrons and protons, whose energy spectrum corresponds to that found on LEOs and GEOs. Given in Tables 1 and 2 is a brief summary of the materials selected for testing.

Table 1

List of materials provided by the Project partner for testing

#	Material Designation	Note
1	1.000 GE 1.0MIL Kapton	Kapton films by Sheldahl
2	1.000A GE 5.0MIL Kapton	
3	1.0MIL Kapton Aluminum	
4	2.0MIL Kapton Aluminum	
5	3.0MIL Kapton Aluminum	
6	ITO 1.0MIL Kapton Aluminum	
7	ITO 2.0MIL Kapton Aluminum	
8	ITO 3.0MIL Kapton Aluminum	
9	2.0MIL Teflon Silver Inconel	Teflon films by Sheldahl
10	5.0MIL Teflon Silver Inconel	
11	10.0MIL Teflon Silver Inconel	
12	ITO 2.0MIL Teflon Silver Inconel	
13	ITO 5.0MIL Teflon Silver Inconel	
14	ITO 10.0MIL Teflon Silver Inconel	
15	Primaire PSX Peinture PCBE	Paints by MAP
16	Primaire PSX Peinture SG121FD	
17	Peinture PU1	
18	Peinture PUK	

Table 2

List of the Russian materials
most important from the point of view of their use in spacecraft
that were selected for testing

#	Russian Material Designation	Type of Material	Application of Material	Chemical Composition of Material
1	EKOM-1 white	TCC (Enamel)	Used as a coating on the external surfaces of radiators of space vehicles (SVs) in conditions of low-earth orbits (LEOs). Has a limited use for short operating times on geostationary earth orbits (GEOs) and high-elliptical earth orbits (HEOs).	<ul style="list-style-type: none"> • Acrylic copolymer; • ZnO pigment.
2	KO-5191 white	TCC (Enamel)	Used as a coating on the external surfaces of radiators of SVs in conditions of LEOs. Has a limited use for short operating times on GEOs and HEOs.	<ul style="list-style-type: none"> • Polysiloxane binder; • ZnO pigment.
3	EKOM-4 white	TCC (Enamel)	Used as a coating on the external surfaces of radiators of SVs in conditions of LEOs. Has a limited use for short operating times on GEOs and HEOs.	<ul style="list-style-type: none"> • Acrylic copolymer; • ZrO₂ pigment.
4	TR-SO-TsM white	TCC (Enamel)	Used as a coating on the external surfaces of radiators of SVs in conditions of LEOs. Has a limited use for short operating times on GEOs and HEOs.	<ul style="list-style-type: none"> • Water solution of potassium silicate; • ZrO₂ pigment.
5	EKOM-2 black	TCC (Enamel)	Used as a coating on the external surfaces of radiators of SVs in conditions of LEOs, GEOs and HEOs.	<ul style="list-style-type: none"> • Acrylic copolymer; • pigment: a mixture of oxides of Fe, Cu, Mn + carbon.

#	Russian Material Designation	Type of Material	Application of Material	Chemical Composition of Material
6	SOT-1S-100	TCC (Metallized film)	Used as a coating on the external surfaces of radiators of SVs in conditions of LEOs, GEOs and HEOs.	<ul style="list-style-type: none"> • Tetrafluoroethylene-hexafluoropropylene copolymer of the F-4MB brand with the thickness 100 μm with a silver coating with the thickness 0.1—0.15 μm; • protective layer over the silver: nichrome of the Kh20N80 brand and EP-730 lacquer; • external surface of the film covered with a conductive transparent coating of indium oxide doped with tin oxide (ITO).
7	PM-1EU-OA	TCC (Metallized film)	Used as part of multi-layer insulation (MLIs) and in on-board cable networks in GEOs and HEOs.	Polyimide film with the thickness 12 μm with single-sided vacuum deposition of an aluminum layer.
8	NIKAM-RAM-2	Fabric	Used for facing MLIs in LEO conditions.	<ul style="list-style-type: none"> • Polyimide film of the PM-1EU-OA brand with the thickness 12 μm with single-sided vacuum deposition of an aluminum layer; • reinforcing layer: polyester fabric; • binding agent between the film and fabric: heat-resistant copolymer; • conductive, optically transparent coating of indium oxide doped with tin oxide (ITO) on the external surface of the polyimide film.
9	Arimide frame fabric TTKA-S 56420	Fabric	Used for facing MLIs and for thermal insulation of propulsion devices in GEO conditions.	<ul style="list-style-type: none"> • Arimide threads; • skeleton cell with the dimensions 10 \times 10 mm made of silvered copper wire wound onto an arimide thread.

#	Russian Material Designation	Type of Material	Application of Material	Chemical Composition of Material
10	TSON-SOT M bts	Fabric	Used for facing MLIs and in on-board cable networks in LEO, GEO and HEO conditions.	<ul style="list-style-type: none"> Fabric obtained by thermochemical treatment of the STMK fabric based on aluminoborosilicate glass; skeleton cell with the dimensions 10×10 mm made of silvered copper wire wound onto a Capron thread.
11	FP-BSFR 100-208	Solar Arrays	Used as part of solar arrays on GEOs and HEOs.	Solar array cells based on crystalline silicon with a rear side reflective coating and protective coatings of the K-208 glass with the thickness $100 \mu\text{m}$ glued to the front and back surfaces.
12	FP-BSFR 200-208	Solar Arrays	Used as part of solar arrays on GEOs and HEOs.	Solar array cells based on crystalline silicon with a rear side reflective coating and protective coatings of the K-208 glass with the thickness $200 \mu\text{m}$ glued to the front and back surfaces.
13	FP 100-208	Solar Arrays	Used as part of solar arrays on LEOs.	Solar array cells based on crystalline silicon, having bifacial sensitivity, with protective coatings of the K-208 glass with the thickness $100 \mu\text{m}$ glued to the front and back surfaces.
14	FP 200-208	Solar Arrays	Used as part of solar arrays on LEOs.	Solar array cells based on crystalline silicon, having bifacial sensitivity, with protective coatings of the K-208 glass with the thickness $200 \mu\text{m}$ glued to the front and back surfaces.

All exposures are made in a good, oil-free vacuum, with dose rates low enough to avoid excessive heating, expansion or destruction of the sample. After irradiation, the samples are placed into an inert atmosphere at room temperature to avoid distortion of the results. After testing, the samples are packed into hermetically sealed containers filled with inert gas and subsequently shipped to the Partner. Photographs of the samples under testing are made both before and after irradiation.

List of the optical parameters investigated:

- α_λ - spectral coefficient of absorptance (0.3—10 μm) and α_s – integral coefficient of solar radiation absorptance;
- R_λ - spectral coefficient of reflectance (0.3—10 μm) and R_s – integral coefficient of solar radiation reflectance;
- T_λ - spectral coefficient of transmittance (0.3—10 μm) and T_s – integral coefficient of solar radiation transmittance;
- BRDF/BSDF;
- ε_H – integral coefficient of heat emission to a hemisphere;
- D and D/x – optical density and relative optical density reduced to the unit of the sample thickness;
- changes in the appearance and color of the samples.

Measurement of the optical parameters of the samples after the impact of the space environment factors was conducted according to standard procedures on spectrophotometers in the wavelength ranges 0.2 — 2.5 and 2.5 — 10 μm . Measurement of the coefficient of heat emission was carried out by means of the TRM-I thermoradiometer.

The scattering indicatrix was measured on a modernized installation for measuring the Bi-Directional Reflectivity Distribution Function (BRDF) and Bi-Directional Scattering Distribution Function (BSDF) in the spectral range (0.3÷2.5 μm). The measurements were conducted under the following conditions:

- radiation sources, monochromatic, with the wavelengths 532 and 1063 nm;
- angular resolution of the installation, 0.2÷0.5°, for carrying out measurements on samples with a mixed, specular and diffuse, type of reflectance (scattering), and 2°, for samples with diffuse reflectance;
- sample size, up to 100 cm^2 , with the possibility of measuring selected sections of the sample;
- recording the BSDF/BRDF outside the plane of incidence of the probing beam — for samples agreed upon with the Partner;

- angles of incidence of the probing beam, 8°, 30° and 60°;
- angular range of the measurements, $\pm 45^\circ$ (depending on material type); measurements conducted every 5° with the purpose of determining the existence of irregular reflection maxima in certain directions;
- for opaque materials, the BRDF was measured; for a limited selection of semi-transparent materials, both the BSDF and BRDF were measured.

To provide for the above-mentioned possibilities, modernization has been carried out of the installation existing at OAO Kompozit. That device is intended for measuring the Bi-Directional Reflectivity Distribution Function (BRDF) and the Bi-Directional Scattering Distribution Function (BSDF) and is currently capable of measuring the BSDF/BRDF on samples with high scattering ability in the spectral range 0.3—2.5 μm . The measurements are only carried out in the plane of incidence of the beam, with an angular resolution of about 2°, at angles of incidence from 0° to 75° and at virtually any observation angles. A sample with a diameter of 30 mm remains stationary; it is the photodetector that rotates.

The modernization completed includes:

- equipping the device with monochromatic radiation sources for the wavelengths 532 nm and 1063 nm;
- increasing the angular resolution of the device to $0.2\div 0.5^\circ$ in order to carry out measurements on samples with a mixed, specular and diffuse, type of reflectance (scattering);
- constructional support for measurements of sample surfaces with an area of up to 100 cm^2 , with the capability of measuring selected sections of the sample;
- providing for the capability to measure the BSDF/BRDF outside the plane of incidence of the beam.

Equipment and materials acquired for the modernization:

- rotation platform (by Standa) with a stepper motor for rotating the MR150 type photodetector; angular resolution, 0.02°;
- low-noise photodetector (by Hamamatsu) with an S8785-02 type preamplifier;
- source of continuous monochromatic radiation, 532 nm, LCM-T-111 model (by Laser-Compact, “Polus”);
- source of continuous monochromatic radiation, 1063 nm, LCM-T-112 model (by Laser-Compact, “Polus”);

- ATmega-USB type measurement control card (by Argussoft), connectable to PC via USB;
- portable PC;
- synchronous detector of the “Lock-In” type;
- radiation modulator (chopper);
- rotary mounts for fixing the radiation sources;
- telescopic beam expander $\lambda=532$ nm, $\lambda=1063$ nm (1:10);
- angular position sensor (2 items);
- sample-inclination device.

To meet the Partner’s requirements as to measurements in the IR range, modernization has been carried out of the IR spectrophotometer IKS-31. An installation was created under the Project to measure the Directed Hemispherical Reflectance (DHR) of material samples in the spectral range $2.5\div 10$ μ m. The measurement technique is based on using an integrating sphere, in the center of which the samples are placed. The sphere is connected to the single-beam IR spectrophotometer IKS-31. Measurements are carried out every 100 nm in the range $2.5\div 10$ μ m, with the spectral resolution of the probing beam being ± 20 nm.

Equipment and materials acquired for the modernization:

- integrating sphere (by Labsphere) with a gold diffuse reflectance coating;
- cooled broadband infrared radiation detector by Hamamatsu;
- comparison standards (by Labsphere) with NIST traceable calibration;
- mirror optics (flat and parabolic mirrors);
- radiation modulator;
- rotary mount for fixing the samples in the center of the integrating sphere;
- motorized rotating platform (by Standa) with a control unit for the stepper motor;
- ATmega-USB type measurement control card (by Argussoft), connectable to PC via USB;
- phase-sensitive voltmeter of the “Lock-In” type;
- PC with an interface unit.

The developed version of the Database includes fifteen tables, thirteen forms and six reports. The lists of these tables, forms and reports are given in Figures 1—3 of Appendix 1.

The table of materials (tbl_MaterialList) contains the following information fields (Figure 2 of Appendix 1):

- auto-number (unique identifier);
- name of the material;

- type of the material;
- chemical composition of the material;
- peculiarities of the fabrication method of the material;
- application of the material;
- reference to the state standard for the manufacture of the material.

The types of materials are presented in tbl_TypeMaterials (Figure 5, Appendix 1). All the materials are divided into six types. The materials that do not come under any of the itemized types are presented in the 'others' category:

- thermal control coverings,
- fabrics,
- MLIs,
- solar arrays,
- structural materials,
- optical materials,
- others.

TCCs are subdivided into the following classes (Figure 6, Appendix 1):

- enamels,
- silicate coverings,
- galvanochemical coverings,
- metallized films,
- non-metallized films,
- metallized glasses,
- non-metallized glasses,
- others.

Structural materials (tbl_TypeStructuralMaterial) used on the external surfaces of spacecraft are subdivided into the following four types (Figure 7, Appendix 1):

- glass plastics,
- carbon plastics,
- thermoplastics,
- metals,
- alloys,

- others.

The table of the type of tests (tbl_TypeTests) includes (Figure 8, Appendix 1):

- in-flight tests,
- laboratory tests,
- prediction results.

The factors of the space environment (tbl_SpaceFactors) are divided into the following classes (Figure 9, Appendix 1):

- electrons,
- protons,
- ultraviolet solar radiation,
- infrared and visible solar radiation,
- vacuum ultraviolet,
- soft X-ray radiation,
- combined action of electrons and protons,
- combined action of electrons, protons and ultraviolet solar radiation,
- atomic oxygen,
- combined action of atomic oxygen and ultraviolet solar radiation,
- thermocycling,
- contamination,
- complex action of the space environment factors,
- others,
- combined action of electrons and ultraviolet solar radiation,
- combined action of protons and ultraviolet solar radiation,
- before irradiation.

The list of optical and thermophysical parameters measured is given in tbl_Parameters (Figure 10, Appendix 1):

- solar absorption,
- spectral absorption coefficient,
- solar reflectance,
- spectral reflectance coefficient,
- solar transmittance,

- spectral transmittance coefficient,
- coefficient of heat emission,
- spectral coefficient of heat emission,
- integral coefficient of heat emission,
- optical density,
- relative optical density reduced to the unit of the sample thickness,
- change of material color and appearance,
- Bi-directional Reflectance Distribution Function (BRDF),
- coefficient of thermal conductivity,
- coefficient of thermal diffusivity,
- specific heat capacity,
- melt temperature,
- density,
- others.

Orbits (tbl_TypeOrbits), taking into account the operating conditions of spacecraft in them, are divided into types as follows (Figure 11, Appendix 1):

- Low Earth Orbit (LEO, 200—600 km, $i = 0—90$),
- Low Earth Orbit (LEO, 600 —1,000 km, $i < 65$),
- Middle Earth Orbit (MEO, 1000—36,000 km, $i < 90$),
- Polar Orbit (POL, 600—1000 km, $i > 65$),
- Geostationary Earth Orbit (GEO, 36,000 km, $i = 0$),
- Highly-Elliptical Earth Orbit (HEO, 500—40,000 km, $i = 65$).

The table tbl_References contains a list of the information sources. The imprint of the publications, such as the author's name, title and the publisher, is presented in this table (Figure 12, Appendix 1).

The results of material tests have been distributed into six tables in accordance with the division of materials into six types. The test results obtained for each of the six material types are entered into a separate table linked to the other tables. The structure of the data tables is presented in Figure 13 of Appendix 1 with TCCs as an example. For the other types of materials, the structure of the tables is similar.

For the presentation of the test results, six forms have been developed, each of them linked to one of the six data tables which, in turn, correspond to the six types of materials (films, MLIs, TCCs,

solar arrays, optical and structural materials). Figures 14—16 of Appendix 1 show examples of records from the TCCs, MLIs and structural materials data tables in data forms. The data form has a similar appearance for the other types of materials.

In the top right corner of each form, there are buttons for print preview of the selected record and for sending it to print to the operating system's default printer. Fig. 17 (Appendix 1) shows an example of a Database record prepared for print.

Fig. 18 (Appendix 1) shows the main form of the Database. The main form allows opening the forms corresponding to all the six material types, as well as the materials table and the table with the list of references. Additionally, the main form allows forming search queries (by orbit type, test type, space environment factor and results of optical and thermophysical measurements). Shown in Figs. 19—21 (Appendix 1) are examples of such queries. For each of the six types of materials, the main form contains buttons allowing to form queries for printing the required Database records. Shown in Figs. 22—23 (Appendix 1) are examples of print preview and sending to print of selected Database records.

A short description of the techniques of conducting the tests and measurements, as well as of the equipment used, is given below.

2. Techniques of conducting the tests and measurements

2.1. Technique of conducting tests of materials under combined exposure

The UV-1/2 automated test bench (Fig. 1) is intended for studying the physico-chemical properties of materials and coatings under the combined action of space environment factors (electron and proton radiation with charged particle energies of up to 50 keV, electromagnetic solar radiation with intensities of up to 10 e.s.i., vacuum of up to 1×10^{-6} Pa, temperature $T = \pm 150^\circ\text{C}$) and for confirming changes in their properties for long operating lives.

The test bench consists of three main parts:

- a vacuum module with an evacuation system and a vacuum control system;
- a unit of simulators of the space environment factors;
- an automated system of measurement, control and monitoring.

Vacuum module

The vacuum module consists of a vacuum chamber, a two-stage evacuation system and a vacuum control system (Positions 1 and 4).

The vacuum chamber is a cylinder with a capacity of 1 m^3 . Located on the front flange are hermetically sealed connectors for information input and output, as well as connecting pipes for connecting the thermostat. Attached to the back flange are the space environment factor simulators. The evacuation system is two-stage and is divided into a fore vacuum evacuation system and a high vacuum evacuation system. The first stage, fore pumping, is carried out using an NVR-16D pump up to a pressure of 1×10^{-1} Pa. The second stage, medium vacuum of up to 1×10^{-3} Pa, is provided by a Turbovac-2000 turbomolecular pump (by Leybold Heraeus); high vacuum, up to 1×10^{-5} Pa, is provided by an EGIN-5/1 sputter-ion pump. Vacuum control is performed using a thermoelectric (13VT3-003) and a magnetic (VMB-14) vacuum gauges. Evacuation control may be carried out remotely.

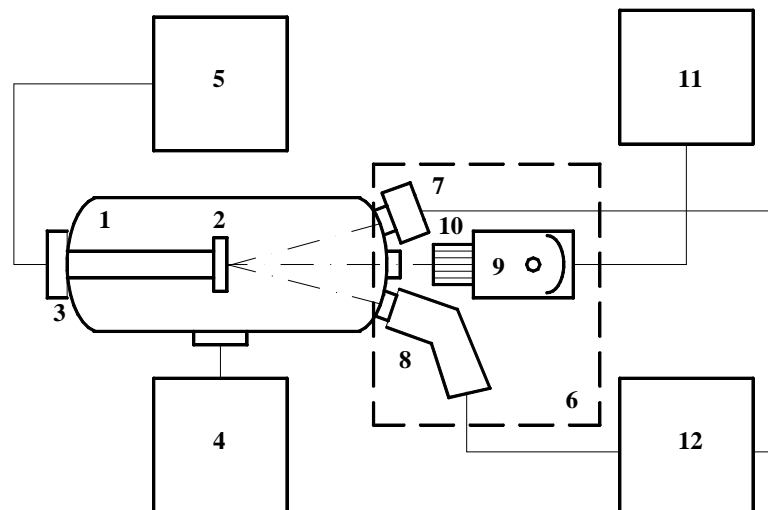


Figure 1. Diagram of the automated test bench UV-1/2

- 1 — vacuum chamber;
- 2 — target;
- 3 — thermostat;
- 4 — system of evacuation and vacuum control;
- 5 — measurements unit;
- 6 — unit of simulators of the space environment factors;
- 7 — electron accelerator;
- 8 — proton accelerator;
- 9 — simulator of concentrated solar radiation;
- 10 — beam-shaping optical device;
- 11 — solar radiation simulator control unit;
- 12 — accelerators control unit.

Located inside the vacuum chamber along the axis of the vacuum module is a target (Position 2), on which the investigated samples are installed. The target is connected to the thermostat (Position 3), which allows keeping its temperature in the range from -150°C to $+150^{\circ}\text{C}$.

Unit of simulators of the space environment factors

The simulators unit (Position 6) consists of an electron accelerator with energies of up to 50 keV (Position 7), a proton accelerator with energies of up to 50 keV (Position 8) and a simulator of electromagnetic solar radiation (Position 9) with a beam-shaping optical device (Position 10). The

electron and proton accelerators are symmetrically connected via vacuum gate valves to the back flange at angles of 30° to the axis of the vacuum module. The simulator of electromagnetic solar radiation is located along the axis of the vacuum module. The luminous flux enters the vacuum chamber through a quartz glass window. The source of light in the simulator is a spherical ultrahigh-pressure xenon arc lamp of the DKsShRB type with water cooling, with a power of 5 kW or 10kW.

Automated system of measurement, control and monitoring

The system consists of a measurements unit (Position 5), a control unit for the electromagnetic solar radiation simulator (Position 11) and an accelerators control unit (Position 12). The system allows controlling the electron, proton and electromagnetic solar radiation fluxes. For this purpose, sensors (Faraday cylinders for the electrons and protons and an S1226 photodiode by Hamamatsu (Japan) for the electromagnetic solar radiation) are installed in the vacuum chamber. Data from them are fed to the measuring devices (a V7E-42 electrometric multipurpose voltmeter and an E7-12 digital L, C, R measuring device) and then to a PC assigned for processing the measurements data and included into the measurements unit (Position 5).

Besides, the accelerators are equipped with sensors, data from which, via an analog-digital converter (a CAMAC crate), are fed to a PC assigned for controlling the ionizing radiation sources and included into the accelerators control unit (Position 12). The operating modes of the accelerators can be set both manually and by PC. The PC also controls these modes during operation. The operating modes of the electromagnetic solar radiation simulator are set and monitored manually on the simulator control unit.

During testing, UV radiation from the electromagnetic solar radiation simulator (Position 9) strikes the sample at a right angle to its surface, while the proton and electron beams reach it at the following angles:

- $+ 30^\circ$, proton beam with an energy of 5 to 50 keV from the proton accelerator (Position 8);
- $- 30^\circ$, electron beam with an energy of 5 to 50 keV from the electron accelerator (Position 7).

The principal technical parameters of the UV-1/2 test bench are given in Table 3.

Table 3.

Technical Parameters of the Installation	
Vacuum	$10^{-1} \dots 10^{-5}$ Pa
Electron energy	10...50 keV
Proton energy	10...50 keV
Current of the electron beam	$10^{-2} \dots 10$ μ A
Current of the proton beam	$10^{-2} \dots 10$ μ A
Electromagnetic solar radiation	1...10 e.s.i.
Temperature	$-150 \dots +150^{\circ}\text{C}$

Processing the measurement results

Calculating the electron and proton fluence

The parameters measured in the course of the experiment are:

- U_i — value of the voltage on the Faraday cylinder (FC) for a single measurement, V;
- t — irradiation time of the sample under investigation, s;
- $P_{\text{in}}, P_{\text{fin}}$ — vacuum level in the measuring chamber (initial and final, respectively), Pa;
- $T_{\text{in}}, T_{\text{fin}}$ — temperature of the target (initial and final, respectively), $^{\circ}\text{C}$.

A program, in the form of an MS Excel table, has been written for calculating the flux density Φ and the fluence F of the electron and proton beams.

The beam current I_j for the j -th point on the irradiation plot is calculated via the formula:

$$I_j = \frac{2U_{\text{av}}}{R_l} (\mu\text{A}),$$

where R_l is the load resistance of the Faraday cylinder ($R_l = 10.0 \text{ M}\Omega$), $\text{M}\Omega$;

U_{av} is the average value of the voltages U_i measured at R_l throughout the experiment for the j -th point on the irradiation plot, V.

The multiplier 2 is connected with the fact that the area of the entrance window of the Faraday cylinder $s = 0.5 \text{ cm}^2$ (the diameter $d = 8 \text{ mm}$).

$$U_{\text{av}} = \frac{\sum U_i}{K} (\text{V}),$$

where U_i is the voltage on the Faraday cylinder (FC) for a single measurement, V;
 K is the number of measurements.

The particle flux density Φ_j for the j -th point on the irradiation plot is calculated via the formula:

$$\Phi_j = L \times I_j \text{ (particles/cm}^2 \times \text{s)},$$

where L is the normalization factor for a current of 1 μA . It is known that a charge of 1 coulomb corresponds to the charge of N particles, i. e. $N = \frac{Q}{e} = 6.24 \times 10^{18}$ particles (as the elementary charge $e = 1.602 \times 10^{-19}$ C). A current of 1 μA corresponds to the flux of N charged particles through the cross-section $s = 1 \text{ cm}^2$ in the time $t = 1 \text{ s}$, that is, $1 \mu\text{A} = 6.24 \times 10^{12}$ (particles/cm²·s). Hence:
 $L = 6.24 \times 10^{12}$ (particles/cm²·s).

The fluence F_j of particles for the j -th point on the irradiation plot is calculated via the formula:

$$F_j = \Phi_j \times t \text{ (particles/cm}^2\text{)},$$

where t is the sample irradiation time, s.

The integral fluence F_Σ for a single sample is calculated via the formula:

$$F_\Sigma = \sum F_j \text{ (particles/cm}^2\text{)},$$

where j is the number of points sufficient for creating the irradiation plot of the sample.

Calculating the equivalent solar exposure

The parameters measured in the course of the experiment are:

- $I_{\text{ph.d}}$ — current of the photodiode, μA ;
- t — irradiation time of the sample under investigation, hrs.

A program, in the form of an MS Excel table, has been written for calculating the equivalent solar exposure H_s . The calculation table is given in Appendix 3.

The equivalent solar irradiance ESI_j for the j -th point on the irradiation plot is calculated via the formula:

$$ESI_j = L \times I_{\text{ph.d}},$$

where L is an empirical coefficient, μA^{-1} ;

$I_{\text{ph.d.}}$ is the average current of the photodiode, μA ;

$$I_{\text{ph.d.}} = \frac{\sum I_i}{K} \text{ (}\mu\text{A)},$$

where I_i is the value of the photodiode current for a single measurement, μA ;

K is the number of measurements.

The equivalent solar exposure H_{s_j} for the j -th point on the irradiation plot is calculated via the formula:

$$Hs_j = ESI_j \times t \text{ (e.s.h.)},$$

where t is the irradiation time of the sample under investigation, hrs;

e.s.h. is the equivalent solar hour.

The integral equivalent solar exposure Hs_{Σ} for a single sample is calculated via the formula:

$$Hs_{\Sigma} = \sum Hs_j \text{ (e.s.h.)},$$

where j is the number of points necessary for creating the irradiation plot of the sample.

The value of the coefficient L was determined through two series of measurements:

1. The total (integral) luminous flux was measured by the calorimetric method using a calorimetric light detector. Then, using a UV filter, the UV component of the total luminous flux was measured.
2. The UV component of the luminous flux was measured in the range 0.3...0.4 nm using an S1226 photodiode by Hamamatsu (Japan). Then, this figure was approximated for the entire UV range in accordance with the spectral distribution of the radiation source (DKsShRB xenon lamp) and the spectral sensitivity of the light detector with the UV filter.

The following value of the coefficient of conversion of the data from the photodiode to the equivalent solar irradiance has been obtained: $L = 1.36 \text{ (}\mu\text{A}^{-1}\text{)}$.

2.2. Technique of conducting tests under separate exposure to electrons and protons

Testing materials under exposure to electrons

Irradiation of materials with accelerated electrons with the energy 50keV was performed on the UV-1/2 test bench at OAO Kompozit. Intensity of the electron flux equaled $1.0 \times 10^{12} \text{ cm}^{-2}\text{s}^{-1}$ (all tests were performed under exposures equivalent to no less that one year of operating the TCCs on GEO). Sample temperature during irradiation did not exceed 20°C.

Tests of Sheldahl films and MAP enamels under the action of electrons with the energies 85 and 170 keV were conducted at MEPhI. A description of the testing technique is given below.

Setup of the electron injector installation

Shown in Fig. 2 is the diagram of the installation (electron injector), which consists of the following components: 1 - high-voltage pulse electron gun with an indirectly heated hot cathode, 2 - focusing coil, 3 - beam transport system in the form of a pipe with magnetic coils, 4 - magnetic screen, 5, 6 - electromagnets, 7 - chamber containing the target (Fig.3) with the samples.

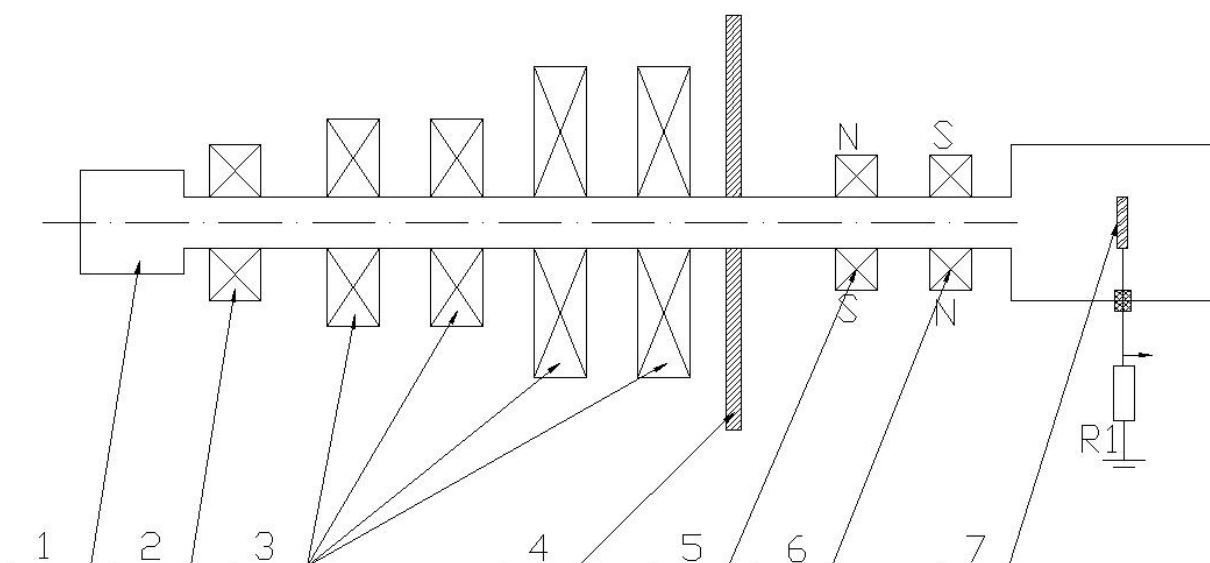


Figure 2. Diagram of the installation (annotated in the text)

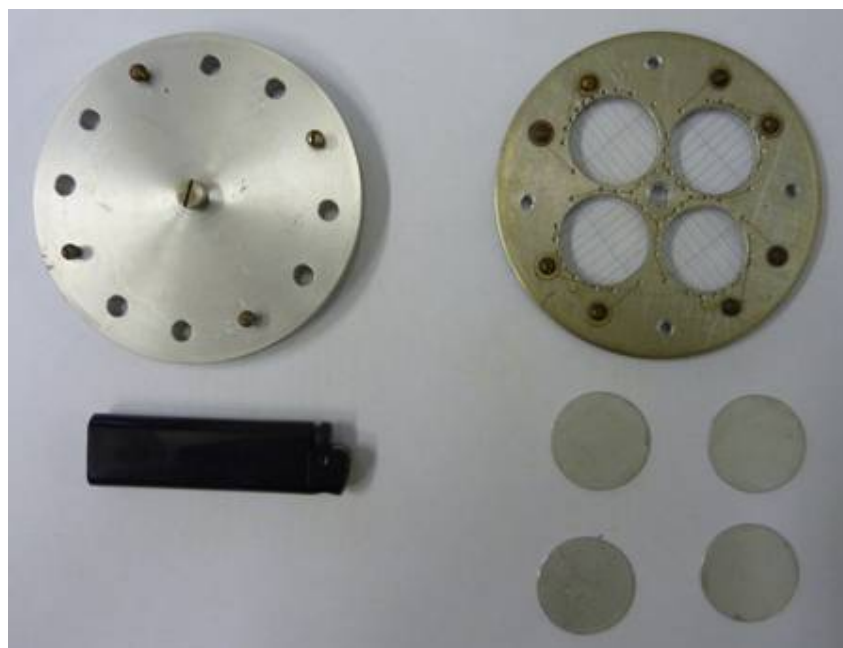


Figure 3. Target for irradiation of the samples

The appearance of the device is shown in Fig. 4.



Figure 4. Appearance of the device (above), complete view of the device (below), electron source with the beam transport system

The control panel of the installation is shown in Fig. 5.

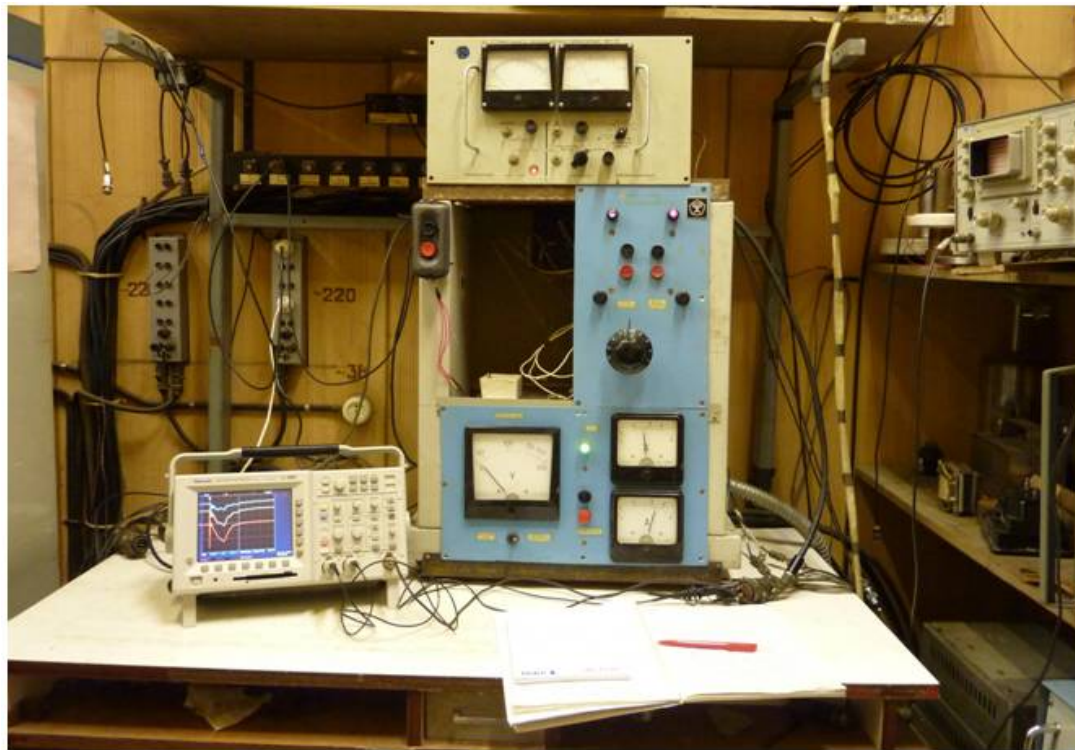


Figure 5. Control panel

Evacuation system

The vacuum pumping system consists of a mechanical fore pump, a cryogenic zeolite pump and three high-vacuum ion pumps: two of the NORD-250 model and one of the NORD-100 model. Vacuum control in the device is carried out using thermocouple and ionization pressure gauges of the types PMT-4M and PMI-2.

Parametres of the installation

The voltage pulse amplitude (Fig. 6) is measured at the exit of a high-resistance divider. The electron current from the target is measured at a resistance of $5\ \Omega$ (Fig. 7) using a Tektronix TDS 3056 digital oscillograph.

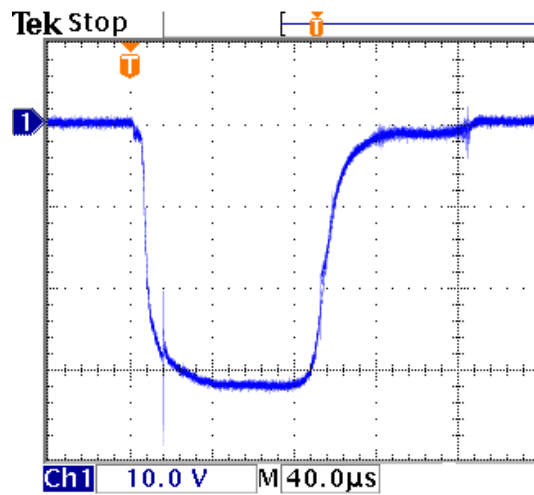


Figure 6. High-voltage pulse

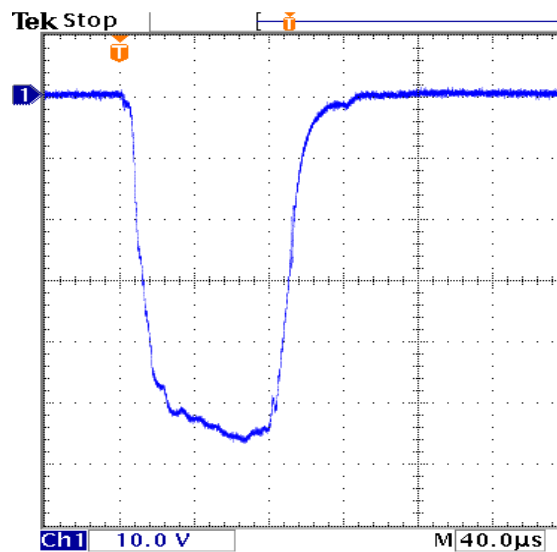


Figure 7. Current pulses from the target

Loss-free passage of the beam through the transport system to the Faraday cylinder strongly depends on current in the focusing coil of the electron gun. When the value of the current is nonoptimal, the beam strikes the walls of the vacuum chamber, which leads to the gradual degradation of the vacuum in the injector up to 5×10^{-5} Torr and to the increase of the gas load on the NORD-250 pumps. On the other hand, with the value of the current in the coil being optimal, the vacuum improves with long-term operation of the injector.

The parameters of the electron injector are given in Table 4.

Table 4

Parameters of the installation

№	Parameters of the installation	Values
1	high-voltage pulse amplitude	0 ÷ 100 kV
2	amplitude of the electron beam current pulse (adjustable)	0 ÷ 20 A
3	diameter of the beam at the exit of the injector (adjustable)	12 mm
4	duration of the high-voltage pulse	100 µs
5	pulse recurrence frequency	1 Hz
6	limit pressure (minimum)	1.5×10^{-6} Torr
7	power consumption	10 kW

Uniformity of the distribution of the electron current

To adjust the device for the required uniformity of the current distribution, a 24-collector Faraday cylinder was used. The Faraday cylinder is shown in Fig. 8.



Figure 8. Multiple-collector Faraday cylinder.

The Faraday cylinder is located in the chamber, instead of on the target with the samples, and signals from each collector are fed, through a vacuum socket, to the oscillograph.

Experimental section

Values of the current of the focusing coil 2 (Fig. 2) and the power voltage of the electromagnets 5 and 6 (Fig. 2) were specially selected to achieve the required uniformity of the current distribution. The electromagnets 5 and 6 (Fig. 9) are necessary for distributing the current in the vertical and horizontal planes.

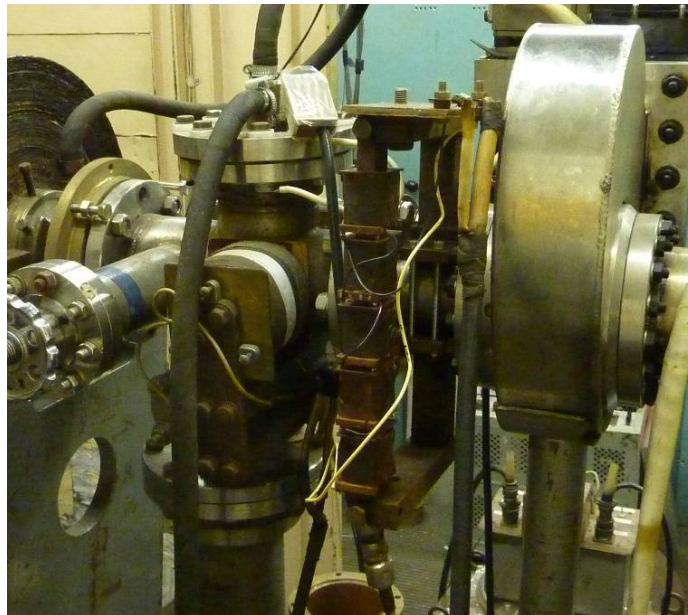


Figure 9. Photograph of the electromagnets

The distribution graph of the current in four directions is shown in Fig. 10.

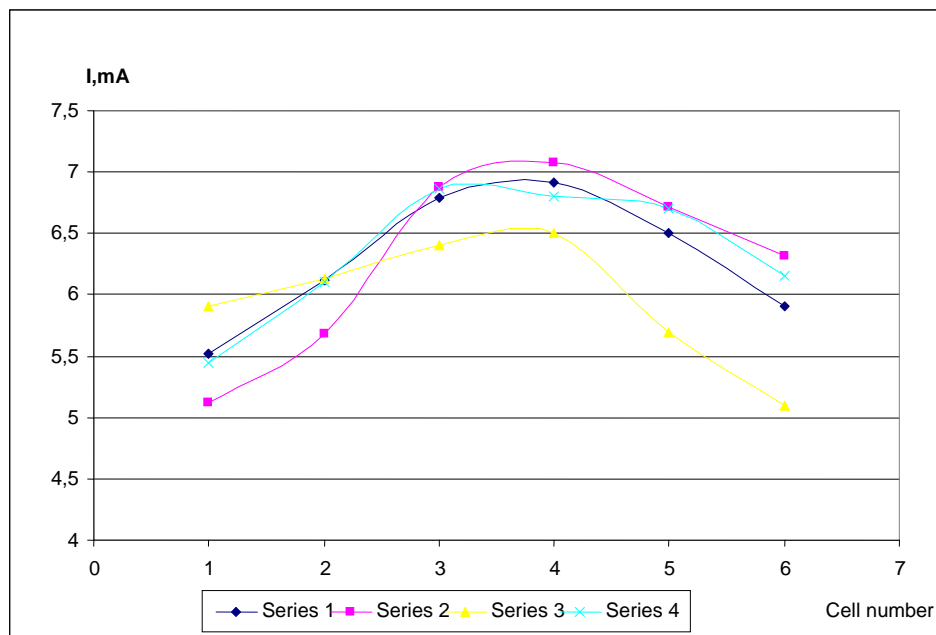


Figure 10. Distribution of the current.

To increase the irradiation energy, an additional high-voltage transformer with a modulator was installed. Shown in Fig. 11 is the diagram of the installation (electron injector), which consists of the following elements: 1 - high-voltage pulse electron gun with an indirectly heated hot cathode, 2 - focusing coil, 3 - beam transport system in the form of a pipe with magnetic coils, 4 - magnetic screen, 5, 6 - electromagnets, 7 - chamber containing the target (Fig. 3) with the samples, PT - pulse transformer, Modulator – modulator for creating a positive rectangular pulse.

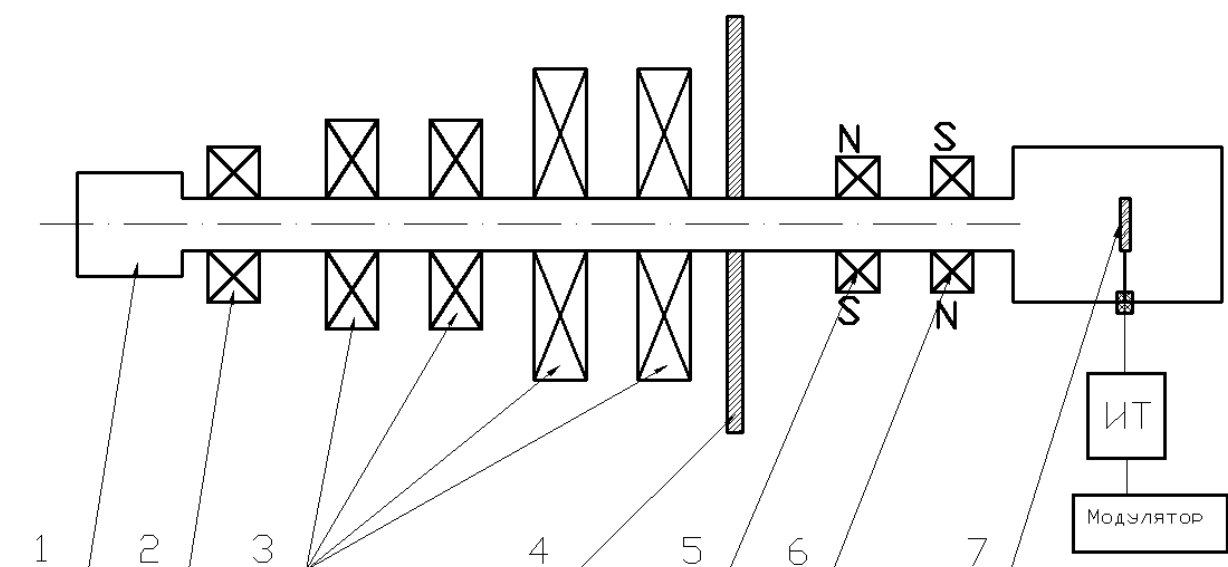


Figure 11. Diagram of the installation for increasing energy (annotated in the text)

The parameters of the modernized electron injector are given in Table 5.

Table 5.

Parameters of the installation

№	Parameters of the installation	Values
1	high-voltage pulse amplitude	$0 \div 200$ kV
2	amplitude of the electron beam current pulse (adjustable)	$0 \div 20$ A
3	diameter of the beam at the exit of the injector (adjustable)	12 mm
4	duration of the high-voltage pulse	100 μ s
5	pulse recurrence frequency	1 Hz
6	limit pressure (minimum)	1.5×10^{-6} Torr
7	power consumption	10 kW

Testing materials under exposure to protons

In accordance with the research program, the Research Institute of Nuclear Physics of Moscow State University has performed irradiation of samples of polymer films used as thermal control coatings (TCCs) of spacecraft with beams of accelerated protons.

The tests were conducted on an experimental installation developed at INP MSU for investigating the changes in the optical properties of TCCs as a result of proton irradiation. The diagram of the experimental installation is shown in Fig. 12.

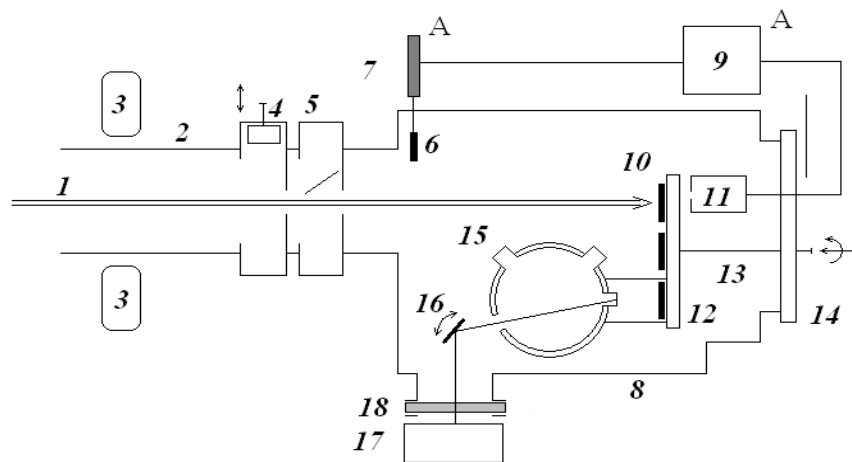


Figure 12. Diagram of the experimental installation

1- proton beam; 2- ion guide; 3- electromagnet; 4- Faraday cylinder; 5- manually operated shutter; 6- automatic shutter; 7- control electromagnet 6; 8- vacuum chamber; 9- scaling unit; 10- samples; 11- Faraday cylinder; 12- turntable; 13- shaft; 14- flange; 15- photometric sphere; 16- scanning mirror; 17- light source; 18- quartz glass

For the purposes of obtaining proton radiation simulating the impact of the space environment factors—which takes place in vacuum—the vacuum system and the working chamber are evacuated up to a forevacuum of 10^{-2} Torr using a fore pump (NRV 20); then, by means of an oil-diffusion pump – 10 (N-160/700) using the polyphenyl ether 5F4E ($C_{30}H_{22}O_4$) for vacuum applications, they are evacuated up to a residual pressure of 1 to 3×10^{-5} Torr. The oil-diffusion pump is separated from the working chamber by a high-vacuum valve. The fore pump is connected to the chamber through the bypass line.

For the period of fore pumping, through the bypass line, the oil-diffusion pump is separated from the fore pump by a valve. Pressure measurement in the vacuum system is performed using a 13VTZ-003 vacuum gauge connected to the PMT-4m vacuum gauge tube. Vacuum measurement in the working chamber is performed by means of a VIT-2 vacuum gauge connected to the vacuum gauge tubes PMT-3, for measuring low vacuum, and PMI-2, for measuring high vacuum.

The working section consists of a vacuum chamber (8), into which the proton beam (1) is injected through the ion guide (2) from the KG-500 accelerator (a cascade generator with a maximum energy of 500 keV). A special deflecting electromagnet (3) shapes the proton beam and provides for its scanning in two planes: the horizontal and the vertical one. A number of electrodes placed at different heights are used to monitor the vertical uniformity of the beam. After this, horizontal scanning is turned on and beam uniformity in this plane is determined. A Faraday cylinder (4) and a beam shutter (5) provide for manual adjustment of the beam. Quartz glass is used as the

beam visualizer. The samples under investigation (10) are mounted on a turntable (12) that is rotated using a shaft (13). Next to each sample on the turntable, there is a slot for the proton beam to pass into the Faraday cylinder (11) that provides for measuring the fluence. The signal from (11) comes to the programmable up/down counter (scaling unit) F5007 (9). When the required accumulated count is reached on it, corresponding to a given fluence value, a signal is applied to the control electromagnet (7) and the beam is automatically cut off via the shutter (6). The sample holder with the sample is pressed against the measuring window of the integrating sphere (15) of the FM-59 photometer. The radiation scattered by the sphere reaches the UV and IR photodiodes and the composite signal from these allows conducting measurement of the reflectance coefficient against the reference samples.

Film irradiation under the ISTC program was conducted at experimentally determined values of the flux density of accelerated protons that do not result in a degradation of the vacuum. It should also be noted that the operation time expenditure of the KG-500 accelerator was determined by the given fluence values, while taking into account the time required for the preliminary starting procedures at the beginning of the working day and the time required to finish work of the accelerator.

2.3. Testing materials in a plasma flux of atomic oxygen

The material samples were irradiated with a beam of oxygen plasma formed in the plasma accelerator (average ion energy, 20—30 eV) of the plasma-beam test bench at INP MSU that simulates conditions existing on low-earth orbits.

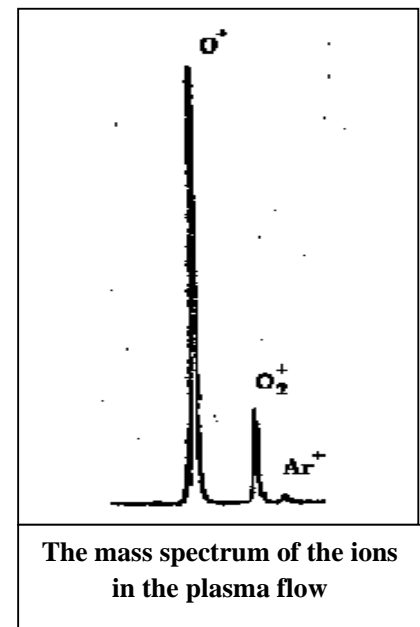
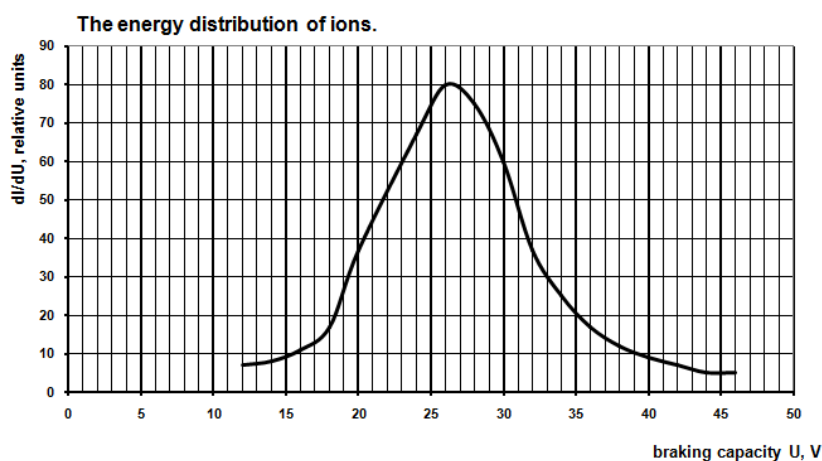


Figure 13. Characteristics of the flux of oxygen plasma.

Flux composition: O and O₂ neutrals, O and O₂ ions, plasma electrons

The diagram of the test bench is shown in Fig. 14. The bench contains a single vacuum chamber (1), divided by the partition (2) into two regions: the section (3) of the plasma source and the measuring section (4). The plasma beam (5) is formed in the accelerator (6) and reaches the sample (7) through the separator (8) of charged particles and an aperture in the partition cooled with water. The material sample (7) is mounted on the holder (9).

Diagnostics of the beam is performed by the sensors (10, 11) of the ion and neutral components, located on the manipulator (12) that allows placing them into the position of the sample. The energy distribution of the ion component is measured using a three-grid retarding-field analyzer. The mass-average parameters of the molecular beam are determined from the values of the energy and momentum fluxes using a thermistor bolometer and a torsion balance. The mass composition of the ion component is recorded using the LM-102 quadrupole mass spectrometer by MKS (US), whose analyzer (13) is mounted on the chamber flange and whose electronic unit (14) is connected to the computer system (15) of information collection, recording and processing. The system was developed based on a Pentium 4 PC, using the LabView programming environment and equipment by National Instruments (US).

The vacuum system of the test bench is implemented with differential pumping of both sections, as well as of the accelerator, using the SA-16 (16), SA-10 (17), SA-4 (18) SPACE TORR cryopumps by Suzuki Shokan (Japan) having the pumping speeds 5.5 , 2.5 and $0.3 \text{ m}^3 \text{ s}^{-1}$. respectively.

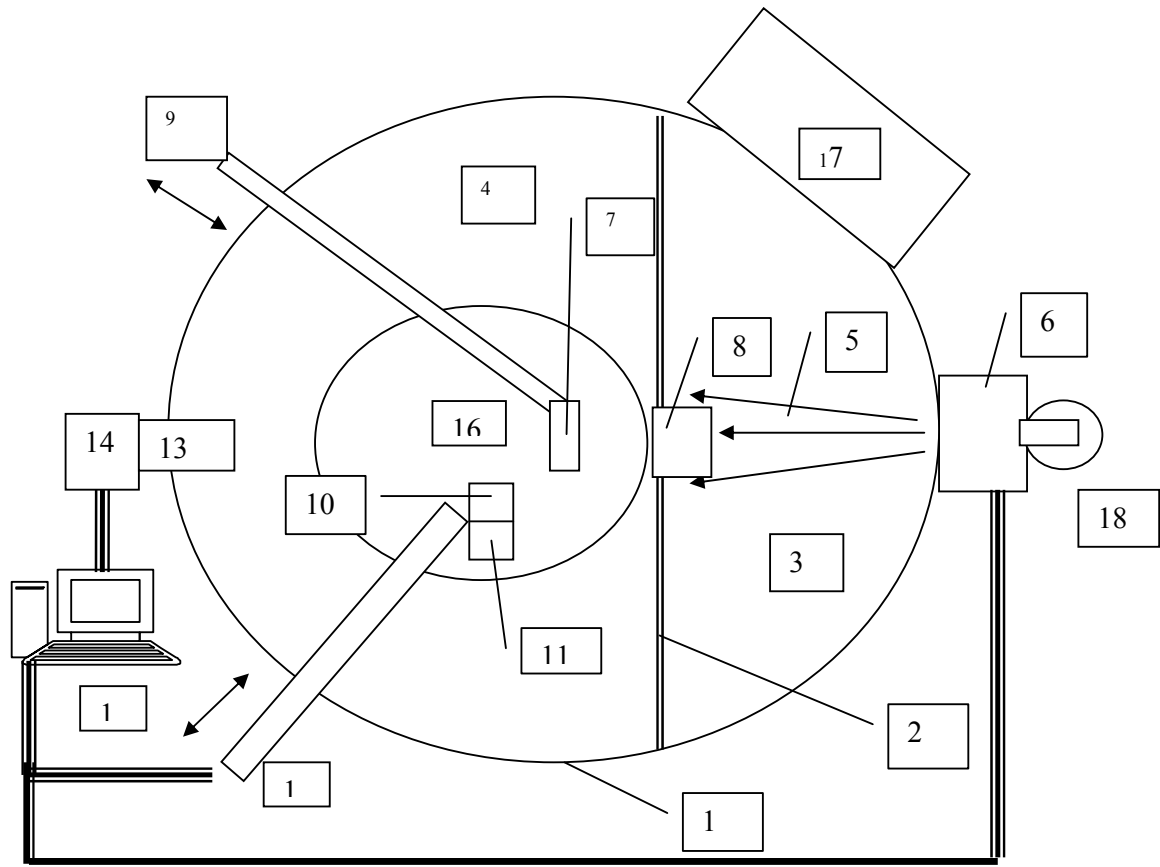


Figure 14. Diagram of the plasma-beam test bench at INP MSU:

1-vacuum chamber, 2-partition, 3-section of the plasma source, 4- measuring section, 5-plasma flux, 6-accelerator, 7-sample, 8-charged particles separator, 9-sample holder, 10-sensor of ions, 11-sensor of neutrals, 12-sensors manipulator, 13- quadrupole analyzer, 14- electronic unit of the mass spectrometer, 15-computer recording system, 16, 17, 18- cryopumps

Residual pressure in the chamber, when it is not warmed up, does not exceed $3 \text{ to } 5 \times 10^{-5} \text{ Pa}$. Operating vacuum is $1 \text{ to } 1.5 \times 10^{-2} \text{ Pa}$ in the section (3) and $3 \text{ to } 5 \times 10^{-3} \text{ Pa}$ in the section (4) for typical consumption levels of the plasma-forming gas (oxygen) being $0.2\text{--}0.5 \text{ cm}^3 \text{ s}^{-1}$ and those of the working gases of the hollow cathode (argon or xenon) being $0.1\text{--}0.2 \text{ cm}^3 \text{ s}^{-1}$. The parameters of the flux are determined at a distance of 0.2 m from the anode face and in the same plane as the material sample is placed.

Selecting the modes of simulation experiments

Simulating the behavior of materials for long flight times calls for the development of accelerated test techniques that would allow making estimates of probable changes of the key material properties in time intervals that are practically feasible. In predicting changes over a period of 10—20 years, an acceleration ratio of no less than one hundred has to be provided for.

In the present experiments, the required acceleration degree was achieved by means of increasing both the flux density and the energy of the particles as compared to their in-flight levels. The beam of accelerated plasma hitting the samples consisted of ions, atoms and molecules of oxygen with a mass-average velocity of 16 km/s (average energy of atoms, 20 eV) and a flux density of $(2.5—3.5) \times 10^{16} \text{cm}^{-2} \times \text{s}^{-1}$. In colliding with the surface, the fast molecules in the flux dissociate, the ions are neutralized and, as a result, the material is impacted by atoms having an average velocity of 16 km/s.

The results of a simulated exposure must be equivalent to the presumed in-flight effects. In the standard technique of measuring fluence in simulation tests, the equivalence criterion is the value of the specific mass losses of polyimide. The procedure corresponds to the generally-accepted technique of determining the equivalent fluence of atomic oxygen (AO) in simulation tests according to the US standard ASTM E 2089-00 (2006).

According to the accepted technique, in irradiating materials, a witness sample made of polyimide film is placed next to the sample being tested and the equivalent fluence of AO is determined from the mass losses of the former. In the present set of experiments, it was the samples of polyimide film to be investigated that served as witness samples.

In interpreting the results of accelerated tests with increased atom energies, the question arises as to their conformity with in-flight data. Using beams of AO with increased energy for simulation tests may be appropriate on condition that the relative reaction efficiency of the material remains constant with respect to polyimide.

As shown by studies using a laser pulse source, the energy dependence in the range 1—16 eV is a universal power dependence for many polymers, as well as graphite. For these materials, the relative reaction efficiency does not change significantly with the growth of the AO energy. Comparing the data of accelerated tests of various polymers on the plasma-beam installation of INP MSU, the AO energy levels being in the range 15—30 eV, with those of the NASA PEACE in-flight experiment on the International Space Station and those of laboratory studies at 5 eV may serve as experimental confirmation of this

For experimental verification of the hypothesis proposed here—about the invariance of the energy dependence of erosion in certain classes of polymers under the action of atomic oxygen in the energy range 2—5 eV, as well as with the energy increased up to 20—30 eV, and about the change of the charge state of the oxygen atoms— the relative erosion factors were previously determined for a

selected set of polymer and carbon materials. The materials—pyrographite (PG), polystyrene (Styroflex) (PS), polyimide (PI), low-density polyethylene (LDPE), polyvinyl fluoride (PVF) (Tedlar), polyethylene terephthalate (PET) (Mylar), polymethyl methacrylate (PMMA)—were studied by the method of Kapton standard in conditions of irradiating the samples with a beam of oxygen plasma with the particle energy 20—30 eV, at which the energy dependence of the erosion factor for the polymers under scrutiny is presumed to be universal. This allows using the properties of materials that are well studied at 5 eV (polyimide) and the results of accelerated comparative tests at higher energies to predict changes in the structure of new materials, too, at 5 eV and high fluences.

Presented in a formalized manner, the proposed approach comes to the following: the erosion factor of a material $Y_m = dM_m/dF$ can be written in the form of a function of the energy E (eV), i. e. $Y_m(E) = Y_m(5) \times f_m(E)$. Then

$$Y_m(5) = Y_m(E) / f_m(E) \quad (1)$$

where $f_m(E)$ is the energy dependence, normalized so that $f_m(E) = 1$ at $E = 5$ eV,

dM_m and dM_k are the specific mass losses of the material and of the witness sample of polyimide (Kapton) respectively,

F is the fluence of AO.

As is usual in the standard technique of in-flight and ground tests, the actuating quantity, the so-called effective fluence (EF) of AO, is determined from the mass losses of a witness sample of the reference material, polyimide (Kapton), whose properties are well understood. At $E = 5$ eV, $Y_k = M_k/F = 4.3 \times 10^{-24} \text{ g} \times \text{cm}^{-2}$. This means that the experiment measures the relative value of the erosion factor for the given material with respect to polyimide (Kapton) Y_m/Y_k . Then, the relative erosion factor sought for the material at 5 eV, taking into account expression (1):

$$Y_m(5)/Y_k(5) = [Y_m(E)/f_m(E)] / [Y_k(E)/f_k(E)] = [Y_m(E)/Y_k(E)] \times [f_k(E)/f_m(E)] = [dM_m(E)/dM_k(E)] \times [f_k(E)/f_m(E)]$$

Consequently, the relative erosion factor, measured, e. g., at $E = 20$ eV, differs from the sought value at 5 eV by the coefficient $q = f_k(20) / f_m(20)$.

The value of $q = f_k(E)/f_m(E)$ was determined from the measurement data for $dM_m(20)/dM_k(20)$ and from literary sources for $Y_m(5)/Y_k(5)$ via the formula $q = [Y_m(5) / Y_k(5)] / [dM_m(20) / dM_k(20)]$.

Given in Table 6 are the obtained erosion factors of polymer materials.

Table 6

Relative erosion factors of polymer materials

Material	PI	PET	LDPE	PG	PVF	PS	PMMA
Y_m/Y_k at 5 eV	1.0	1—1.1	> 0.8	0.23	1.02— 1.12	0.91	> 1.8
Y_m/Y_k at 20 eV	1.0	1.07	0.93	0.23	1.11	0.94	2.5
$q = f_k(20)/f_M(20)$	1.0	0.93— 1.03	> 0.86	1.0	0.93-1.01	0.97	> 0.7

It can be seen from the table that, for these materials, q is close to 1: $Y_m(5)/Y_k(5) \sim Y_m(E)/Y_k(E)$.

Thus, it has been shown that, with increasing the energy of AO to 30 eV, the relative erosion factor, determined from the polyimide equivalent, is virtually equal to the value at the energy 5 eV for polyethylene, Mylar, Tedlar, epoxide, coal plastic, which testifies to the rather high degree of conformity of simulation tests with in-flight conditions in what concerns mass losses. It should be said that the equivalent flux density of AO achieved increases by more than an order of magnitude, from $5 \cdot 10^{15} \text{ cm}^{-2} \text{ s}^{-1}$ to $80 \cdot 10^{15} \text{ cm}^{-2} \text{ s}^{-1}$, which, in turn, increases the acceleration ratio of the tests

Irradiation of polyimide film samples by Sheldahl was conducted at a normal incidence of the beam, in several cycles with increasing equivalent fluences. The equivalent fluence of AO, reduced to the velocity 8 km/s, was estimated from the mass losses of the film, on the assumption that its erosion factor $Y = 4.4 \times 10^{-24} \text{ g/O atom}$.

In each irradiation cycle, the polyimide sample was weighed outside the chamber both before and after the AO treatment, using the analytical balance HR-202i with the error 0.05 mg. The area of the exposed section was measured and the value of the specific mass losses was calculated.

The equivalent fluence F of atomic oxygen was calculated via the formula

$$F = M/(A \times Y), \text{ atom/cm}^2$$

where M are the mass losses of the sample, g;

A is the area of the sample surface exposed to AO, cm^2 ,

$Y = 4.4 \times 10^{-24} \text{ g/O atom}$, is the erosion factor of polyimide measured in space for the energy of AO being 5 eV.

Proton irradiation has been carried out on five samples of polymer films: ITO 2.0MIL Teflon Silver Inconel; ITO 10.0MIL Teflon Silver Inconel; ITO 1.0MIL Kapton Aluminum; 2.0MIL Kapton Aluminum; 1.000 GE 1.0MIL Kapton. Samples of these films were irradiated in two modes: with a proton energy of 150 keV and with a proton energy of 500 keV. The total fluence, at which irradiation was stopped for all types of films, was equal to of $5 \times 10^{15} \text{ cm}^{-2}$. Besides, a single sample (ITO

10.0MIL Teflon Silver Inconel) was irradiated with protons with the energy 500 keV up to a total fluence of $5 \times 10^{16} \text{ cm}^{-2}$.

At the initial stage of work, it was necessary to determine experimentally the maximum possible flux density of accelerated protons that is endured by the above-mentioned films under irradiation in vacuum. This parameter was determined by monitoring the operating vacuum in the chamber for different currents of the beam hitting the samples. When the permissible threshold of the proton flux density was crossed, a drastic increase of residual pressure was observed during the experiment, due to intense gas release from the films being irradiated. The endurance of the films was determined at a proton energy of 500 keV. It was established that, for samples of Teflon films (ITO 2.0MIL Teflon Silver Inconel and ITO 10.0MIL Teflon Silver Inconel), the flux density of the proton beam, at which, in experimental conditions, a drastic degradation of the vacuum was observed, is $\sim 10^{11} \text{ cm}^{-2} \text{ s}^{-1}$. For Kapton films (ITO 1.0MIL Kapton Aluminum film; 2.0MIL Kapton Aluminum film; 1.000A GE 1.0MIL Kapton film), the maximum flux density amounted to $2 \times 10^{11} \text{ cm}^{-2} \text{ s}^{-1}$.

2.4. Measuring the spectral and integral optical parameters

Measurements of the spectral and integral reflectance and absorptance in the wavelength range 0.3 — 2.5 μm have been carried out for both pristine and irradiated samples of all the researched during this year materials (MAP enamels and Kapton and Teflon Sheldahl films). Lambda-9 and Shimadzu MPS-2000 spectrophotometers were used for the measurements. According to spectral measurements integrated factors of absorptance and reflectance have been calculated.

In addition to values of integrated factor of absorptance of the sunlight calculated from the spectral data, measurement of α_s of the irradiated samples after their carrying out from the vacuum chamber was performed using photometer FM-59M. Measurements of α_s were performed for final and four intermediate values of time of an irradiation. The solar radiation absorptance of the TCC samples was measured on a FM-59M photometer relative to the reference samples, whose spectra had been recorded on the Cary 500 spectrophotometer.

Measurements of the diffuse reflectance or the directional-hemispherical reflectance (DHR) are performed using a special accessory, DRA-CA-55, with which the Cary 500 spectrophotometer is equipped.

Description of the samples: rectangular plates with dimensions 70 \times 70 mm and disks with diameters of 30 — 50 mm. The parameter measured is the spectral directional-hemispherical reflectance $R(\lambda)$ in the range 200 — 2,500 nm; angle of incidence, 8°. The parameter calculated is the solar radiation absorptance A_s .

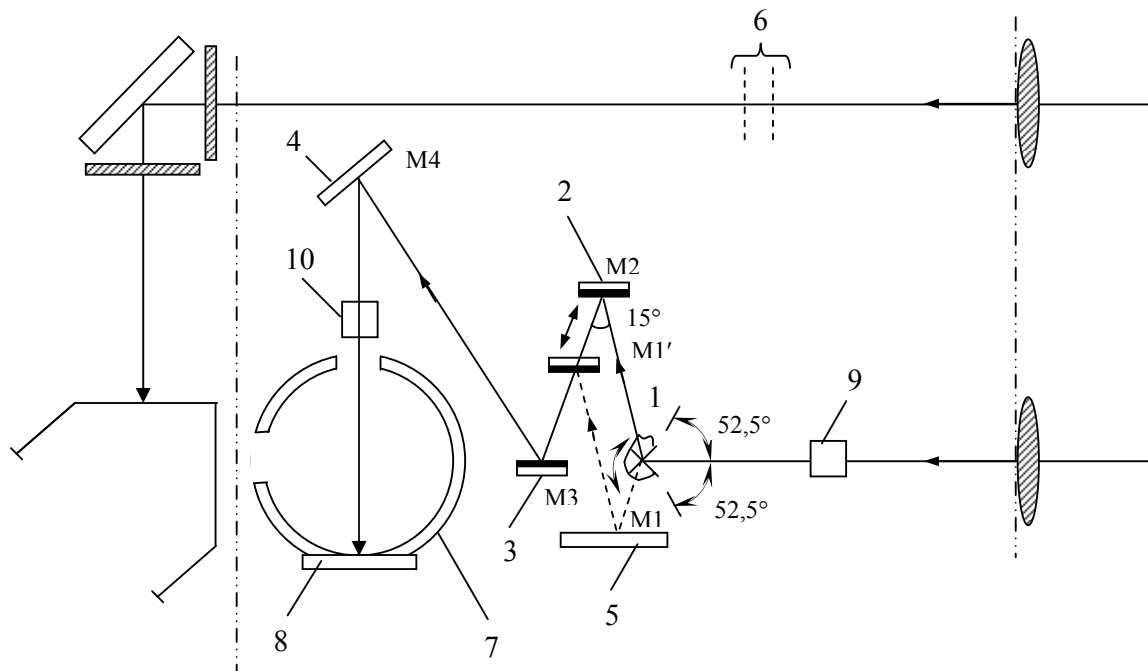


Figure 15. Optical diagram of measuring the solar radiation reflectance R_s (with an integrating sphere).

1. Rotating mirror (flat mirror) M1
2. Sliding mirror (flat mirror) M2
3. Flat mirror M3
4. Concave mirror M4
5. Sample tested for specular reflectance
6. Screen filter (optical attenuator)
7. Integrating sphere with an internal diameter of 150 mm
8. Sample tested for diffuse reflectance
9. Cell for measuring transparent samples
10. Cell for measuring suspensions

The equipment used was an automated Cary 500 spectrophotometer with a DRA-CA-55 integrating sphere coated with Spectralon (internal diameter, 150 mm); standard used, Spectralon reflectance standard, I.D.: SRS-99-020 (calibration date April 4, 2002, Labsphere, Inc., Reflectance Calibration Laboratory, certificate No. 35778-1-1); photometric precision of measurements, $\pm 0.5\%$.

The reflectance spectrum of the sample under investigation is recorded on the Cary 500 spectrophotometer in digital format (ASCII codes); the discretization step in wavelength is 1 nm; the

spectrophotometer setup parameters are standard Processing the spectral data are carried out on the computer, using the Origin 5 software. In calculation, the spectral reflectance $R(\lambda)$ is determined while taking into account the spectral data of the reflectance standard given in the certificate of the SRS-99-020 standard.

Used for calculating A_s were the well-known expression and the data on the spectral density $S(\lambda)$ of the exoatmospheric Sun:

$$A_s = 1 - R_s = \frac{\int_{200 \text{ nm}}^{2500 \text{ nm}} (1 - R(\lambda)) \times S(\lambda) d\lambda}{\int_{200 \text{ nm}}^{2500 \text{ nm}} S(\lambda) d\lambda}$$

The optical diagram of the measurements is given in Fig. 2

Estimates of the absolute values of the normal degree of blackness ε were made in air at room temperature using the TRM-I thermoradiometer.

Shown in Fig. 15 are the reflectance spectra of the reference samples, measured on the Cary 500 spectrophotometer, which were afterwards used in the measurements of the irradiated samples on the FM-59M photometer.

For all pristine and irradiated samples measurements of integral coefficient of heat radiation in hemisphere and reflectance spectra in a range of 2.5-10 microns using themoradiometer TRMI and an add-on device of mirror reflectance on IR-435 spectrophotometer were performed for all pristine and irradiated samples.

2.5. Technique of measuring the BRDF (BSDF)

Measurements of the BRDF of pristine samples have been carried out on the wavelength 532 nm, at the angles of incidence 8° , 30° and 60° and with the angular resolution 1° without using an analyzer of the polarization of reflected radiation.

All the works on modernization of installation for measurements BRDF (BSDF) in a plane of falling and in all 2π - hemisphere- are completely finished. By installation of an additional drive of rotation which was installed on the main rotating platform, signals from the radiation disseminated by samples within a 2π -space angle are registered. Thus movement of the receiver of radiation is carried out by turn of the main rotating platform within azimuthal corners (0-3600 turn of an additional drive within polar corners (0-900). Thus the sample is placed on a table in a horizontal plane and can have the sizes exceeding 100 cm^2 . The modulated radiation of lasers of 532 nanometers and 1064 nanometers goes practically at any angle to a surface of the sample. There are some well known restrictions - area of shadowing near surface normal line and the corner of sliding limit depending on

the sizes of the sample and section of the falling bunch of radiation. Diameter of a probing bunch is defined by the installed telescopic dilators and makes 14 mm and 7 mm (1 mm without dilators). Real angles of falling can be set within (5-800) from a normal to a surface of the sample with accuracy not worse than 0.10. By the installation of precision step-by-step drives with reducers (1:15) FL57STH56-2804AG15, the angular permission at movement of drives isn't worse than 0.1° .

Along with measurements BRDF within a hemisphere, which are realized in the top semispace ("the second floor"), divided by a plane of the main rotating platform, measurements in a falling plane are realized in the bottom part of semispace ("ground floor"). The plane of the sample in this case takes place in a vertical plane which can turn, changing a radiation falling angle on the sample while a source of radiation is motionless. The angular permission at measurements in a plane of falling isn't worse than 0.02° . By the special device turning the plane of the sample installation of a falling angle is set with accuracy not worse than 0.1° is provided. Other device provides an inclination of a plane of falling of the sample within $\pm 10^{\circ}$.

A silicon photo diode S8745-01 ("Hamamatsu") with an active photosensitive platform 2.4x2.4 mm with sensitivity area in a range of (190 nm-1100 nm) is used as the radiation receiver, and also photo diode G8370-02 ("Hamamatsu") on the basis of InGaAs ($\varnothing 2\text{mm}$) with sensitivity area in a range of (0.9-1.7 μ) for measurements on wavelength of 1.064 μ . Special cases which the rotating polarizer of optical radiation is established on were made for photodetectors. The maximum photodetector angle of capture of radiation (without a diaphragm) equals 10^{-4} sr ($\approx 0.5^{\circ}$).

Radiation detecting is carried out with a method called "lock-in", for which "Optical Chopper" OCV-4800FD and "DSP Lock-in Amplifier" SR830 are used. Both devices have a communication channel with the personal computer through RS-232 and USB. The variant of registration a system with a method of "DSP lock-in" with use of 16-digit ADC (200 kSPS) and "Atmel" microcontroller has been developed and made in parallel.

Management of two step-by-step drives of device is carried out with use of "Atmel" microcontrollers and drivers MA335B with step-by-step engines FL57STH56-2804AG15, communication with the personal computer is carried out through USB port. Measurements has been completely automated, the software has been realised on C++ Builder 2006.

To except a flare from external sources of radiation the light-absorbing cover is used. The optical gages fixing extreme angular positions of turns of a platform and a photodetector were installed and the corresponding software of processing of interruptions on operation of optical gages is developed and debugged.

3. Results

of performing work under the Project

During the first phase (first year) of the Project (November 01, 2007—October 31, 2008) the following activities were carried out:

- (1) tests of four brands of MAP enamels under the action of protons with the energy 50 keV (Task 1, Subtask 1.1);
- (2) tests of four brands of Russian materials—EKOM-1 (white), EKOM-2 (black), FP-BSFR-100-208 and FP-BSFR-200-208—under combined exposure to electrons, protons and UV radiation (Task 2, Subtasks 3, 5);
- (3) measurement of the optical parameters of all materials before and after exposure to protons (with the energy 50 keV) and combined exposure to electrons, protons and UV radiation (Task 4, Subtasks 1—4);
- (4) part of the work on modernizing the experimental equipment for carrying out measurements of the optical parameters (Task 5, Subtasks 1 and 2);
- (5) processing the tests results and entering them into the Database (Tasks 1, 2, 4).

During the second phase (second year) of the Project (November 01, 2008—October 31, 2009) the following activities were carried out:

- (1) tests of four brands of MAP enamels under the action of electrons with the energy 50 keV (Task 1, Subtask 1.2);
- (2) tests of 8 brands of Kapton films and 6 brands of Teflon films by Sheldahl under the action of electrons with the energy 100 KeV (Task 1, Subtask 1.2);
- (3) tests of four brands of MAP enamels under combined exposure to electrons, protons and UV radiation (Task 2, Subtask 2);
- (4) measurement of the optical parameters of all materials before and after exposure to electrons (with the energies 50 and 100 KeV) and combined exposure to electrons, protons and UV radiation (Task 4, Subtasks 1—4);
- (5) part of the work on modernizing the experimental equipment for carrying out measurements of the optical parameters (Task 5, Subtasks 1 and 2);
- (6) processing the test results and entering them into the Database (Tasks 1, 2, 4).

During the third phase (third year) of the Project (November 1, 2009—October 31, 2010) the following activities were carried out:

- (1) tests of the films by Sheldahl and the enamels by MAP under the action of accelerated protons with the energies 50, 150, 300 and 500 keV (Task 1, Subtask 1);
- (2) tests of four brands of films by Sheldahl under the combined action of simulated electromagnetic solar radiation, electrons and protons (Task 2, Subtask 1);
- (3) measurement of the spectral parameters of the materials before and after exposure to different types of space radiation (Task 4);
- (4) work on modernizing the installations for measuring the BRDF and for measuring the Directed Hemispherical Reflectance (DHR) (2.5—10 μm) (Task 5, Subtask 1).
- (5) processing the test results and entering them into the Database (Tasks 1, 2, 4).

During the fourth phase (fourth and fifth years) of the Project (November 1, 2010 – October 31, 2012) the following activities were carried out:

- (1) tests of the films by Sheldahl under the action of protons with the energies 150 and 500 keV (Task 1, Subtask 1);
- (2) tests of the films and fabrics under combined exposure to electrons, protons and UV radiation (Task 2);
- (3) tests of the films by Sheldahl and the enamels by MAP under combined exposure to atomic oxygen and UV radiation (Task 3, Subtask 1);
- (4) measurements of the optical parameters of the samples after exposure to the space environment factors (Task 4, Subtasks 1—4);
- (5) modernization of the installation for measuring the Directed Hemispherical Reflectance (DHR) in the range 2.5—10 μm (Task 5, Subtask 2).
- 6) processing the test results and entering them into the Database (Tasks 1—4).

The results of the experimental studies conducted of the complex impact of the space environment factors on the optical properties of spacecraft materials have been entered into the Database in digital and graphic forms. The resulting Database is in Microsoft Access 2000 format and contains about 3,500 records.

Characteristic test results obtained in the course of realizing the stated tasks of the Project are presented in Appendix 2 to the present Report.

4. Conclusion

The present Project is a complex of experimental investigations on the degradation of the optical properties of materials used on the external surfaces of spacecraft in conditions of the space environment.

The present Project is a continuation of ISTC Project #2342p “Development of a Database on the Changes in the Optical Properties of Materials Used on the External Surfaces of Spacecraft under the Action of the Space Environment Factors.” Studied under the previous Project were Russian materials under the separate action of high-energy electrons, high-energy protons and UV radiation. The simultaneous action of those space environment factors was not investigated in that Project. In the present one, the goal was set to find out how these factors act upon the materials together. Moreover, the number of subjects of inquiry was increased. In addition to Russian materials, Sheldahl polymer films (USA) and MAP paints (France) have been tested under the present Project.

The Project has been realized by employees of three institutions: MEPhI, OAO Kompozit and INP MSU. The work stipulated for by the Project was divided into four phases and carried out in five years (November 1, 2007—October 31, 2012). The following has been achieved during the course of the Project:

1. Tests have been conducted of the Sheldahl films, MAP paints and the Russian materials EKOM-4 and the arimide fabric TTKA-S 56420 under the separate action of protons with the energies 50, 150 и 500 keV, electrons with the energies 50, 100 and 200 keV and UV radiation (all tests were carried out with exposures equivalent to one year on GEO).

2. Tests have been conducted in simulating the combined effects of space environment factors, such as electromagnetic solar radiation (visible, ultraviolet, vacuum ultraviolet and soft X-rays) and charged particles (electrons and protons), at GEO altitudes. For such a simulation, simultaneous tests (e + p + UV) have been conducted at an acceleration factor equal to three for UV and an equivalent fluence corresponding to three years. The energy levels of e + p for this test series were 50 keV. These tests have been conducted on the Russian materials, Sheldahl films, and MAP paints.

3. Laboratory tests have been performed in simulating the combined effects of space environment factors, such as atomic oxygen, electromagnetic solar radiation (visible, ultraviolet, vacuum ultraviolet and soft X-ray radiation) at an altitude of 400 km. For LEO simulation, a limited number of simultaneous tests (AO + UV) have been conducted with an acceleration factor equal to one for UV radiation and an equivalent fluence corresponding to three years at an altitude of 400 km. A 20 eV installation was used to conduct these tests on a very limited section of the samples, so that the results could be compared to tests performed in the US using a 5 eV device in other conditions on the same materials

4. BSDF/BRDF measurements have been conducted for the wavelengths 532 and 1063 nm. With this purpose, a BSDF/BRDF measuring device has been developed.

5. Measurements have been conducted of the Directed Hemispherical Reflectance (DHR) in the range 2.5—10 μm . With this purpose, modernization has been carried out of the IKS-31 spectrophotometer.

6. The test results have been entered (both in digital and in graphical form) into the Database developed previously, under ISTC Project #2342p, in Microsoft Access 2000 format.

The data obtained under this Project are the joint property of MEPhI and EOARD. The handing over of any reports and material samples to the Partner is only to be done with permission from the bodies responsible for state export control in Russia. The test data on the Sheldahl films and MAP paints will be also available to the organizations that have delivered these materials, i. e. to the companies Sheldahl and MAP respectively. Neither MEPhI nor EOARD will distribute or transmit information about the Sheldahl and MAP materials without their permission.

5. References

1. Henly E., Johnson E. Radiazionnaya khimiya. M.: Atomizdat, 1974. 415 s.
2. Pykaev A.K. Sovremennaya radiazionnaya khimiya. Osnovnie polojeniya. Experimental'naya tekhnika i metodi. M.: Nauka, 1985. 374 s.
3. Kaplan I.G. Myterev A.M. Pervichnie processi v radiazionnoi khimii i ikh osobennosti v kondensirovannoi faze. Khimiya visokikh energii. 1985. T. 19. # 3. S. 208-217.
4. Feldman V.I. Molekulyarnie mekhanizmi selectivnich effectov v radiazionnoi khimii organicheskikh i polymernich system. Vestnik Moskovskogo Universiteta. Seriya 2. Khimiya 2001. T. 42 # 3 S 194-205.
5. Feldman V.I. Selective localization of primary radiation-chemical events in solid aliphatic hydrocarbons and related polymers as evidenced by ESR. Appl. Radiat. Isot. 1996. V. 47. # 11. P. 1497-1501.
6. Gilett D. Photophysics i fotokhimiya polimerov. M.: Mir, 1988. 435 s.
7. Feldman V.I., Sukhov F.F., Slovokhotova N.A. Selectivnost' radiazionno-khimicheskikh protsessov v nizkomolekulyarnikh i polymernikh uglevodorodakh. Visokomolekulyarnie soedineniya. B. 1994. T. 36 # 3. S. 519-543.
8. Feldman V.I. Osnovi selectivnosti radiazionno-khimicheskikh processov v polymernikh systemakh. Rossiiskiy khimicheskij jurnal. 1996. T.40. # 6. S. 90-97.
9. Pykaev A.K. Sovremennaya radiazionnaya khimiya. Tverdoe telo i polymeri. Prikladnie aspecti. M.: Nauka, 1987. 448 s.
10. Radiazionnaya Khimiya makromolekul. Pod redakziy M. Doula. M.: Atomizdat, 1978. 326 s.
11. Kozlov L.V., Nusinov M.D., Akishin A.I., Zaletaev V.M., Kozelkin V.V. Modelirovanie teplovich rejimov kosmicheskikh apparatov. M.: Masinostroenie. 1971. 225 s.
12. Radiazionnaya stoikost' organicheskikh materialov. Spravochnik. Pod redakziei V.K. Milinchuka i V.I. Tupikova. M. Energoatomizdat, 1986. 171 s.
13. Milinchuk V.K., Klinshpont E.R., Tupikov V.I. Osnovi radiazionnoi stoikosti organicheskikh materialov. M. Energoatomizdat, 1994. 251 s.

Appendix 1

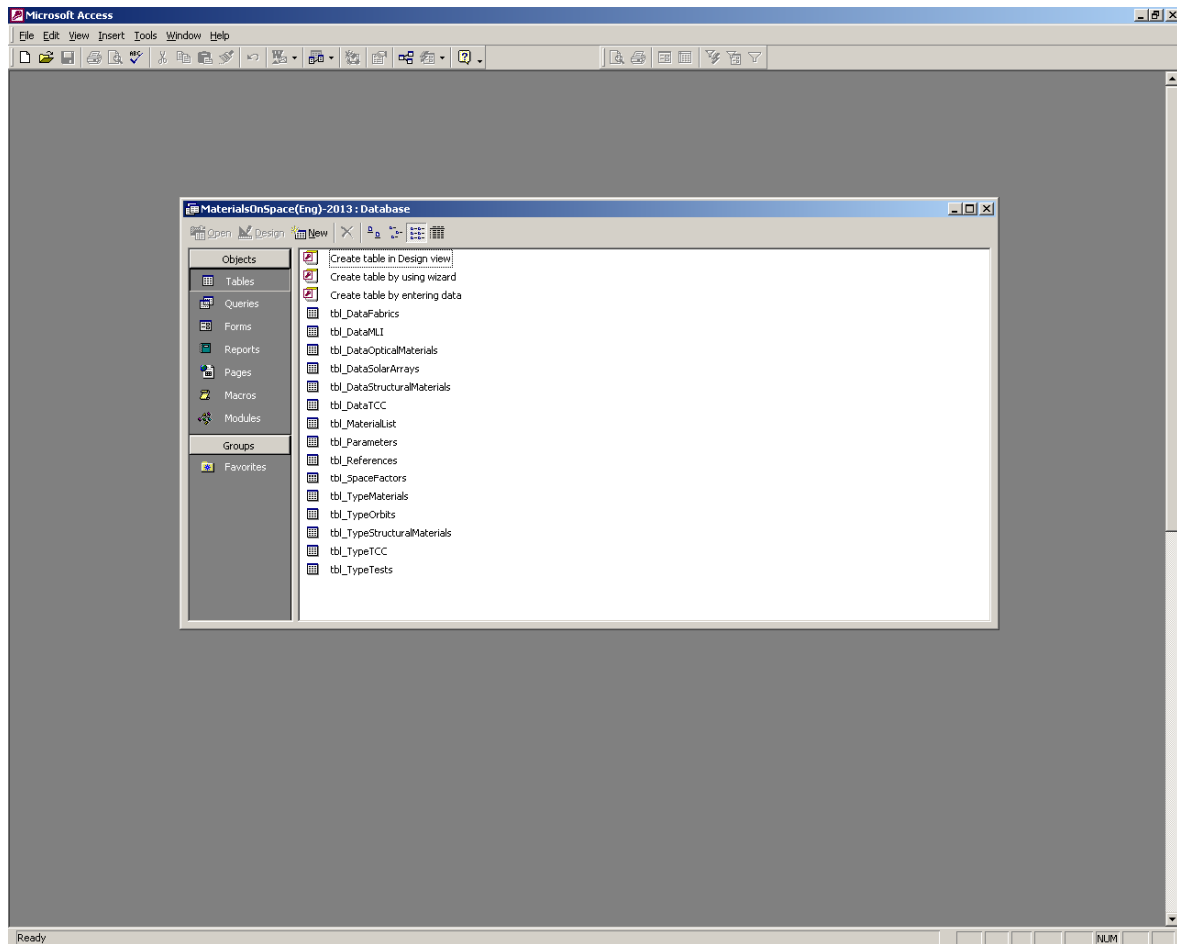


Figure 1

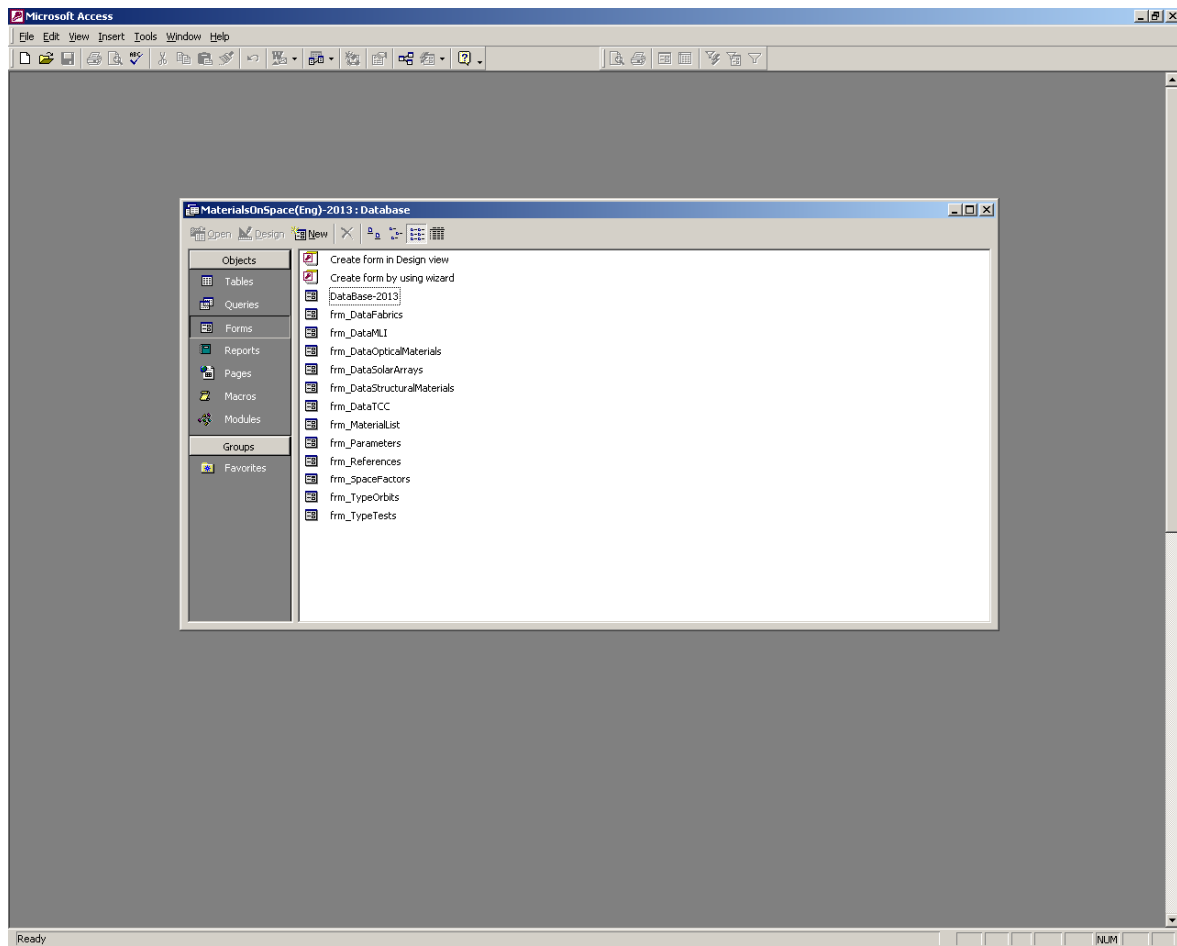


Figure 2

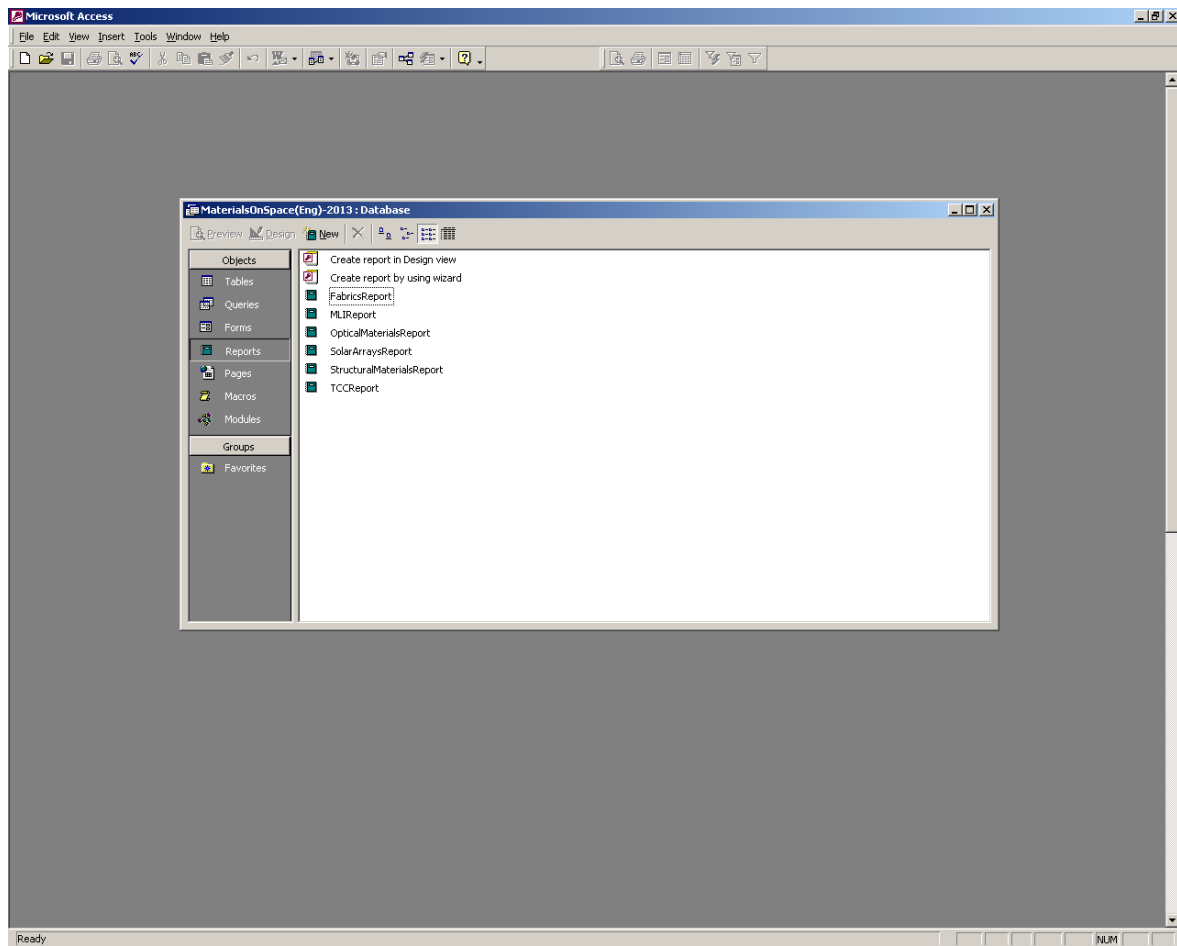


Figure 3

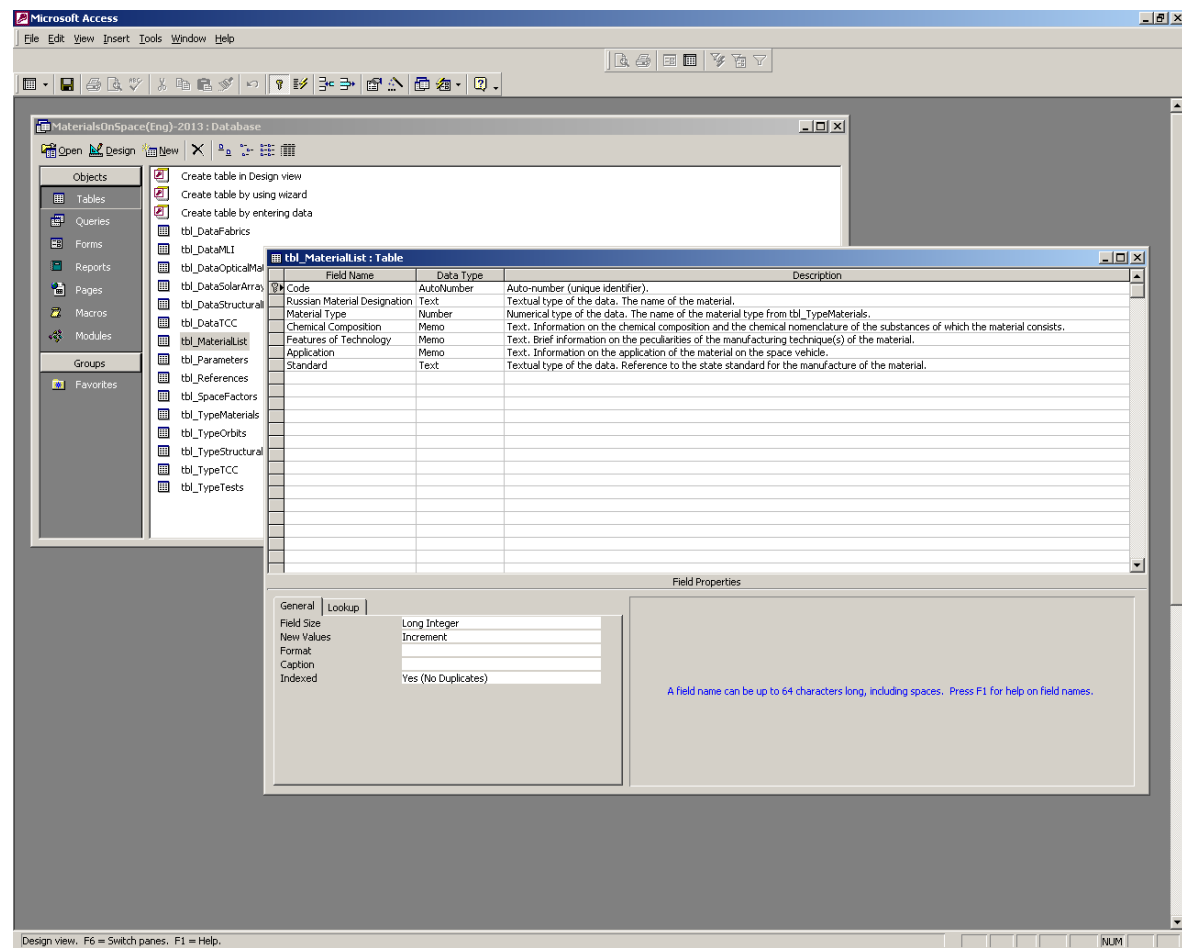


Figure 4

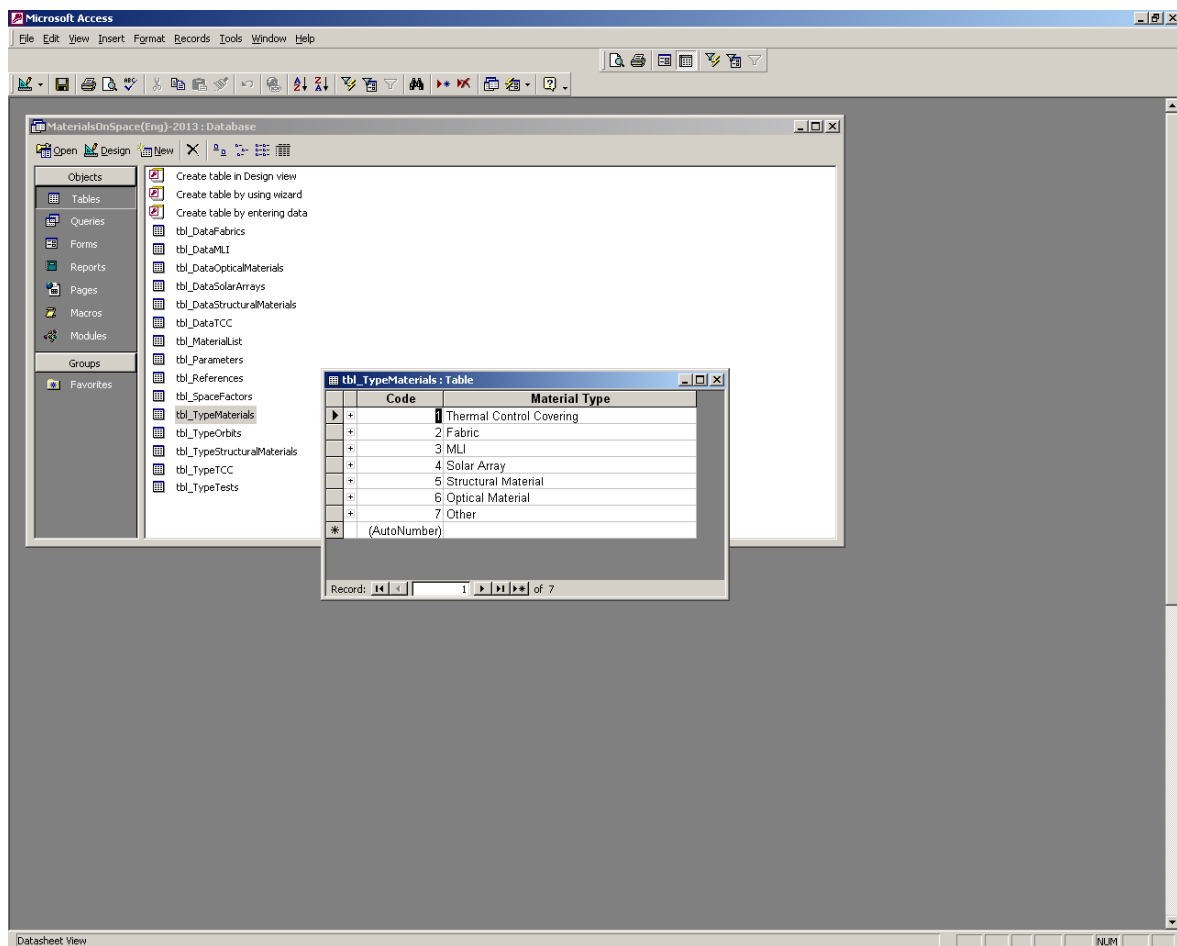


Figure 5

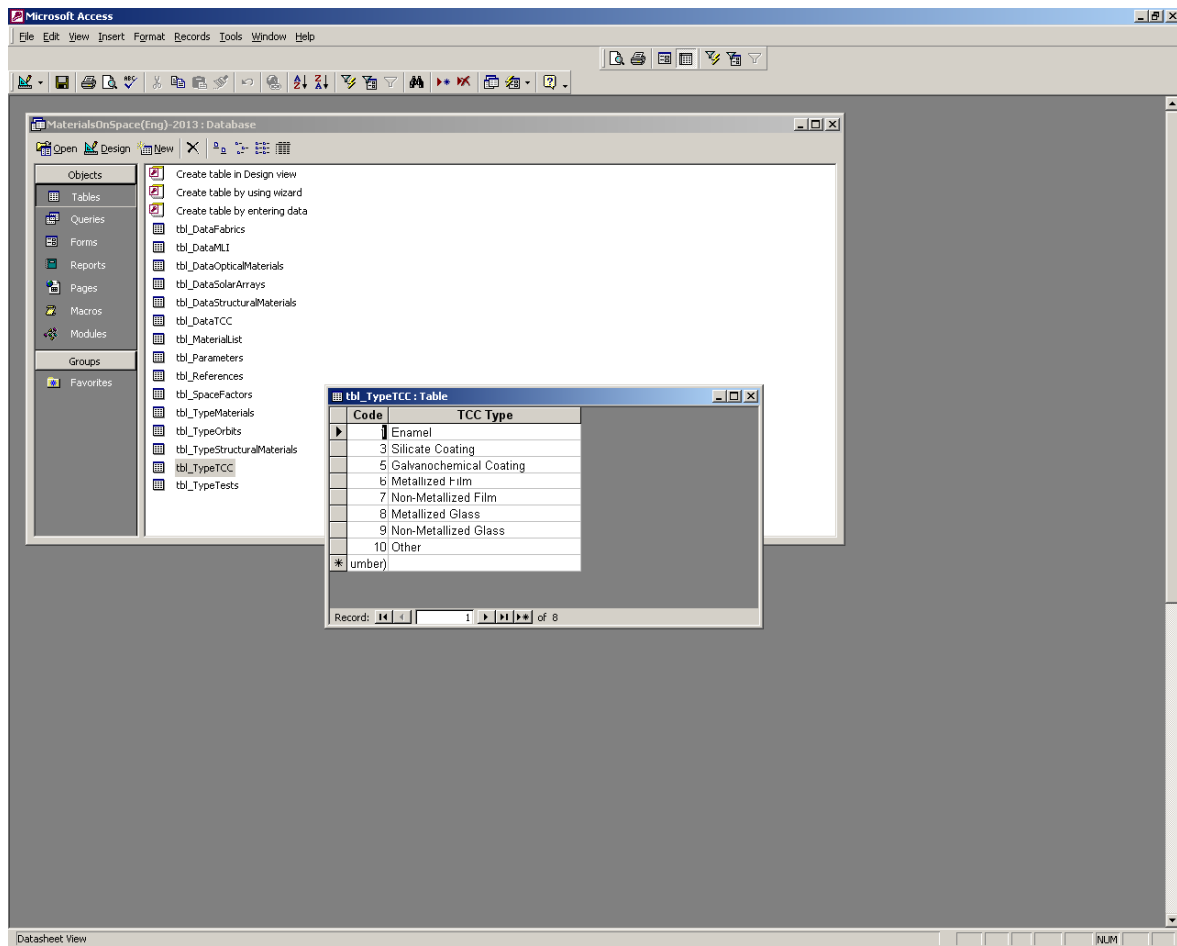


Figure 6

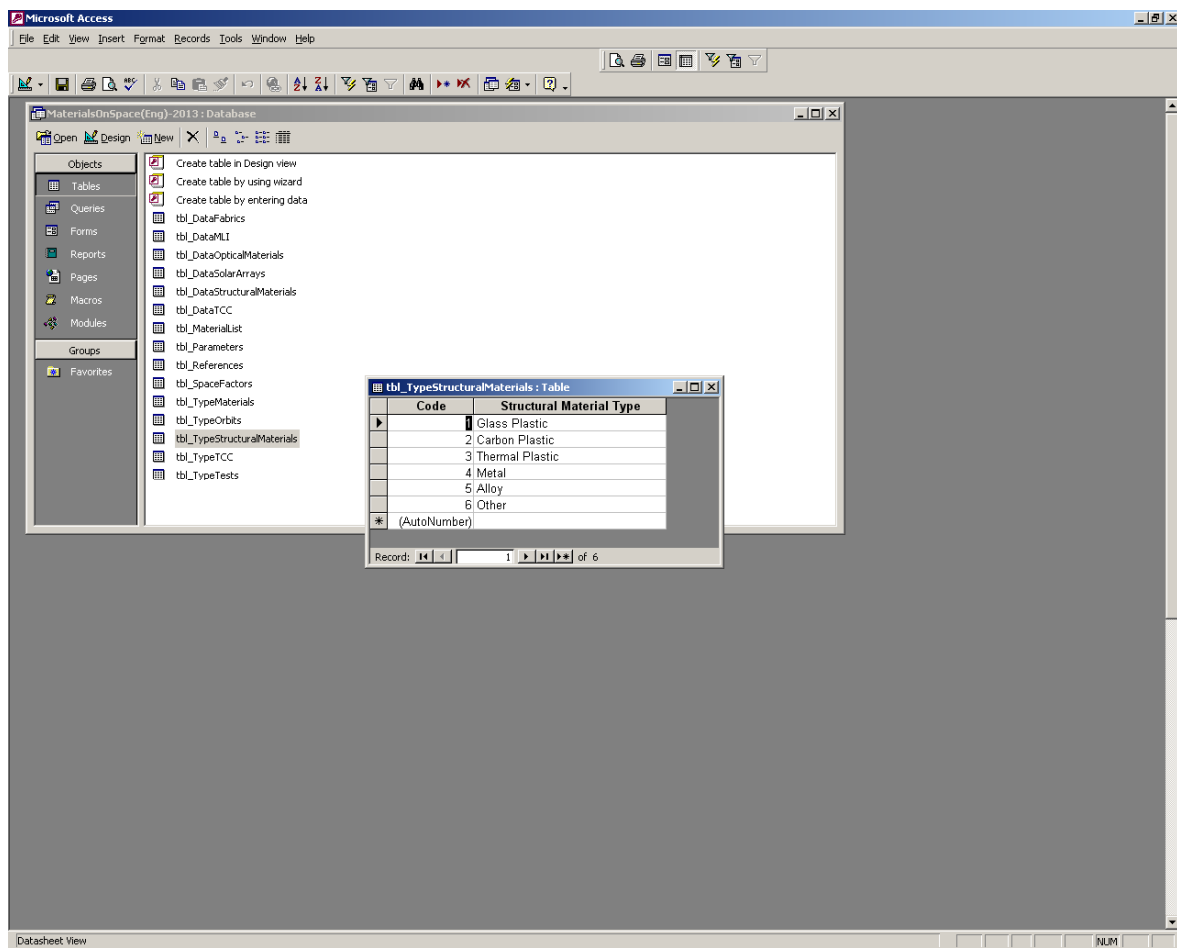


Figure 7

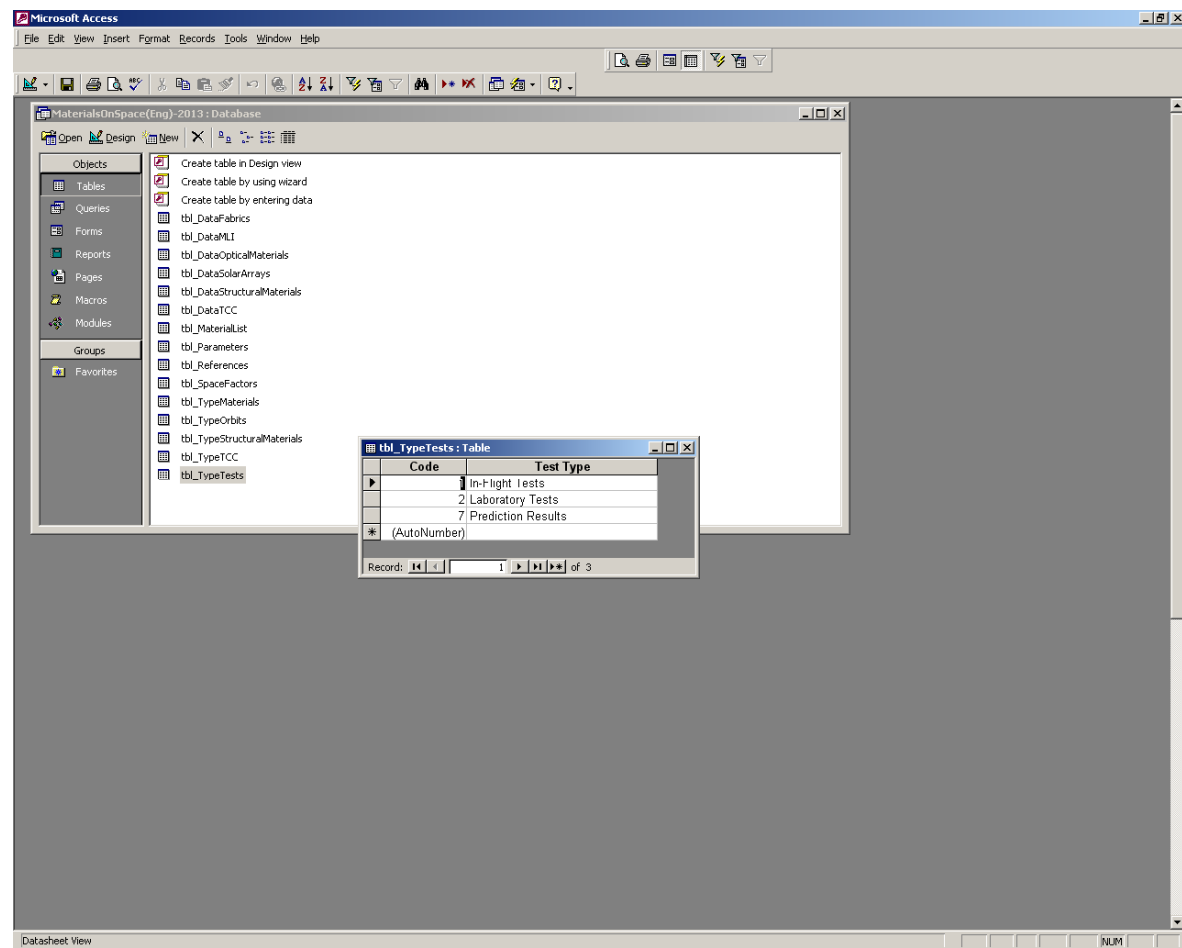


Figure 8

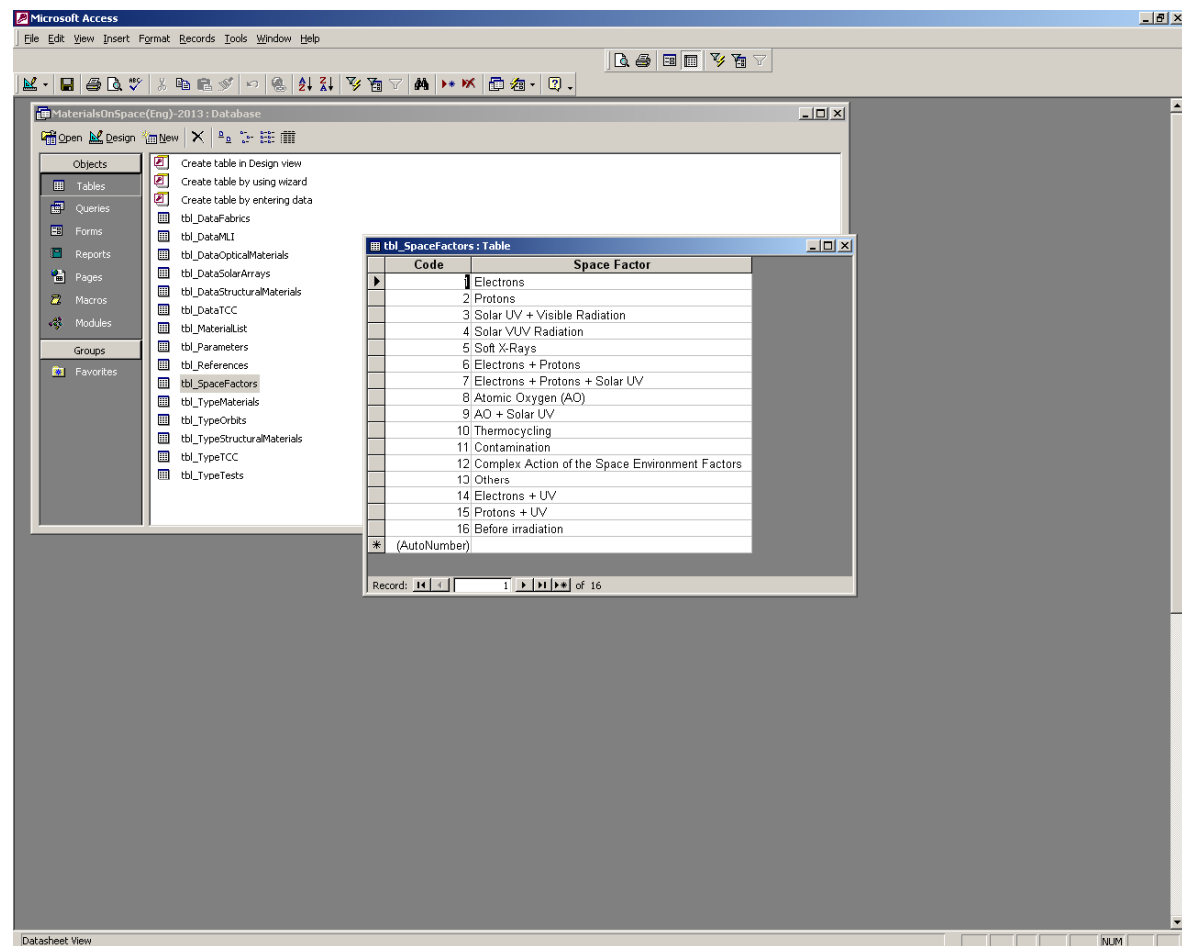


Figure 9

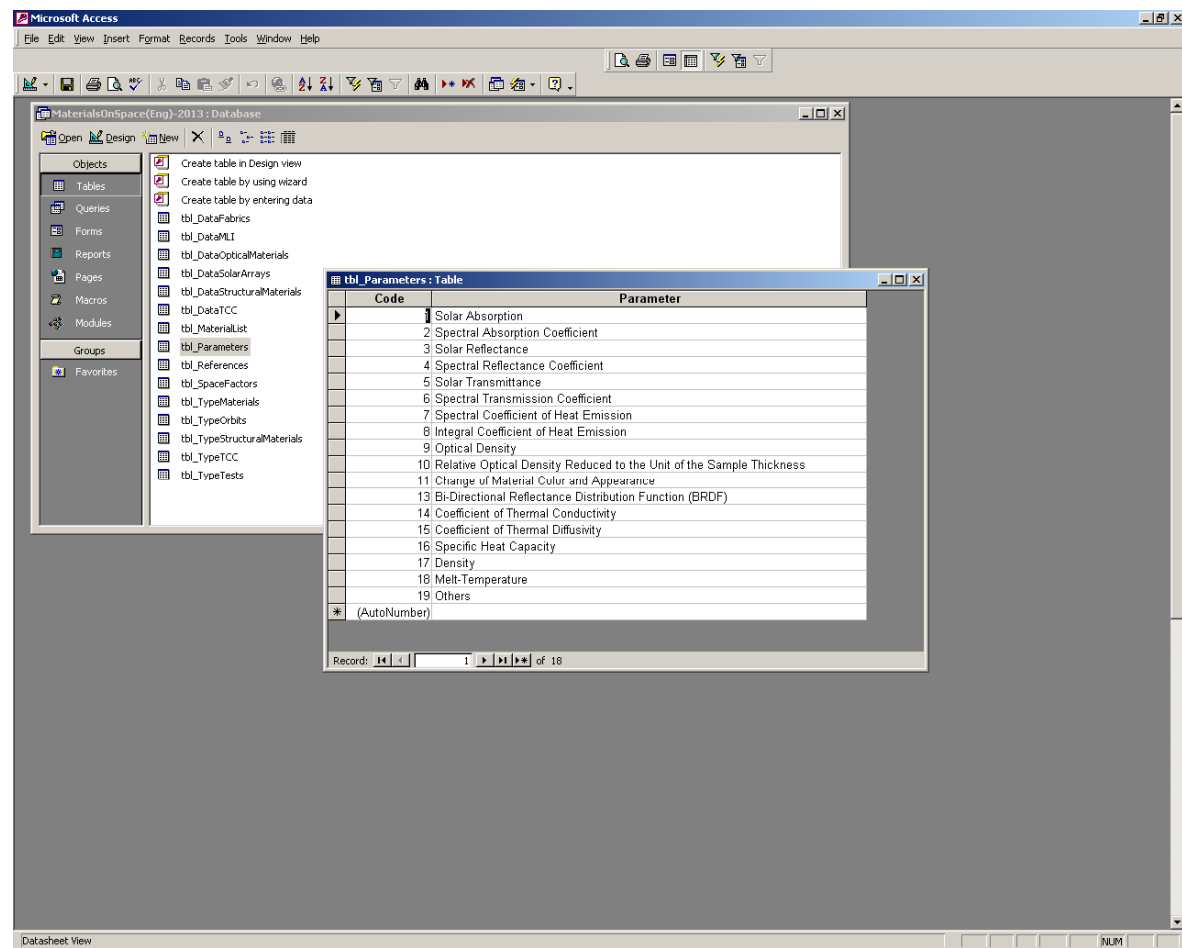


Figure 10

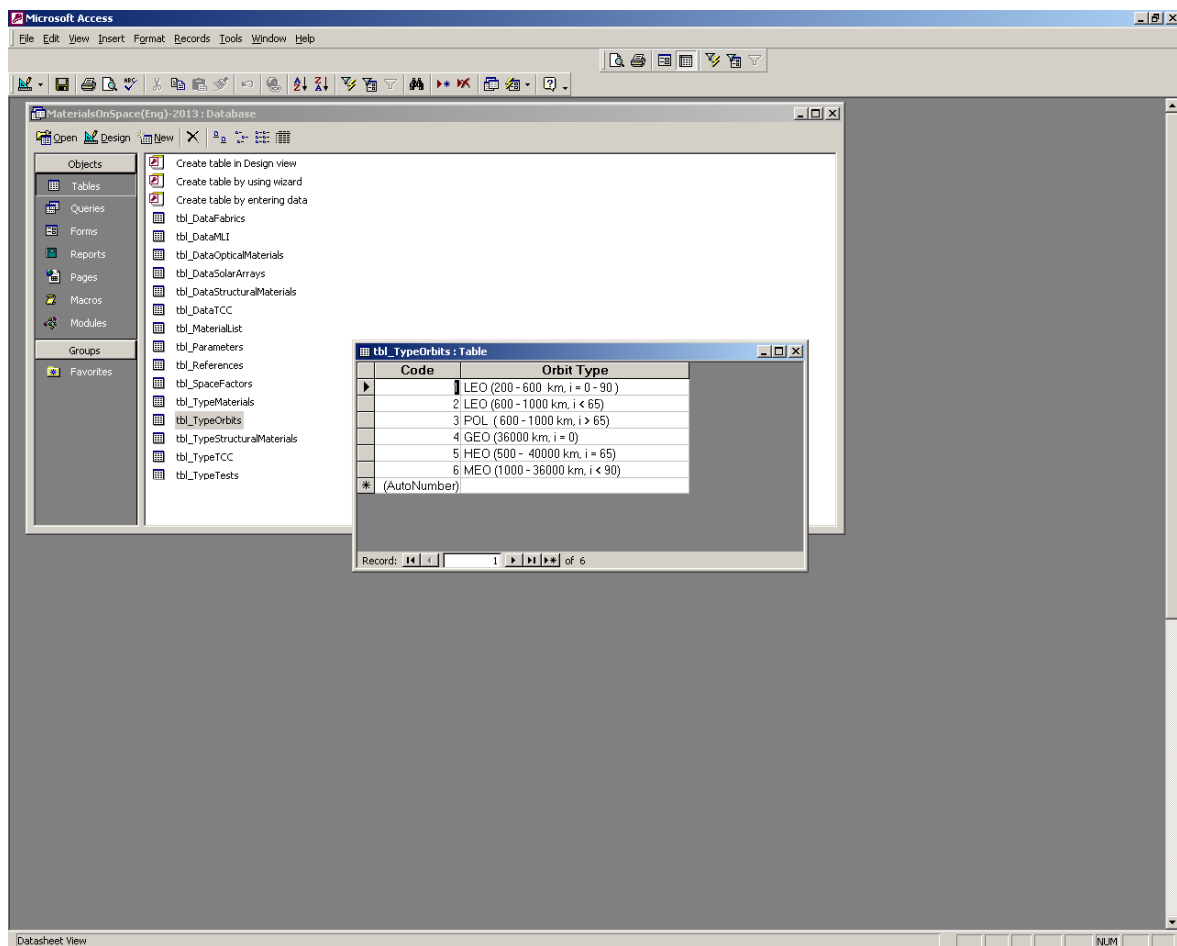


Figure 11

Cod	Authors	Name	Name English
22	Dvoretzky M. I., Mikhailov M. M., Kositsyn L. G. et al.	Issledovaniye spektrov otrazheniya beloi emali, obluchennoi razdel'no i sovместno elektronami, pr	Study of the Reflection Spectra i
23	Malov M. M., Chetverikov A. N., Solov'yev G. G. et al.	Izmeneniye opticheskikh svoystv TRP na osnove oksii tsinka pod vozddeystviyem protonnogo izluchi	Changes of the Optical Propertie
24	Malov M. M., Chetverikov A. N., Abramova R. I. et al.	Vliyaniye UF-izlucheniya na opticheskiye svoystva poroshkov oksii tsinka, perspektivnykh dlya so	Influence of UV Radiation on the
29	Barbashev E. A., Bogatov V. A., Kozin V. I. et al.	Vliyaniye elektronno-protonnogo oblucheniya v vakuumе na opticheskiye svoystva TRP.	Influence of Electron-Proton Irrac
132	Shavarin Yu. Ya., Blinova S. L., Abyzov N. M. et al.	Simulation Tests of Polymeric Materials Intended for Long-Term Spacecraft Missions in Radiation	
133	Final Technical Report.	Research Program for Radiation Stability of the Aerospace Materials - Transfer of the Karpov Instit	
136	Novitsky P. A., Stepanov B. M.	Opticheskiye svoystva materialov pri nizkikh temperaturakh. Spravochnik.	Optical Properties of Materials a
137	Voitsenya V. S., Guzhova S. K., Titov V. I.	Vozdeystviye nizkotemperaturnoi plazmy i elektromagnitnogo izlucheniya na materialy.	Action of Low-Temperature Plas
78	Akishin A. I., Grigoryeva G. M., Zvyagina K. N. et al.	Issledovaniye rabotosposobnosti fotoprebrazovatelei s kontsentratorami v usloviyakh vozddeystviya	Study of the Efficiency of Solar A
79	Akishin A. I., Grigoryeva G. M., Zvyagina K. N.	Degradatsiya opticheskikh svoystv vneshei poverkhnosti SB. Naturniye i nazemniye ispytaniya.	Degradation of the Optical Prope
80	Demidov S. A., Rekant N. B., Kuz'minsky L. I.	Ekspериментальное исследование полусферической отражательной способности технических ма	Experimental Study of the Hemi
81	Romanov B. S., Markus A. M., Udovenko V. F. et al.	Vliyaniye oblucheniya protonami s energiyey do 200 keV na strukturniye i ekspluatatsionniye svoi	Influence of Proton Irradiation wit
84	Knefts K. F., Trofimova A. A., Galkina N. S. et al.	Spektral'niye svoystva metallizirovannykh PETF-plenok.	Spectral Properties of Metallizec
87	Gavrilova I. P., Groshkova G. N., Koltun M. M.	Effektivnost' teploizluchayushchikh pokrytii s peremennoi stepenyu chernoty.	Efficiency of Heat-Radiating Coa
85	Kolchenogova I. P.	Osobennosti opredeleniya radiatsionnykh kharakteristik tkanei.	Peculiarities of Determining the I
86	Gorodetsky A. A., Demidov S. A., Ivanchenko A. S. et al.	Issledovaniye termoreguliruyushchikh pokrytii na orbital'noi kosmicheskoi stantsii "Salyut-6."	Study of the Thermal Control Co
91	Akishin A. I., Bessonova T. S., Berbash N. V. et al.	Vliyaniye korpuskulyarnykh izlucheni na opticheskiye materialy.	Influence of Corpuscular Radiat
93	Tsaplin S. V., Rutner J. F., Konnov A. V. et al.	The Kinetic Model of Thermal Control Coatings Degradation by Action of Ultraviolet Radiation and	
94	Tsaplin S. V., Rutner J. F., Kharkovskii S. I.	The Kinetic Model of Change of Reflectability of Thermoregulating Covers by Action of Ultraviolet	
96	Tenditnyi V. A., Smirnov-Vasiliev K. G., Yevkin I. V. et al.	Laboratory and In-Flight Tests of Spacecraft Thermal Control Coating Degradation.	
98	Barbashev E. A., Bogatov V. A., Deev I. S. et al.	The Contribution of Different Factors of a Space Environment in the Conditions of Low-Earth Orbit	
99	Kuznetsov V. N.	Beryllium Oxide as an Advanced Material for Vacuum Light-Reflecting Coatings in the 6 - 0.5 eV R	
100	Kuznetsov V. N., Lisachenko A. A., Prudnikov I. M. et al.	Comparative Studying of the UV Induced Reflectivity Degradation of the Al-Oxide Anodic Films an	
101	Vdovenko N., Kuznetsov V., Lisachenko A.	Changes in the Reflectivity of Finally Divided ZnO on Vacuum Heat Treatment.	
105	Naumov S. F., Gorodetsky A. A., Demidov S. A.	Research of Thermal Control Coating Optical Characteristics during Long-Term Near Earth Orbital	
108	Naumov S., Demidov S., Sokolova S. et al.	Atomic Oxygen Ground and MIR Flight Testing of Polyimide Films with Various Protective Coatin	
113	Vasilyev V. I., Dvoretzky M. I., Ignatyev V. N. et al.	Imitatsiya kompleksnogo vozddeystviya kosmicheskikh izlucheni na termoreguliruyushchiye pokryt	Simulation of the Complex Actio
114	Pankratova L. N.	IK-spektry i gibkost' svyazei Si-O-Si v poliorganosiloksanakh.	Infrared Spectra and the Flexibili
115	Malov M. M., Chetverikov A. N., Rabukhin A. I. et al.	Opticheskiye svoystva poroshkov oksii tsinka, legirovannykh litiyem.	Optical Properties of Zinc Oxide
138	Project 2342p		
122	Leksin A. N., Agafontsev V. F.	Vliyaniye khimicheskoi obrabotki na opticheskiye svoystva poroshkov oksida tsinka "nitevidnye kr	Effects of Chemical Processing
124	Yagushkin N. I., Grafodatsky O. S., Islyayev Sh. N. et al.	Radiatsionno-elektricheskiye yavleniya v materialakh kosmicheskikh apparatov pri elektrizatsii.	Radiation-Electrical Phenomena
125	Mikhailov M. M., Dvoretzky M. I., Bulanakov Yu. K. et al.	Issledovaniye zavisimosti koeffitsienta pogloshcheniya solnechnoi radiatsii TRP ot intensivnosti po	Study of the Dependence of the
126	Koltun M. M.	Optika i metrologiya solnechnykh elementov.	Optics and Metrology of Solar A
117	Akishin A. I., Guzhova S. K., Tarasov Yu. I.	Modelirovaniye vozddeystviya ionosfery zemli i solnechnogo vetra na materialy vneshei poverkhn	Modeling the Action of the Ionos
118	Vasilyev V. N., Dvoretzky M. I., Kozelkin V. V. et al.	Modelirovaniye vozddeystviya luchistogo potoka Solntsa na termoreguliruyushchiye pokrytiya.	Modeling the Action of the Radia
116	Pankratova L. N., Titov V. I., Goryachev A. N.	Spektrokhimicheskoye izucheniye deystviya izlucheniya na poliorganosiloksany, soderzhashchiye	Spectrochemical Study of the Av
128	Barbashev E. A., Dushin M. I., Ivonin Yu. N. et al.	Nekotoryye rezultaty ispytaniy polimernykh materialov posle ekspozitsionirovaniya v usloviyakh otkryto	Some Test Results for Polymer
129	Pankratova L. N., Goryachev A. N., Zhelezniyova M. V. et al.	Izucheniye deystviya izlucheni na poliorganosiloksany, soderzhashchiye silafluorenilnye zvenya.	Study of the Action of Various T
130	Pankratova L. N.	Ob otsenke radiatsionnoi stoikosti poliorganosiloksanov.	On Estimating the Radiation Sta
131	Zhukova-Khovanskaya O. B., Artyukhin Ye. A., Barantsevich V.	Metody i algoritmy identifikatsii radiatsionnykh kharakteristik termoreguliruyushchikh pokrytii po	Methods and Algorithms of Ident
17	Koshelyayev V. M., Kudrin A. I.	TRP s optimizatsiyey po spektru.	TCCs Optimized for Spectral Pro
139	Project 3806p		
139	Project 3806p		

Figure 12

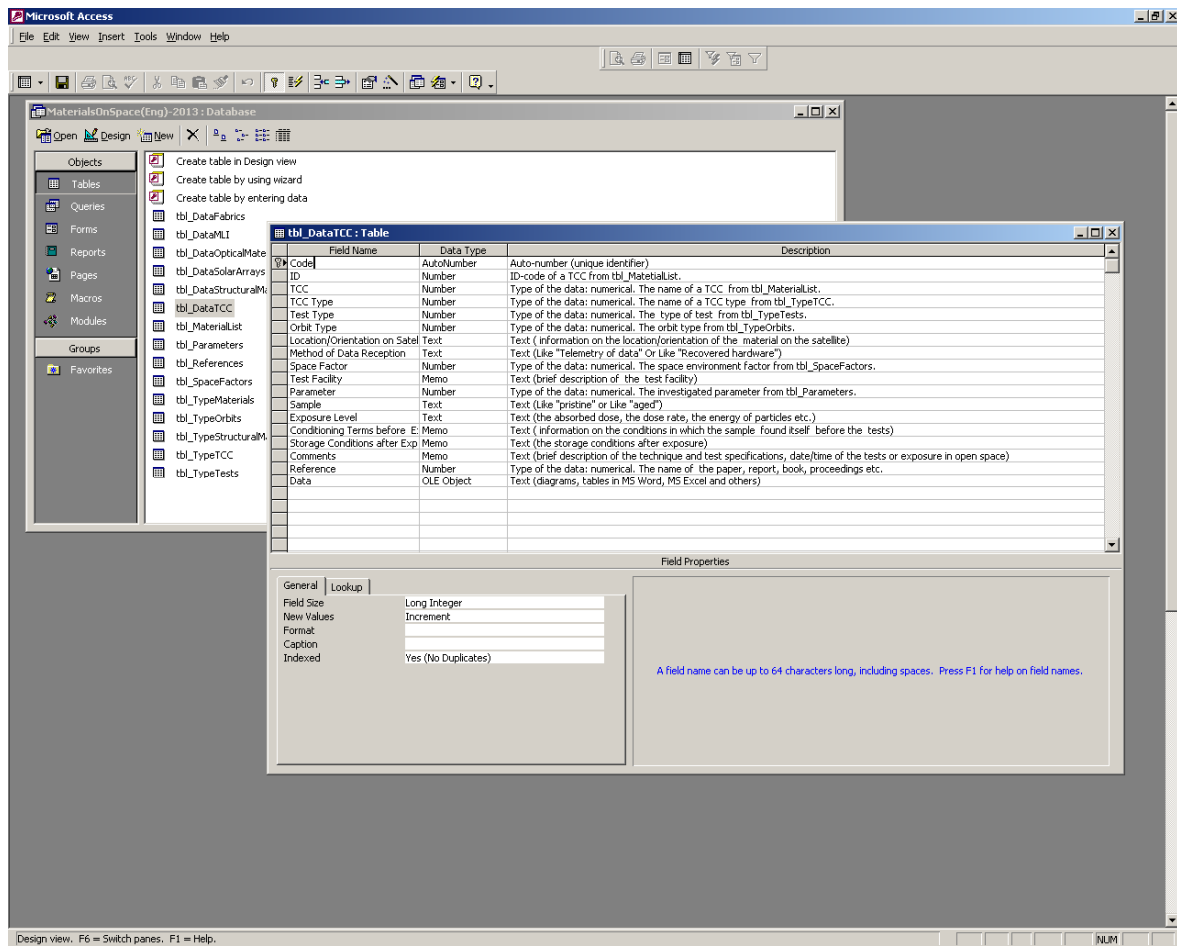


Figure 13

Microsoft Access

File Edit View Insert Format Records Tools Window Help

MaterialsOnSpace(Eng)-2013 : Database

Open Design New

Objects

- Tables
- Queries
- Forms
- Reports
- Pages
- Macros
- Modules
- Groups
- Favorites

Create form in Design view

Create form by using

- DataBase-2013
- frm_DataFabrics
- frm_DataMLI
- frm_DataOpticalMe
- frm_DataSolarArra
- frm_DataStructure
- frm_DataTCC
- frm_MaterialList
- frm_Parameters
- frm_References
- frm_SpaceFactors
- frm_TypeOrbits
- frm_TypeTests

TCC

TCC: PCBE Conductive White Paint

TCC Type: Enamel

Test Type: Laboratory Tests

Orbit Type:

Location/Orientation on Satellite:

Method of Data Reception:

Space Factor: Electrons

Energy and Fluence Level: 100 keV, 6E11 e/cm2s, 2E16 e/cm2

Test Facility: electron accelerator at MIFI

Parameter: Change of Material Color and Appearance

Sample: aged

Conditioning Terms before Exposure: vacuum

Storage Conditions after Exposure: air

Comments:

1 2

PCBE (Conductive White Paint)
(1) - original, (2) - after electron irradiation. $E_e=100$ keV,
flux - 6×10^{11} e/cm²s, fluence - 2×10^{16} e/cm²

Project 3806p

Reference >>

Record: 1646 of 1647

Number (unique identifier of a TCC material from tbl_Material)

Figure 14

MaterialsOnSpace(Eng)-2013 : Database

MLI

MLI: ITO 2.0MIL Kapton Aluminum film

Test Type: Laboratory Tests

Orbit Type:

Location/Orientation on Satellite:

Method of Data Reception:

Space Factor: Electrons + Protons + Solar UV

Energy and Exposure Level: 3 year at GEO

Test Facility: UV-1/2 at Komposit

Parameter: Solar Absorption

Sample: aged

Conditioning Terms before Exposure: vacuum

Storage Conditions after Exposure: air

Comments:

E_p=50 keV (5E10 p/cm²), E_e=50 keV (5E11 e/cm²), 3 e.s.i.
 Electron and proton irradiation was carried out in discrete mode. Average flux density equaled 5E7 p/cm²s and 4.6E8 e/cm²s.
 In order to measure a change in solar absorptance, the sample was extracted into the air. Having been measured, the sample was placed into a vacuum testing chamber, and the irradiation continued until the next value exposure was reached. The given sample was used after irradiation for measuring spectral characteristics.

Solar absorptance α_s for ITO/2.0 mil Kapton/WO A during combined irradiation (electrons + protons + UV solar radiation)

Φ_p , e/cm ²	Φ_e , p/cm ²	Hs, e.s.h	T, hours	α_s
0	0	0	0	0.437
4.10 $\times 10^{16}$	3.34 $\times 10^{18}$	1739	580	0.553
8.55 $\times 10^{16}$	6.60 $\times 10^{18}$	3544	1181	0.627
1.24 $\times 10^{17}$	9.68 $\times 10^{18}$	5239	1746	0.652
1.71 $\times 10^{17}$	1.29 $\times 10^{19}$	7035	2345	0.679
2.17 $\times 10^{17}$	1.61 $\times 10^{19}$	8761	2920	0.701

Φ_p is the proton fluence, Φ_e is the electron fluence, Hs is the equivalent solar exposure (equivalent solar hours), T is the irradiation time.

Project 3806p

Reference

Record: 557 of 558

Figure 15

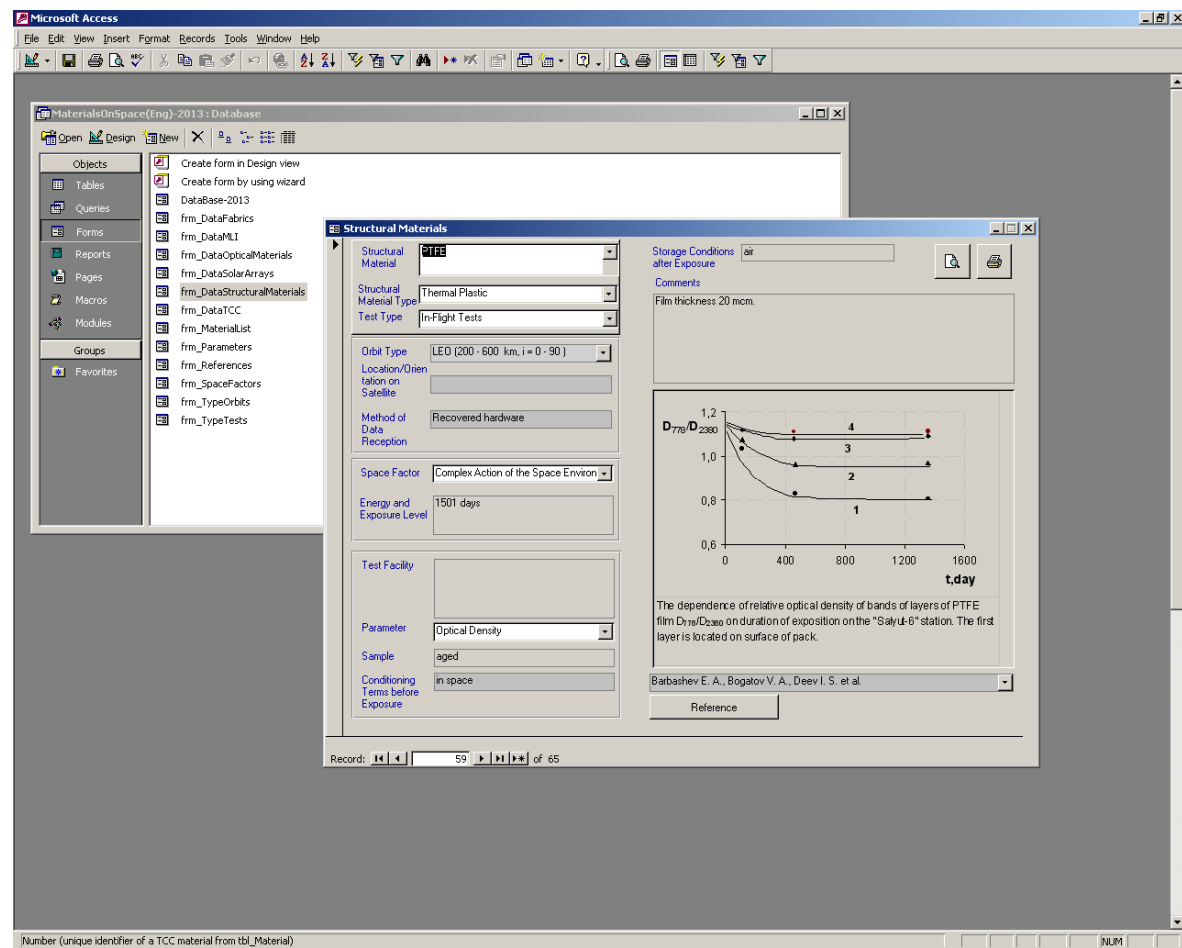


Figure 16

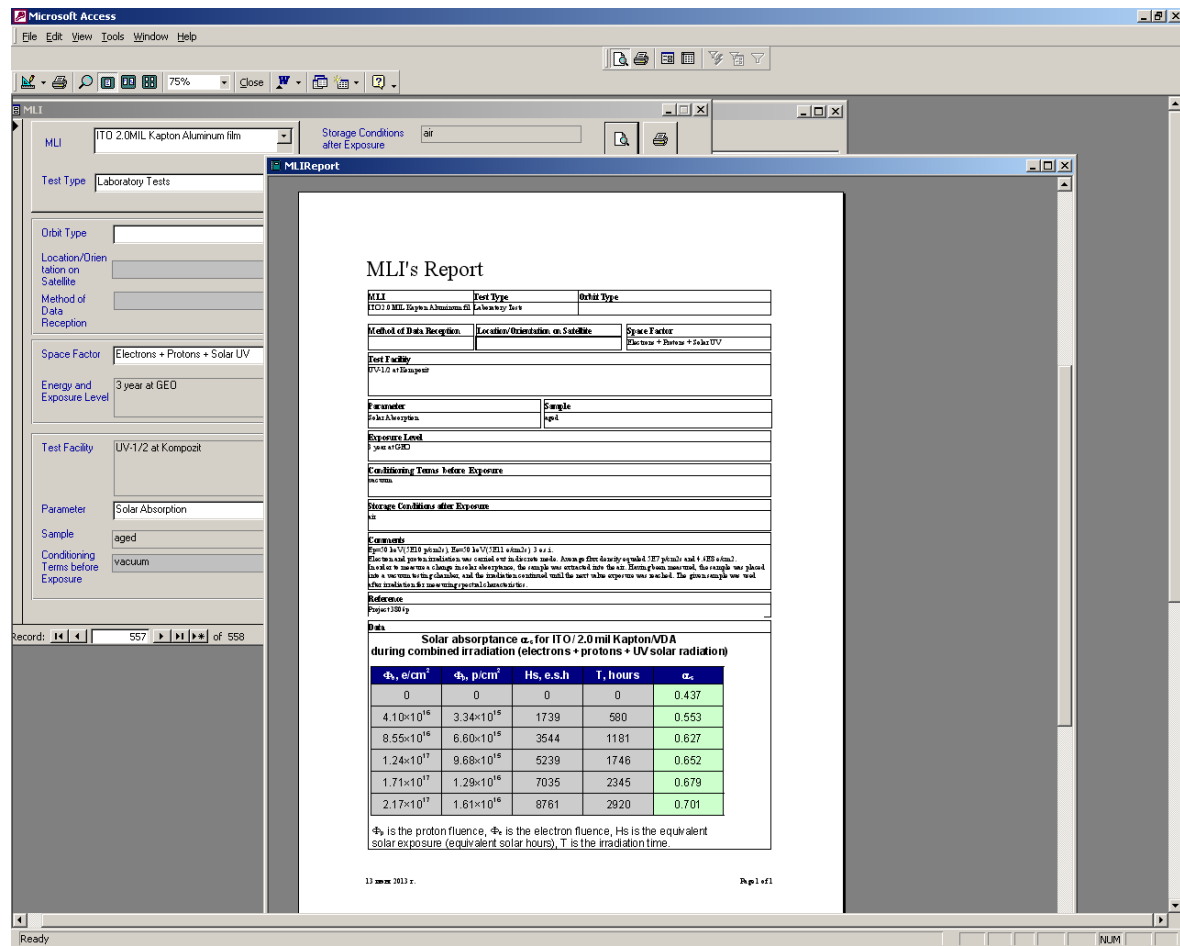


Figure 17



Figure 18

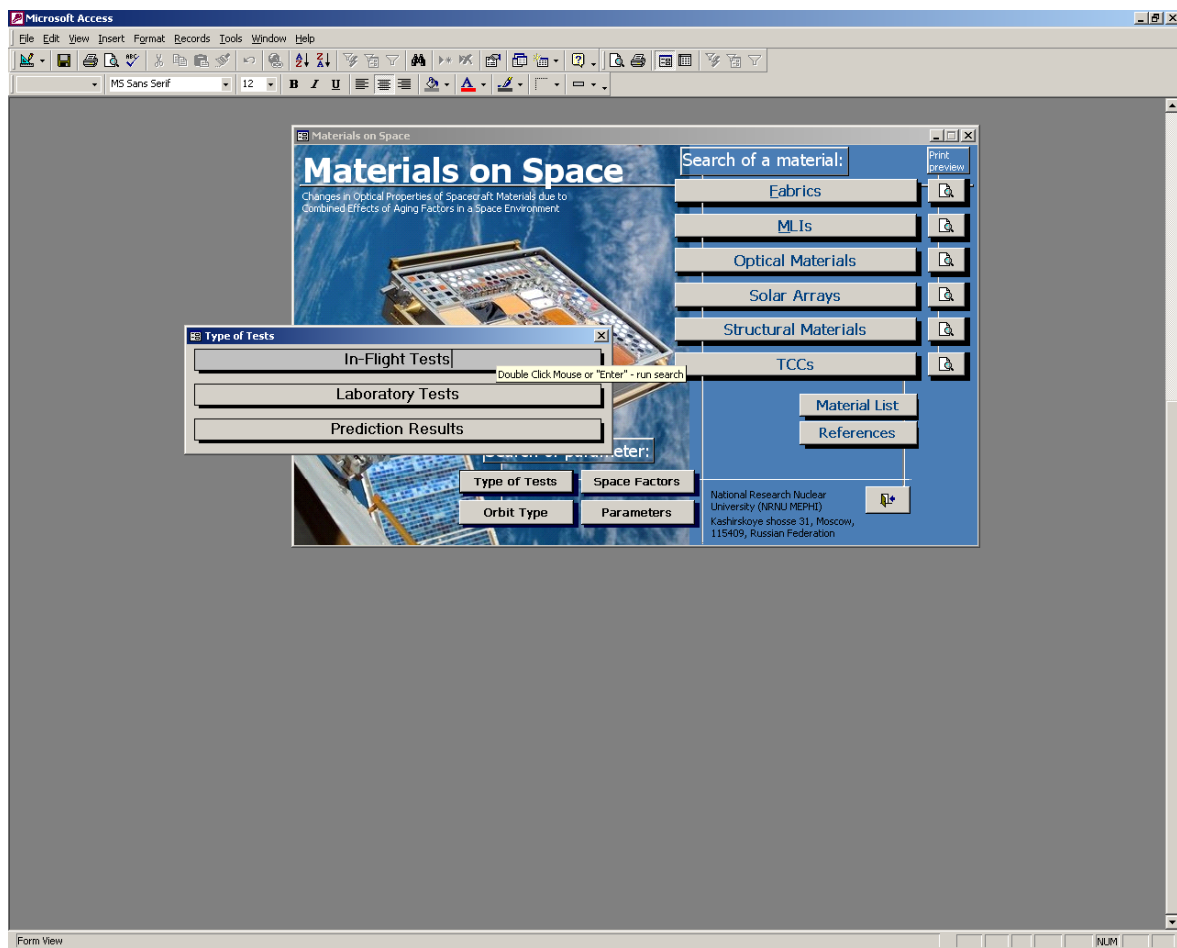


Figure 19

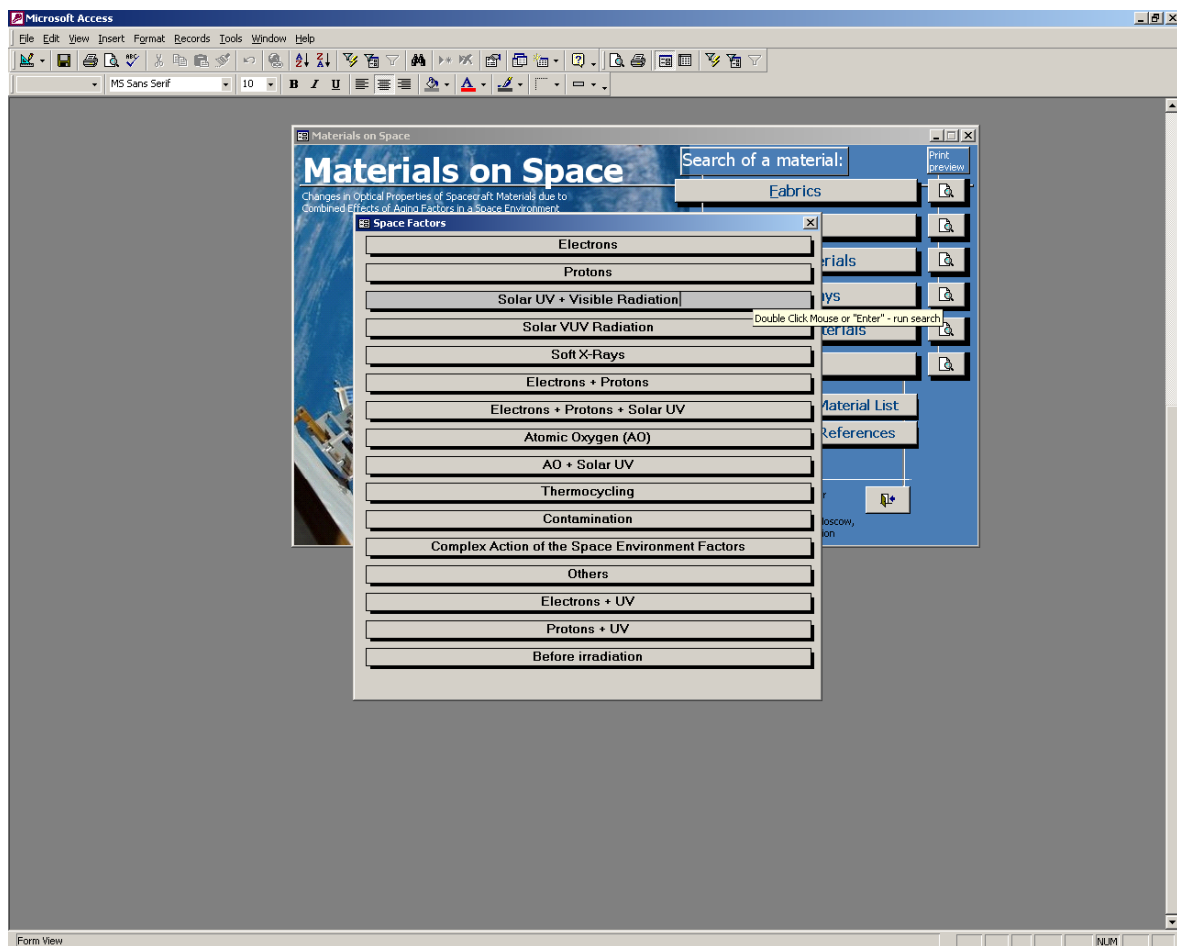


Figure 20

The screenshot shows a Microsoft Access database window titled 'Materials on Space'. The window is in 'Form View' and displays a search interface. At the top, there is a search bar labeled 'Search of a material:'. Below the search bar is a list of material parameters, each with a corresponding input field. The parameters are:

- Solar Absorption
- Spectral Absorption Coefficient
- Solar Reflectance
- Spectral Reflectance Coefficient
- Solar Transmittance
- Spectral Transmission Coefficient
- Spectral Coefficient of Heat Emission
- Integral Coefficient of Heat Emission
- Optical Density
- Relative Optical Density Reduced to the Unit of the Sample Thickness
- Change of Material Color and Appearance
- Bi-Directional Reflectance Distribution Function (BRDF)
- Coefficient of Thermal Conductivity
- Coefficient of Thermal Diffusivity
- Specific Heat Capacity
- Density
- Melt-Temperature
- Others

On the right side of the form, there is a 'Print preview' button and a 'Material List' button. A tooltip is visible over the 'Material List' button, stating 'Double Click Mouse or "Enter" - run search'. The bottom status bar indicates 'Form View' and '9/9/01'.

Figure 21

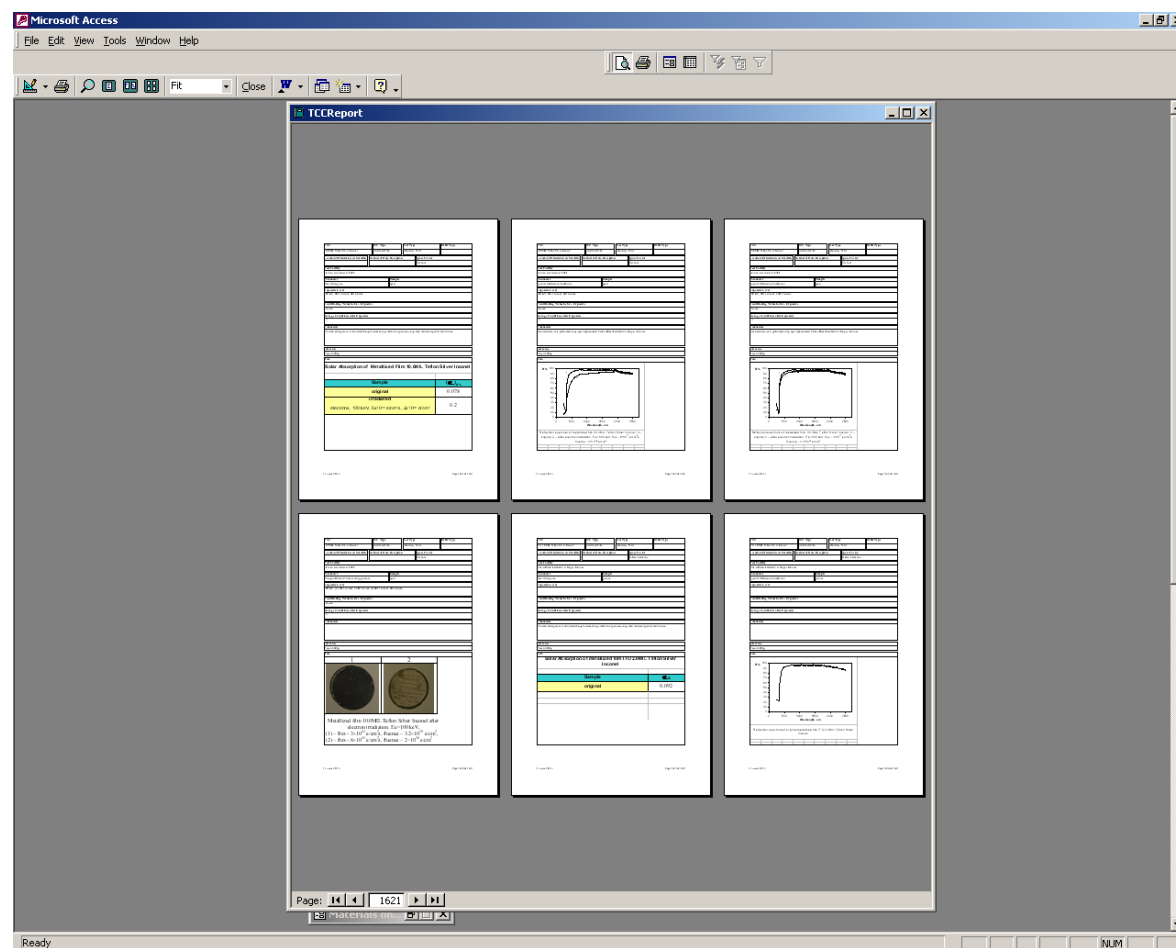


Figure 22

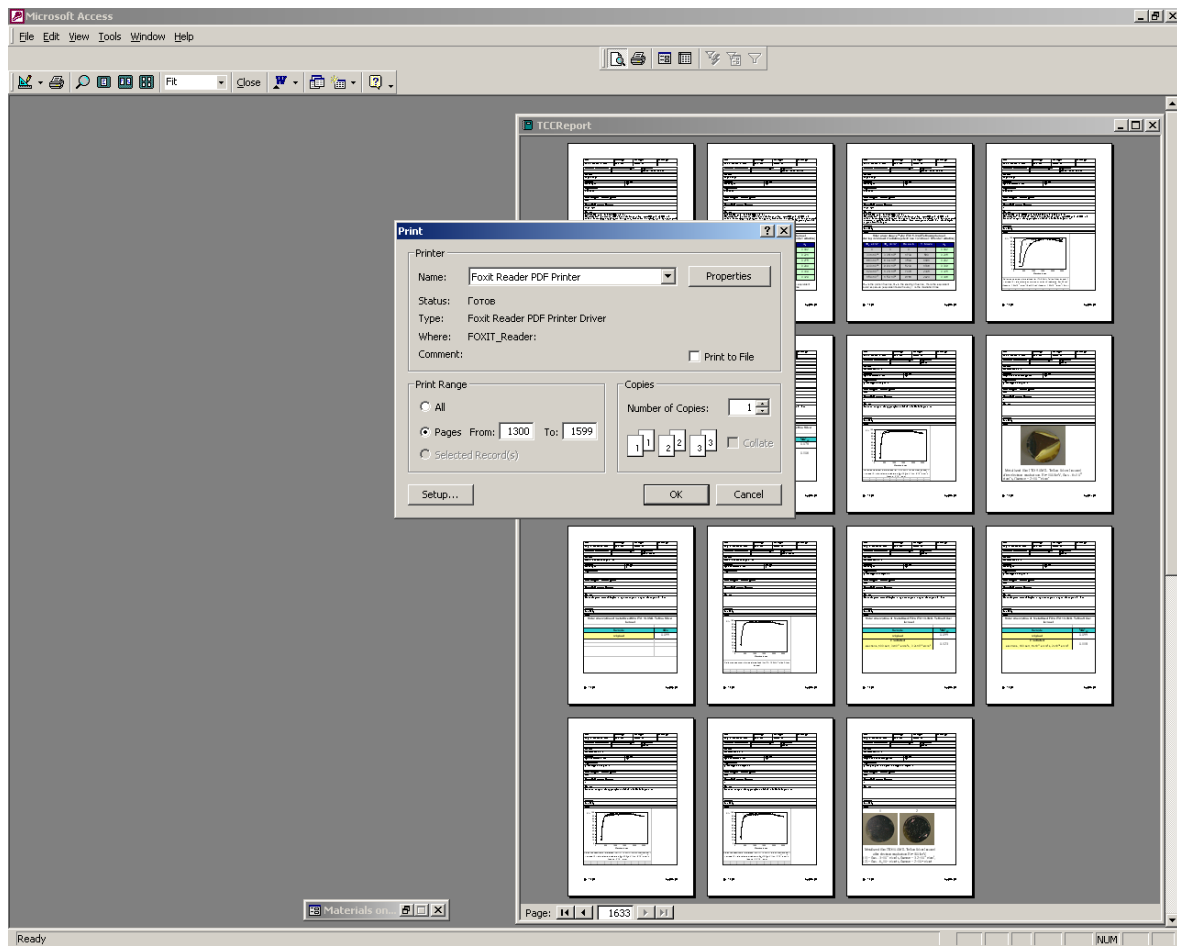


Figure 23

Appendix 2

Shown in Fig. 1 are the reflectance spectra of the reference samples, measured on the Cary 500 spectrophotometer, which were afterwards used in the measurements of the irradiated samples on the FM-59M photometer.

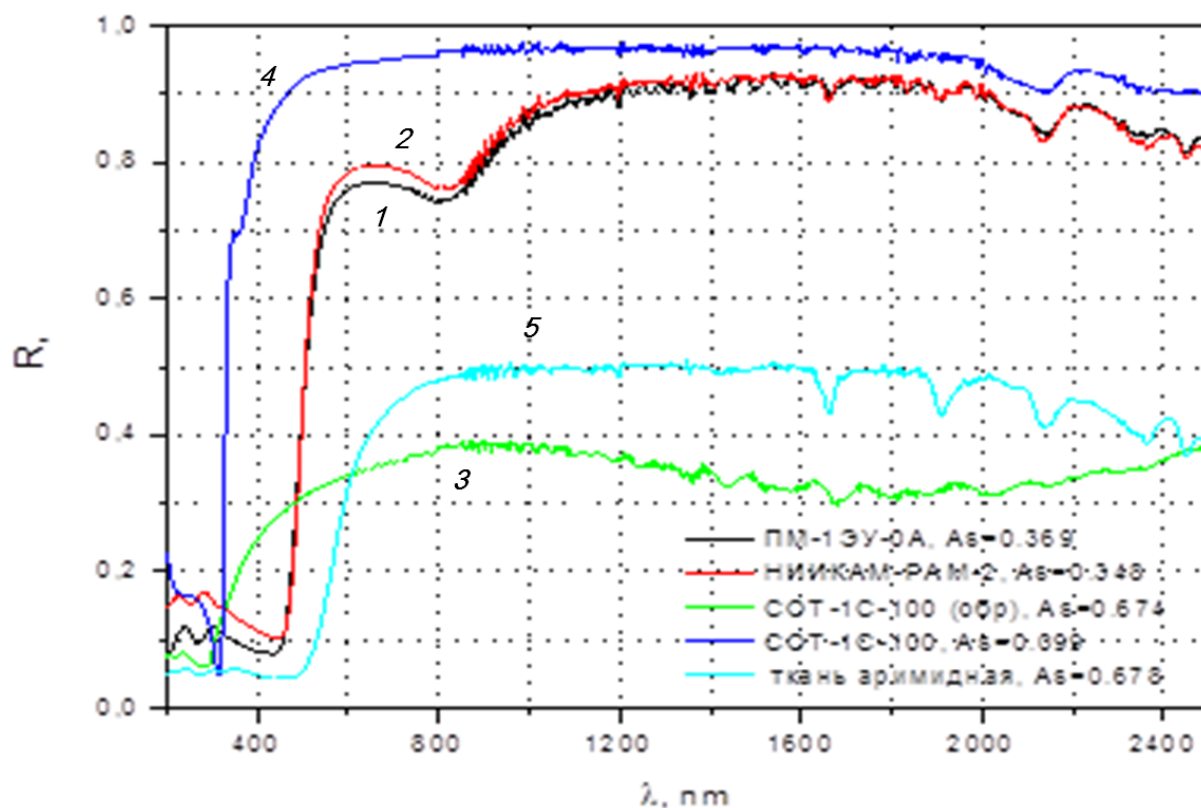


Figure 1. Spectrum of reference samples.

Curve 1 – PM-1EU-OA; Curve 2 – NIIKLAM-RAM-2; Curve 3 – SOT-1-S-100 (back); Curve 4 – SOT-1-S-100 (face); Curve 5 – Arimide frame fabric (article 56420)

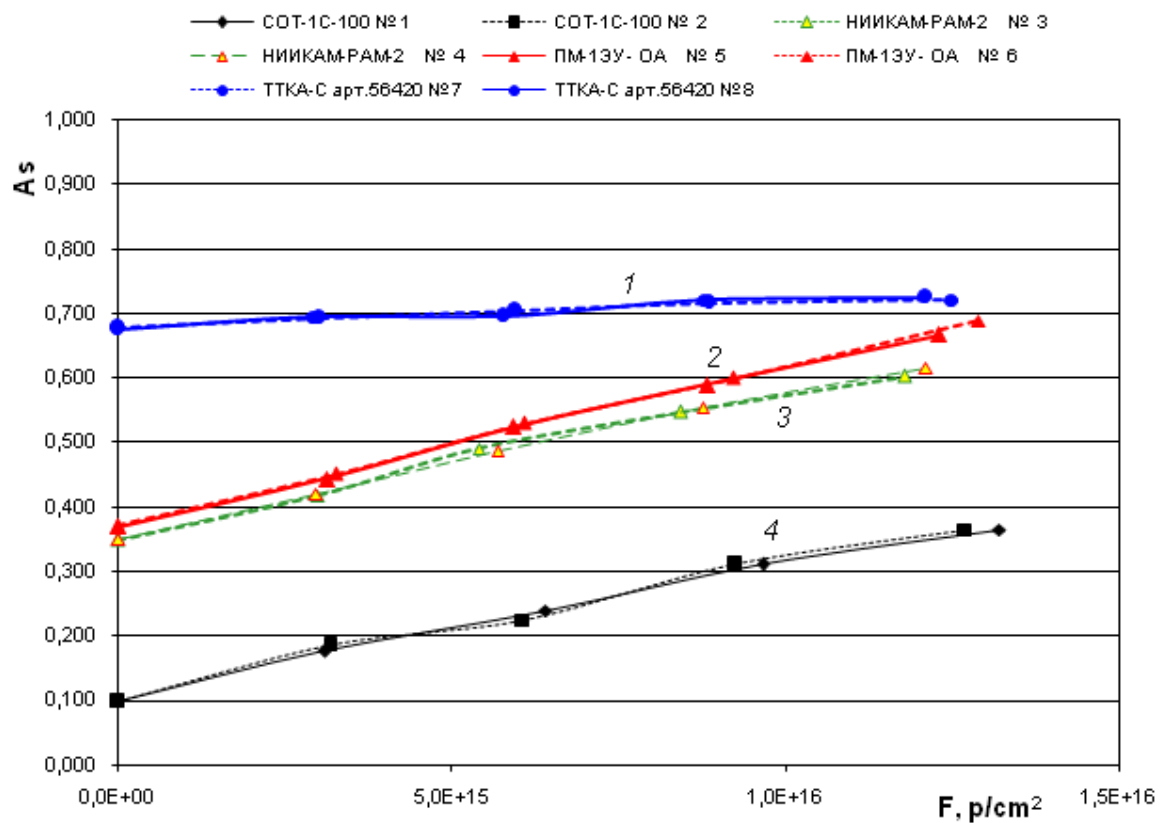


Figure 2. Dependence of solar absorbance A_s of samples of Russian materials on the fluence proton irradiation of a complex irradiation (electrons + protons + UV Sun radiation).
Curves 1 – Arimide frame fabric (article 56420); Curves 2 – PM-1EU-OA; Curves 3 – NIIKLAM-RAM-2; Curves 4 – SOT-1-S-100 films.

Shown in Figs. 3 — 6 are the dependences of the solar radiation absorbance of Russian materials on the time of their exposure of the combined action of different radiations.

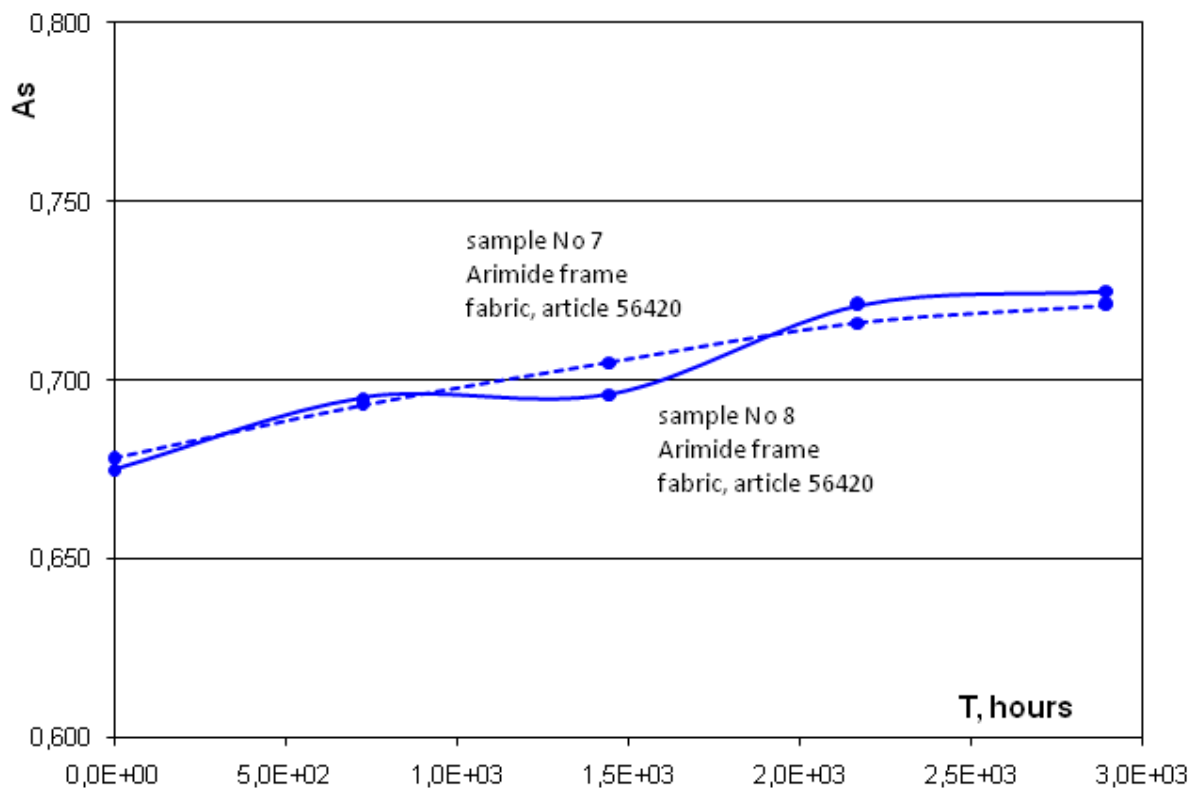


Figure 3. Dependence of solar absorbance A_s of samples of Arimide frame fabric (article 56420) on time of a complex irradiation (electrons + protons + UV Sun radiation)
Curve 1 (top) - sample No 7, Curve 2 (bottom) - sample No 8

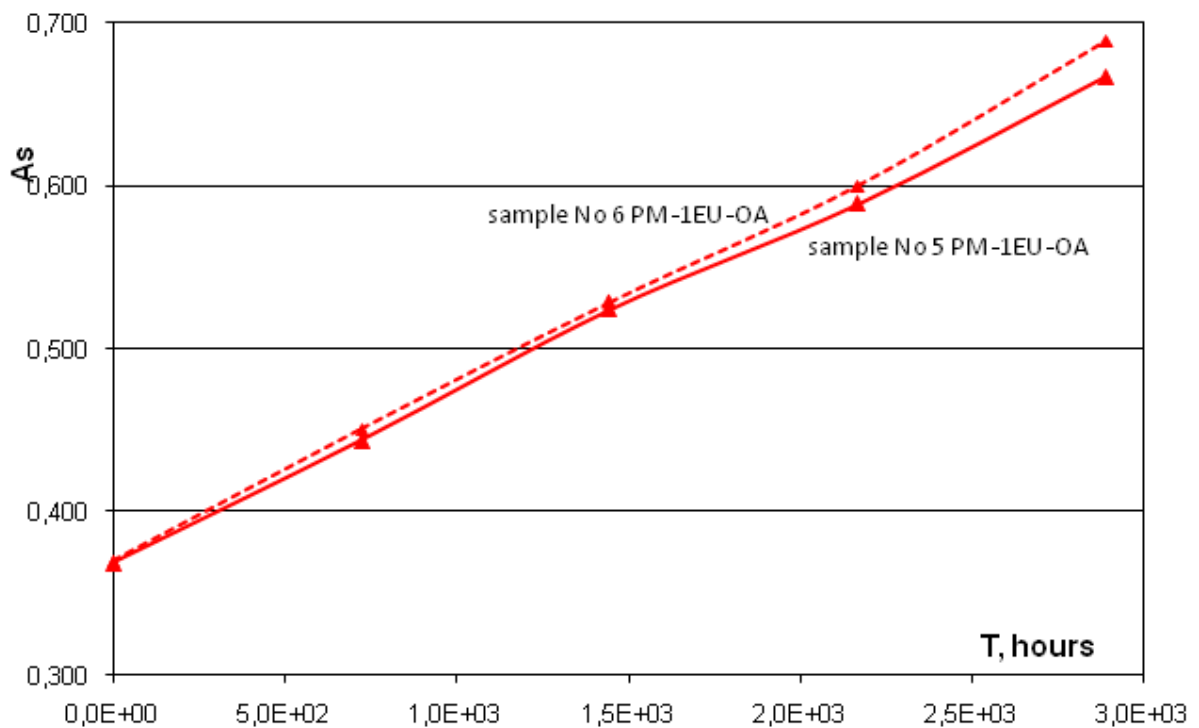


Figure 4. Dependence of solar absorbance A_s of samples of PM-1EU-OA on time of a complex irradiation (electrons + protons + UV Sun radiation)
Top curve - sample No 6 PM-1EU-OA, bottom curve - sample No 5 PM-1EU-OA

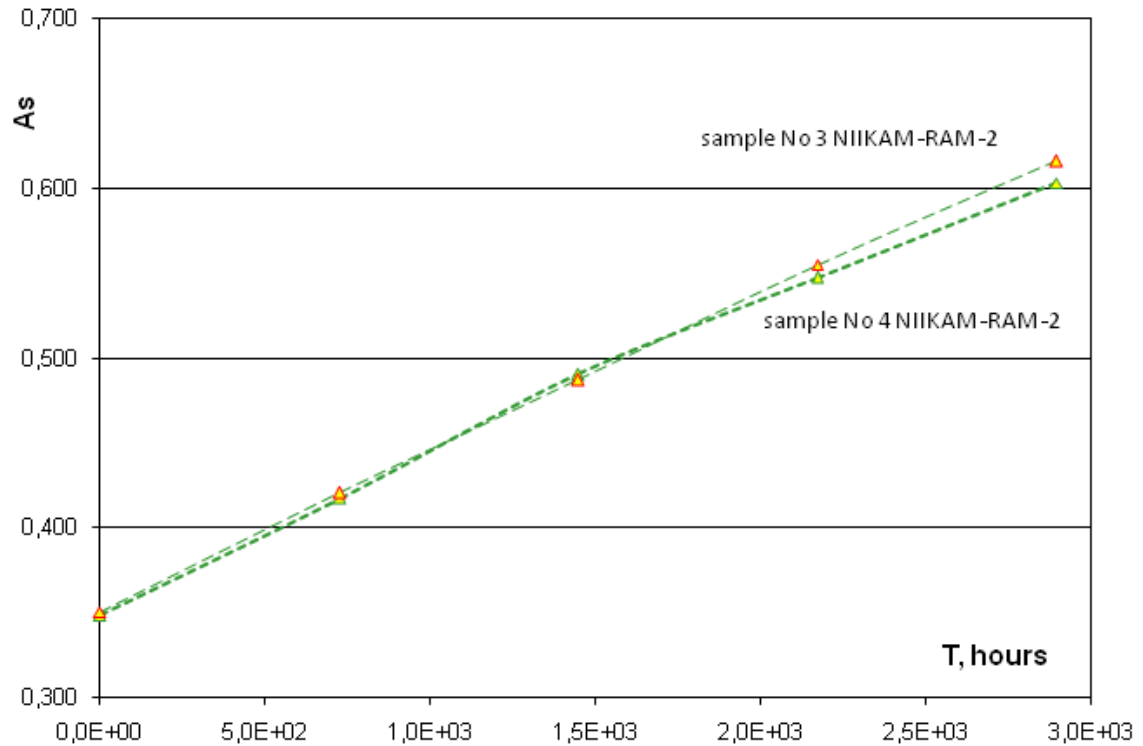


Figure 5. Dependence of solar absorbance A_s of samples of NIIKAM-RAM-2 on time of a complex irradiation (electrons + protons + UV Sun radiation)
Top curve - sample No 3, bottom curve - sample No 4

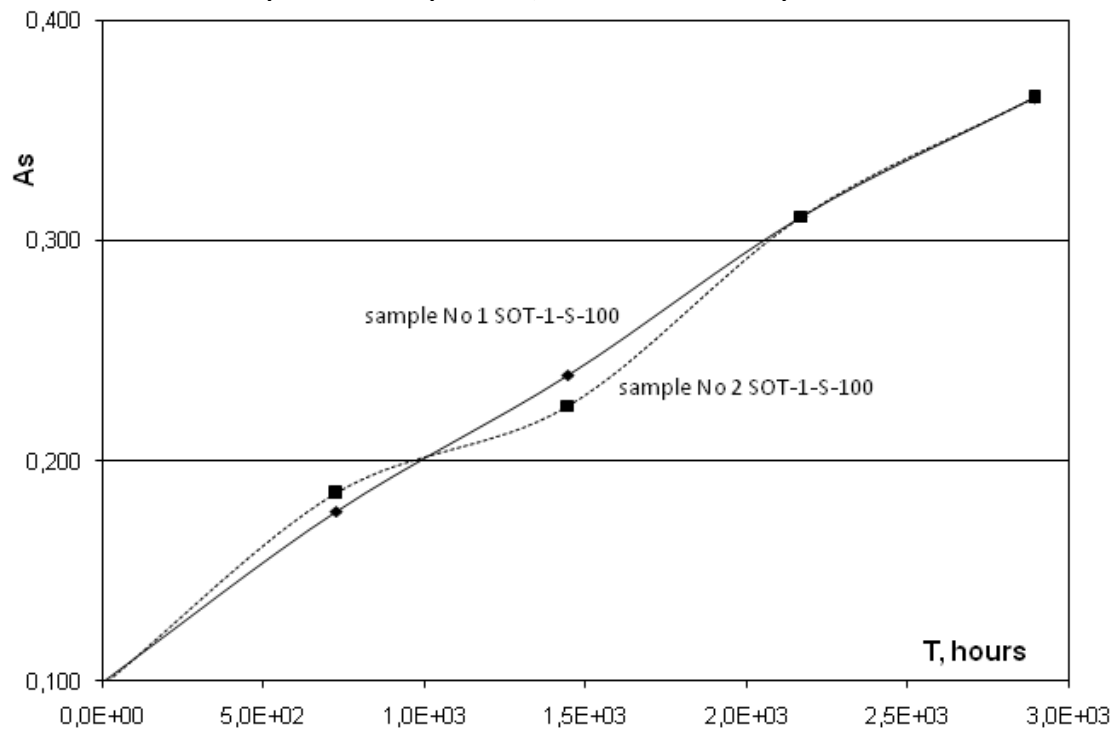


Figure 6. Dependence of solar absorbance A_s of samples of SOT-1-S-100 films on time of a complex irradiation (electrons + protons + UV Sun radiation)
Top curve - sample No 1, bottom curve - sample No 2

Shown in Fig. 7 are the reflectance spectra of the reference samples, measured on the Cary 500 spectrophotometer, which were afterwards used in the measurements of the irradiated samples on the FM-59M photometer. The corresponding Database records are shown also.

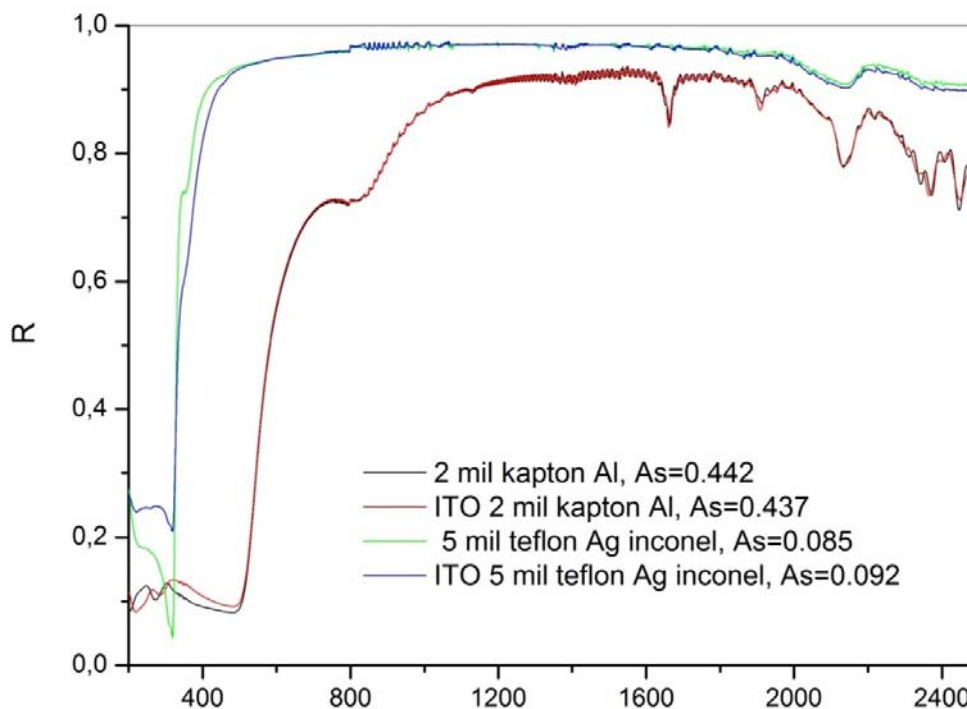
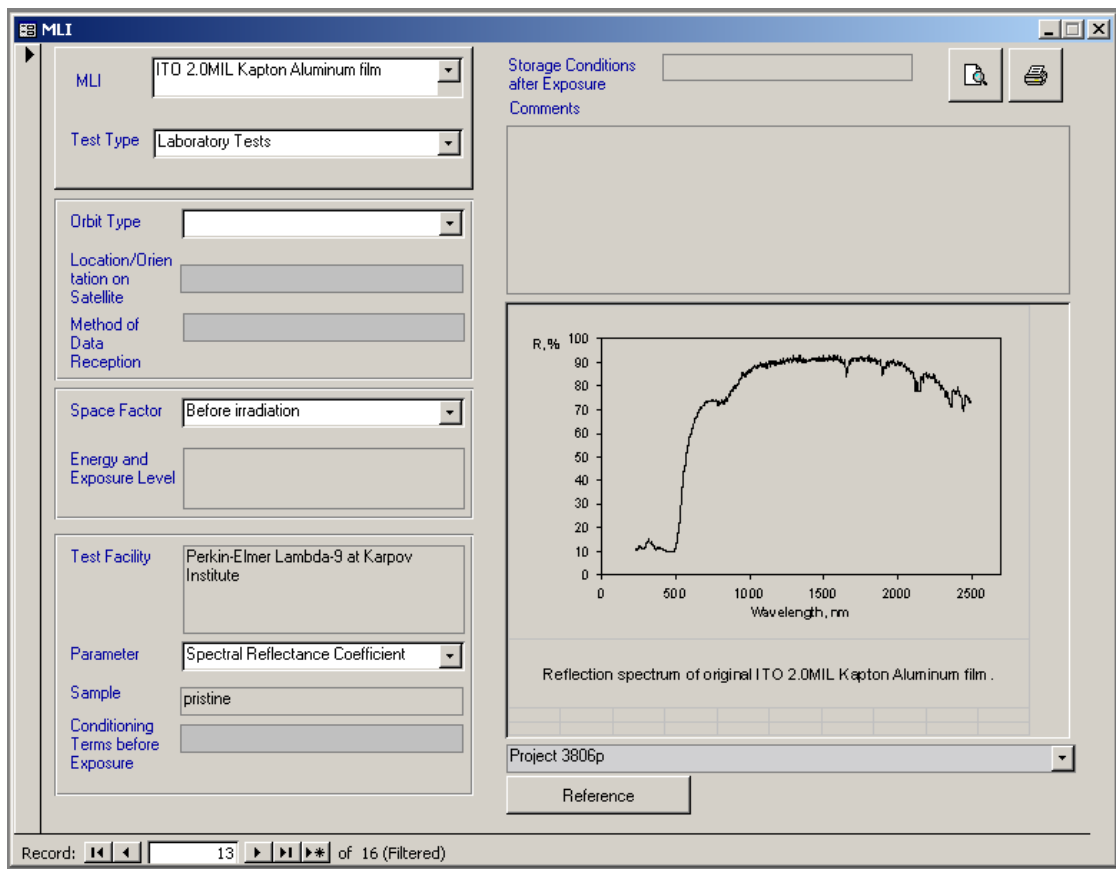
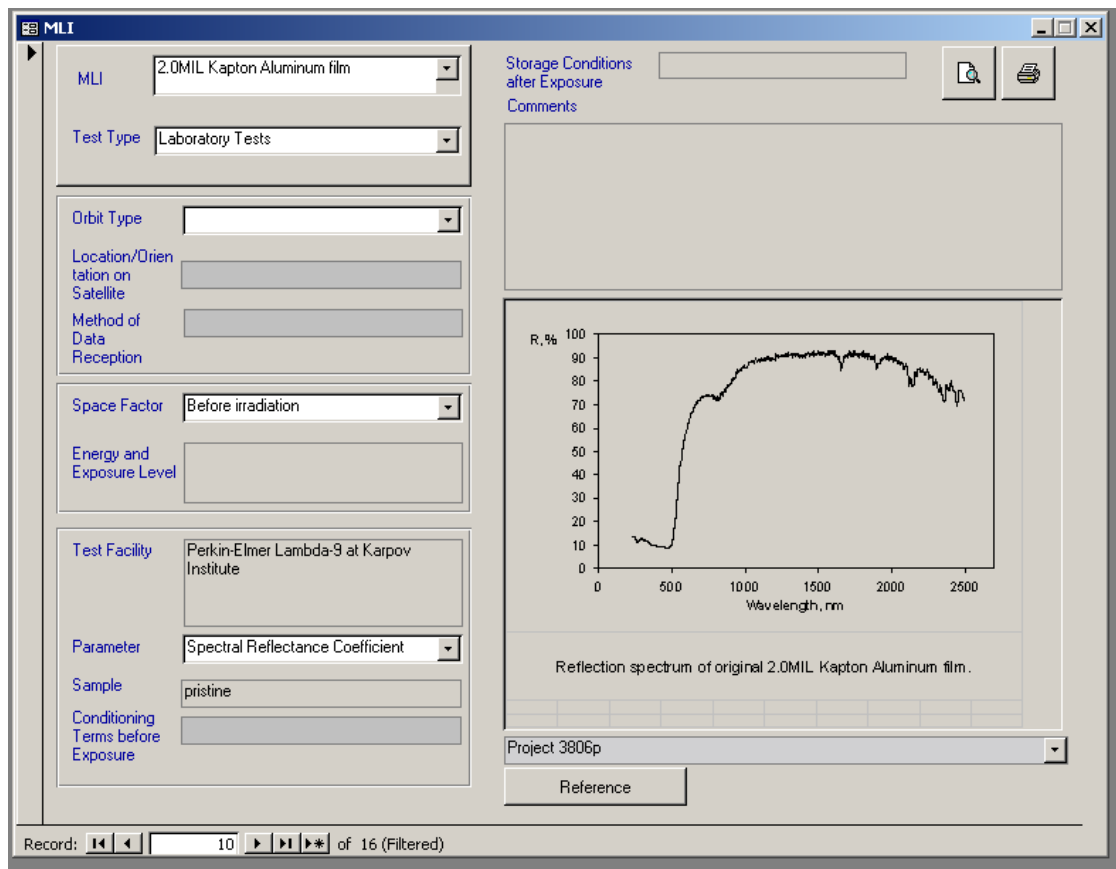
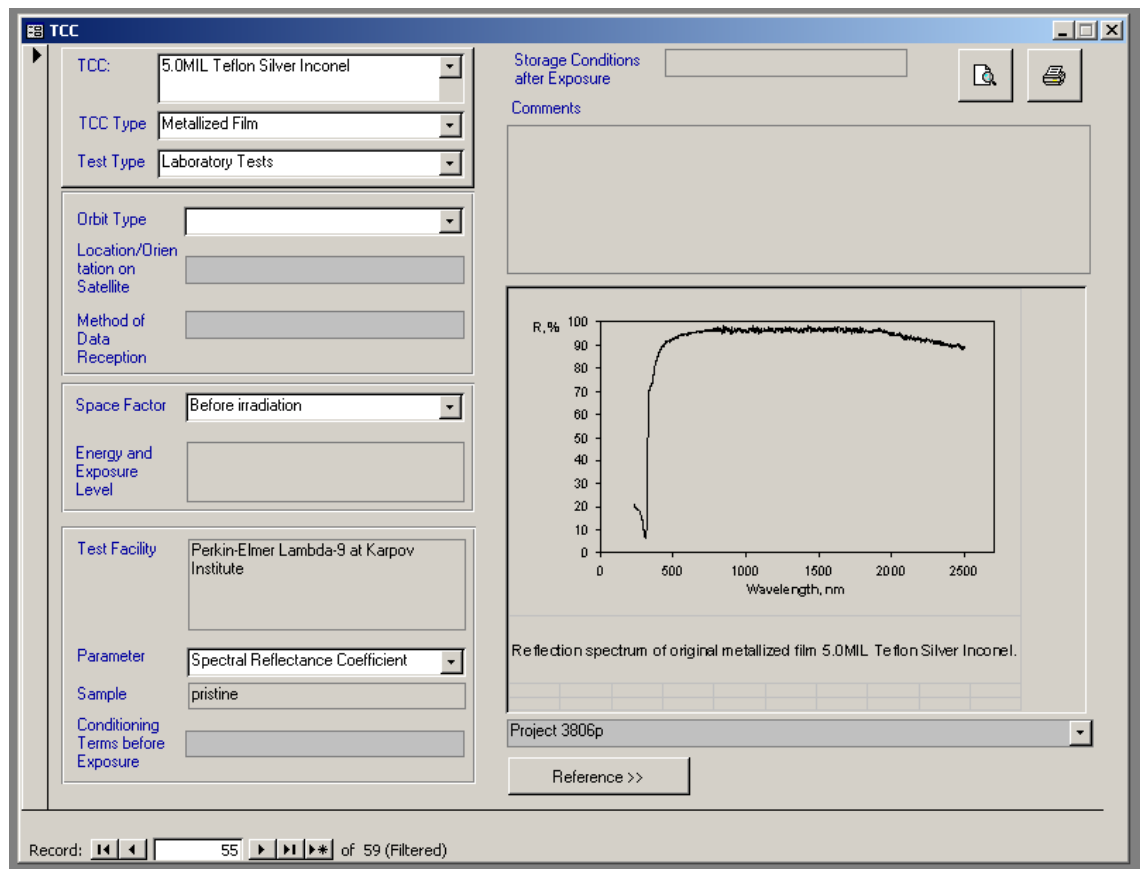
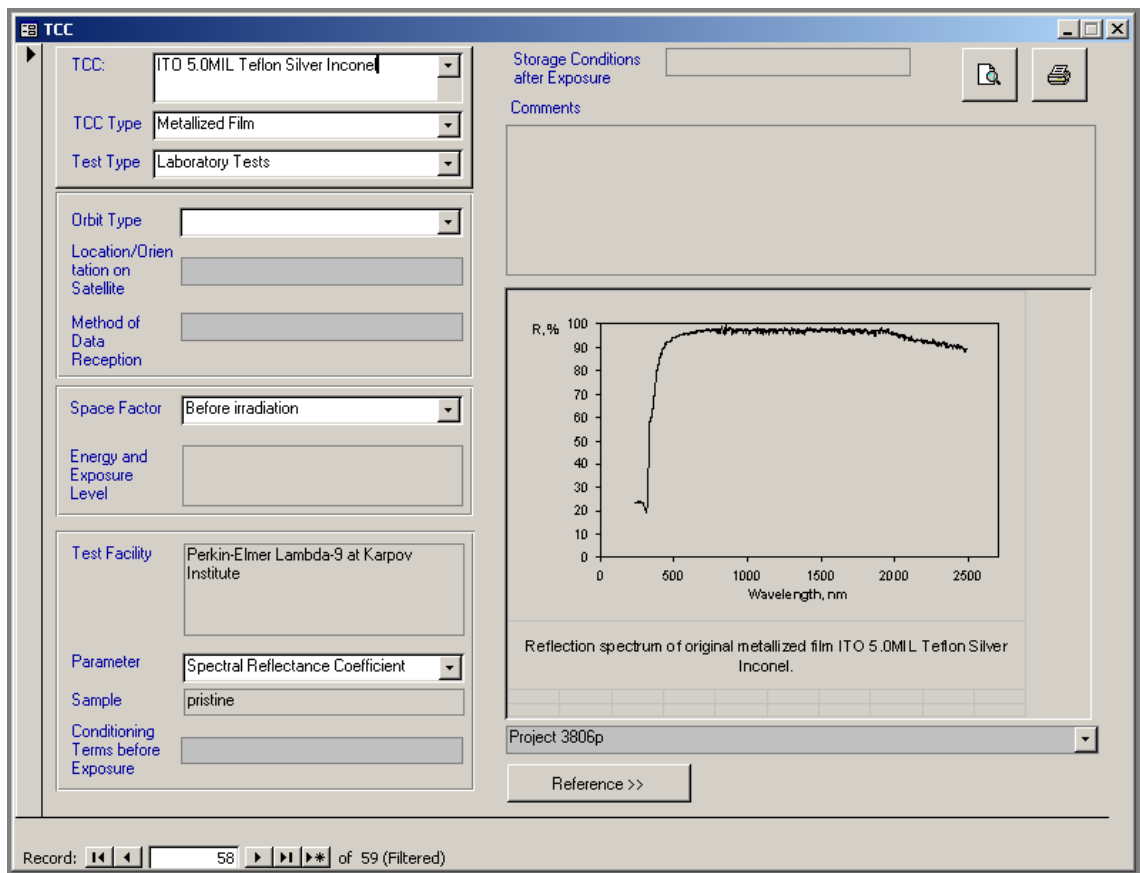


Figure 7. Spectrum of reference samples of Sheldahl (2 mil Kapton Al, ITO 2 mil Kapton Al, 5 mil Teflon Ag inconel and ITO 5 mil Teflon Ag inconel) films.





In Fig. 8-11 dependence of solar absorbance A_s for samples of Sheldahl films on level of influence of complex radiation is presented. The corresponding Database records are shown also.

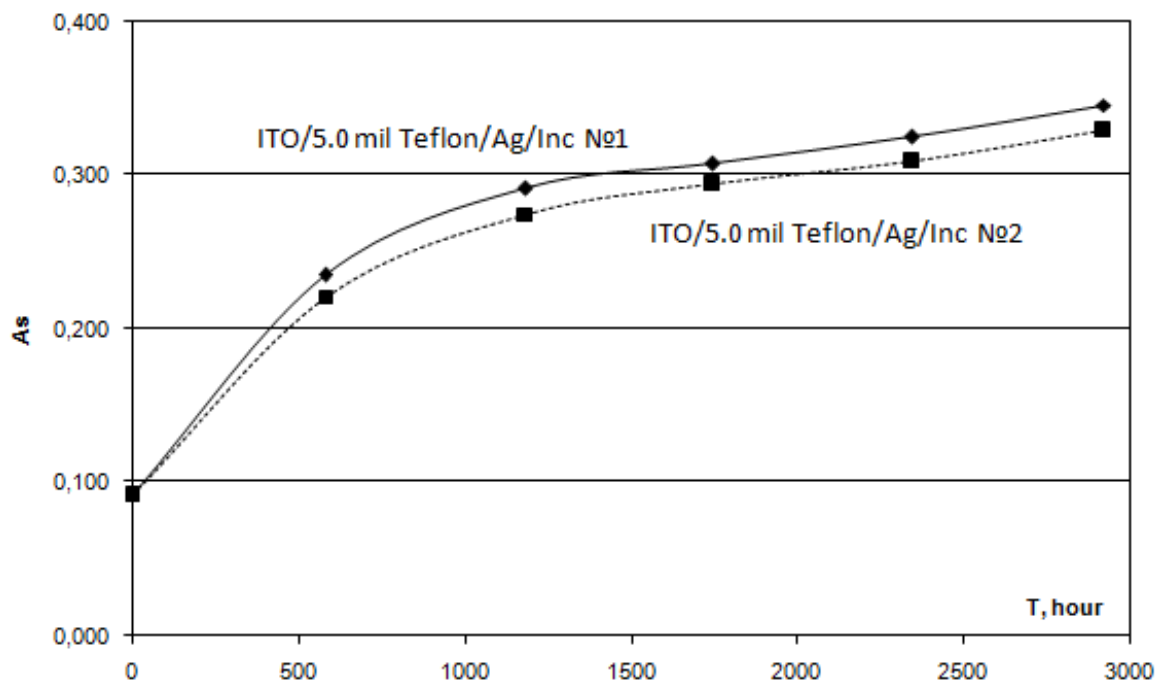


Figure 8. Dependence of solar absorbance A_s of samples of Sheldahl films on time of a complex irradiation (electrons + protons + UV Sun radiation)
Curve 1 (top) - sample ITO/5.0 mil Teflon/Ag/Inc №1,
Curve 2 (bottom) - sample ITO/5.0 mil Teflon/Ag/Inc №2

TCC

TCC: ITO 5.0MIL Teflon Silver Inconel

TCC Type: Metallized Film

Test Type: Laboratory Tests

Orbit Type:

Location/Orientation on Satellite:

Method of Data Reception:

Space Factor: Electrons + Protons + Solar UV

Energy and Exposure Level: 3 year at GEO

Test Facility: UV-1/2 at Kompozit

Parameter: Solar Absorption

Sample: aged

Conditioning Terms before Exposure: vacuum

Storage Conditions after Exposure: air

Comments:

Ep=50 keV (5E10 p/cm2s), Ee=50 keV (5E11 e/cm2s), 3 e.s.i.
Electron and proton irradiation was carried out in discrete mode. Average flux density equaled 5E7 p/cm2s and 4.6E8 e/cm2.
In order to measure a change in solar absorptance, the sample was extracted into the air. Having been measured, the sample was placed into a vacuum testing chamber, and the irradiation continued until the next value exposure was reached. The given sample was used after irradiation for measuring spectral characteristics.

Solar absorptance for ITO/5.0 mil Teflon/Ag/Inconel during combined irradiation (electrons + protons + UV solar radiation). The energy of the protons and electrons amounted to 50 keV. The average flux density for the protons and electrons equaled $\phi = 5 \times 10^7$ p/cm² × s and $\phi = 4.6 \times 10^8$ e/cm² × s respectively. The intensity of the simulated electromagnetic solar radiation was equal to 3 e.s.i.

Project 3806p

Reference >>

Record: 50 of 61 (Filtered)

TCC

TCC: ITO 5.0MIL Teflon Silver Inconel

TCC Type: Metallized Film

Test Type: Laboratory Tests

Orbit Type:

Location/Orientation on Satellite:

Method of Data Reception:

Space Factor: Electrons + Protons + Solar UV

Energy and Exposure Level: 3 year at GEO

Test Facility: UV-1/2 at Kompozit

Parameter: Solar Absorption

Sample: aged

Conditioning Terms before Exposure: vacuum

Storage Conditions after Exposure: inert gas (argon)

Comments:

Ep=50 keV (5E10 p/cm2s), Ee=50 keV (5E11 e/cm2s), 3 e.s.i.
Electron and proton irradiation was carried out in discrete mode. Average flux density equaled 5E7 p/cm2s and 4.6E8 e/cm2.
In order to measure a change in solar absorptance, the sample was extracted into the air. Having been measured, the sample was placed into a vacuum testing chamber, and the irradiation continued until the next value exposure was reached. After irradiation the given sample was delivered to the partner.

Solar absorptance for ITO/5.0 mil Teflon/Ag/Inconel during combined irradiation (electrons + protons + UV solar radiation). The energy of the protons and electrons amounted to 50 keV. The average flux density for the protons and electrons equaled $\phi = 5 \times 10^7$ p/cm² × s and $\phi = 4.6 \times 10^8$ e/cm² × s respectively. The intensity of the simulated electromagnetic solar radiation was equal to 3 e.s.i.

Project 3806p

Reference >>

Record: 51 of 61 (Filtered)

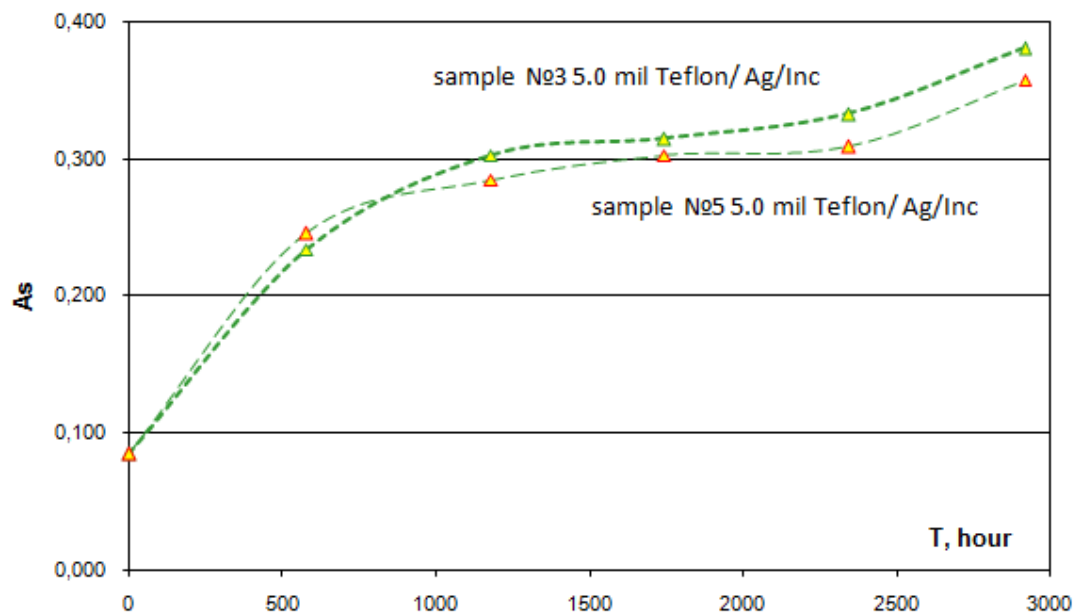
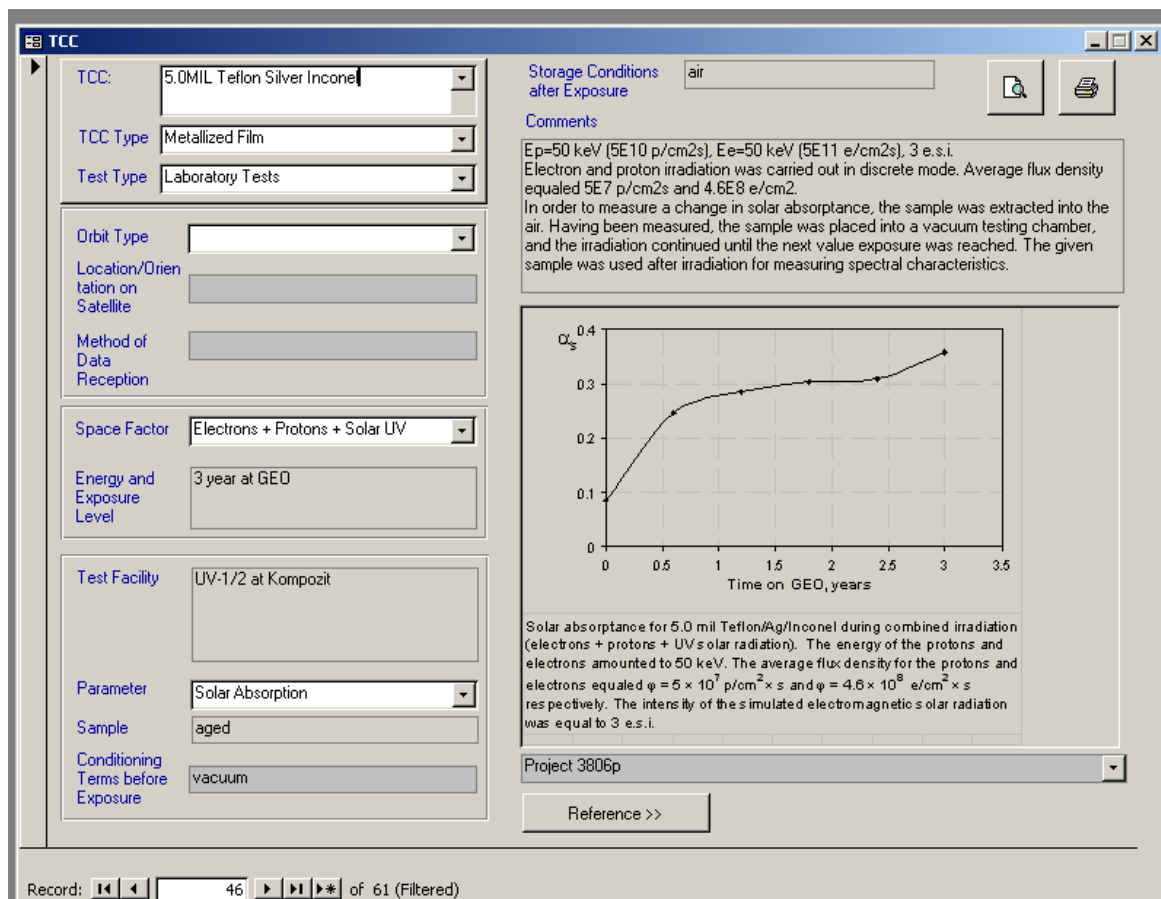


Figure 9. Dependence of solar absorbance A_s of samples of Sheldahl films on time of a complex irradiation (electrons + protons + UV Sun radiation)

Curve 1 (top) - sample 5.0 mil Teflon/ Ag/Inc №3,
Curve 2 (bottom) - sample 5.0 mil Teflon/ Ag/Inc №4



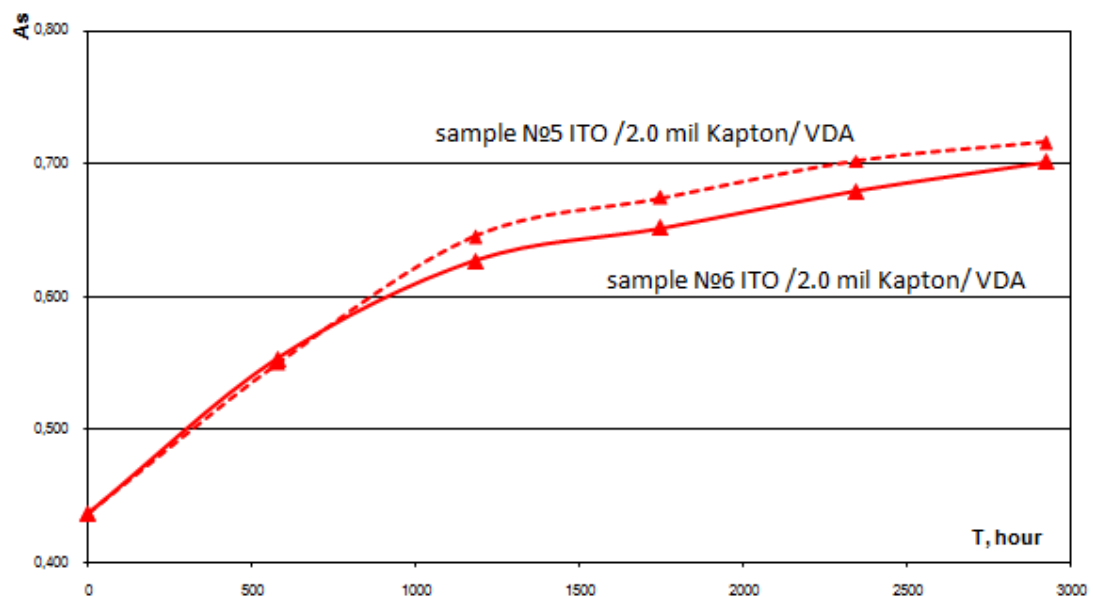
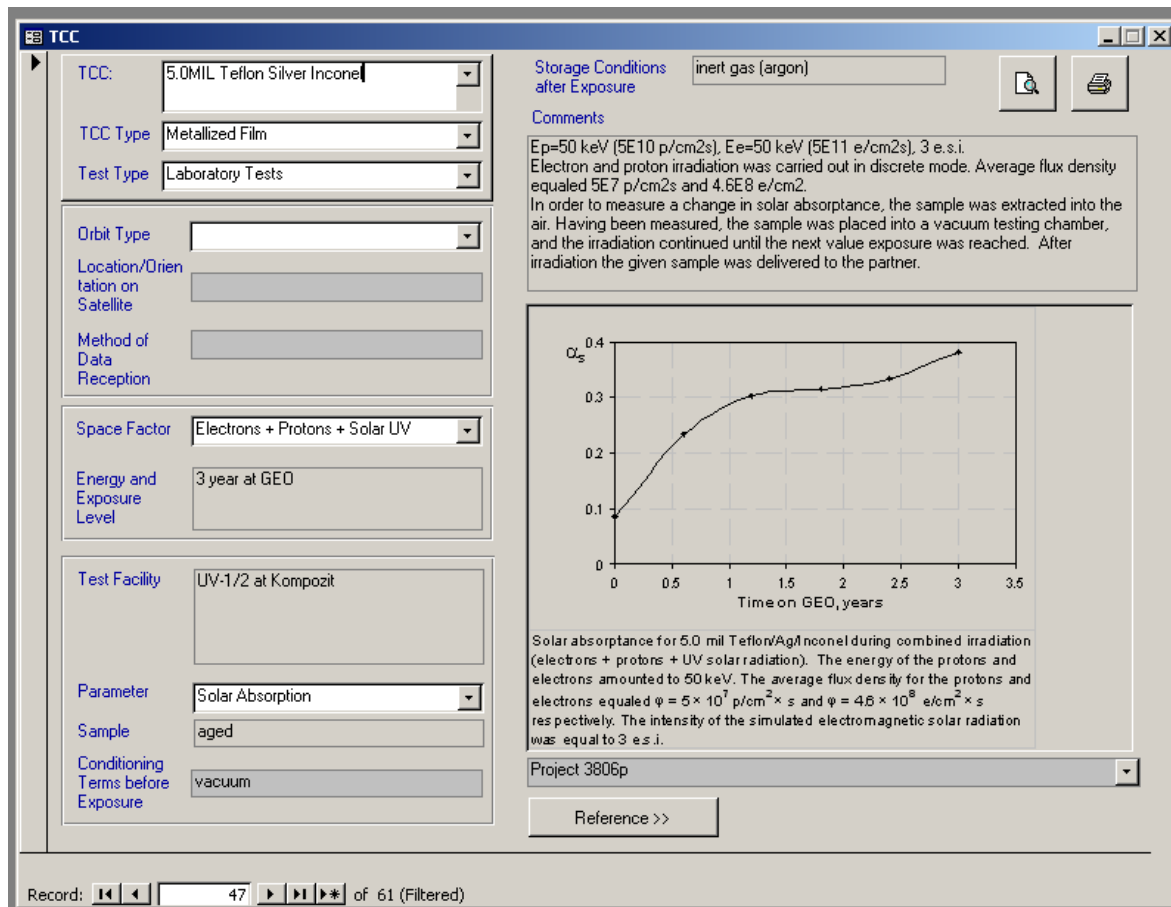


Figure 10. Dependence of solar absorptance A_s of samples of Sheldahl films on time of a complex irradiation (electrons + protons + UV Sun radiation)
 Curve 1 (top) - sample ITO /2.0 mil Kapton/ VDA №5,
 Curve 2 (bottom) - sample ITO /2.0 mil Kapton/ VDA №6

MLI

MLI: ITO 2.0MIL Kapton Aluminum film

Test Type: Laboratory Tests

Orbit Type:

Location/Orientation on Satellite:

Method of Data Reception:

Space Factor: Electrons + Protons + Solar UV

Energy and Exposure Level: 3 year at GEO

Test Facility: UV-1/2 at Komposit

Parameter: Solar Absorption

Sample: aged

Conditioning Terms before Exposure: vacuum

Storage Conditions after Exposure: air

Comments:

Ep=50 keV (5E10 p/cm2s), Ee=50 keV (5E11 e/cm2s), 3 e.s.i.
 Electron and proton irradiation was carried out in discrete mode. Average flux density equaled 5E7 p/cm2s and 4.6E8 e/cm2.
 In order to measure a change in solar absorptance, the sample was extracted into the air. Having been measured, the sample was placed into a vacuum testing chamber, and the irradiation continued until the next value exposure was reached. The given sample was used after irradiation for measuring spectral characteristics.

Solar absorptance for ITO/2.0 mil Kapton/VDA during combined irradiation (electrons + protons + UV solar radiation). The energy of the protons and electrons amounted to 50 keV. The average flux density for the protons and electrons equaled $\phi = 5 \times 10^7$ p/cm² × s and $\phi = 4.6 \times 10^8$ e/cm² × s respectively. The intensity of the simulated electromagnetic solar radiation was equal to 3 e.s.i.

Project 3806p

Reference

Record: 6 of 6 (Filtered)

MLI

MLI: ITO 2.0MIL Kapton Aluminum film

Test Type: Laboratory Tests

Orbit Type:

Location/Orientation on Satellite:

Method of Data Reception:

Space Factor: Electrons + Protons + Solar UV

Energy and Exposure Level: 3 year at GEO

Test Facility: UV-1/2 at Komposit

Parameter: Solar Absorption

Sample: aged

Conditioning Terms before Exposure: vacuum

Storage Conditions after Exposure: inert gas (argon)

Comments:

Ep=50 keV (5E10 p/cm2s), Ee=50 keV (5E11 e/cm2s), 3 e.s.i.
 Electron and proton irradiation was carried out in discrete mode. Average flux density equaled 5E7 p/cm2s and 4.6E8 e/cm2.
 In order to measure a change in solar absorptance, the sample was extracted into the air. Having been measured, the sample was placed into a vacuum testing chamber, and the irradiation continued until the next value exposure was reached. After irradiation the given sample was delivered to the partner.

Solar absorptance for ITO/2.0 mil Kapton/VDA during combined irradiation (electrons + protons + UV solar radiation). The energy of the protons and electrons amounted to 50 keV. The average flux density for the protons and electrons equaled $\phi = 5 \times 10^7$ p/cm² × s and $\phi = 4.6 \times 10^8$ e/cm² × s respectively. The intensity of the simulated electromagnetic solar radiation was equal to 3 e.s.i.

Project 3806p

Reference

Record: 2 of 6 (Filtered)

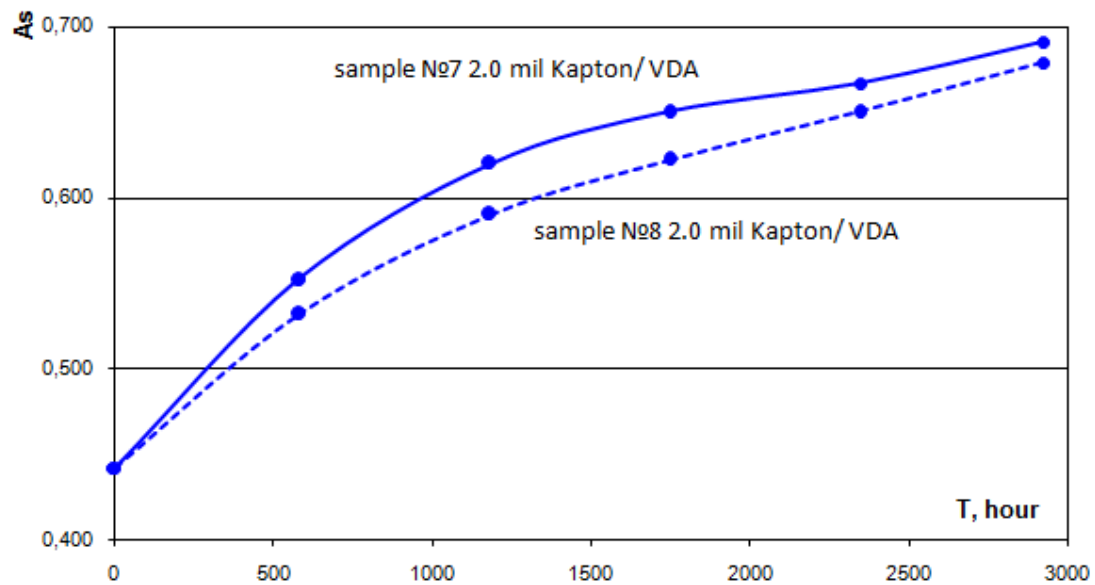
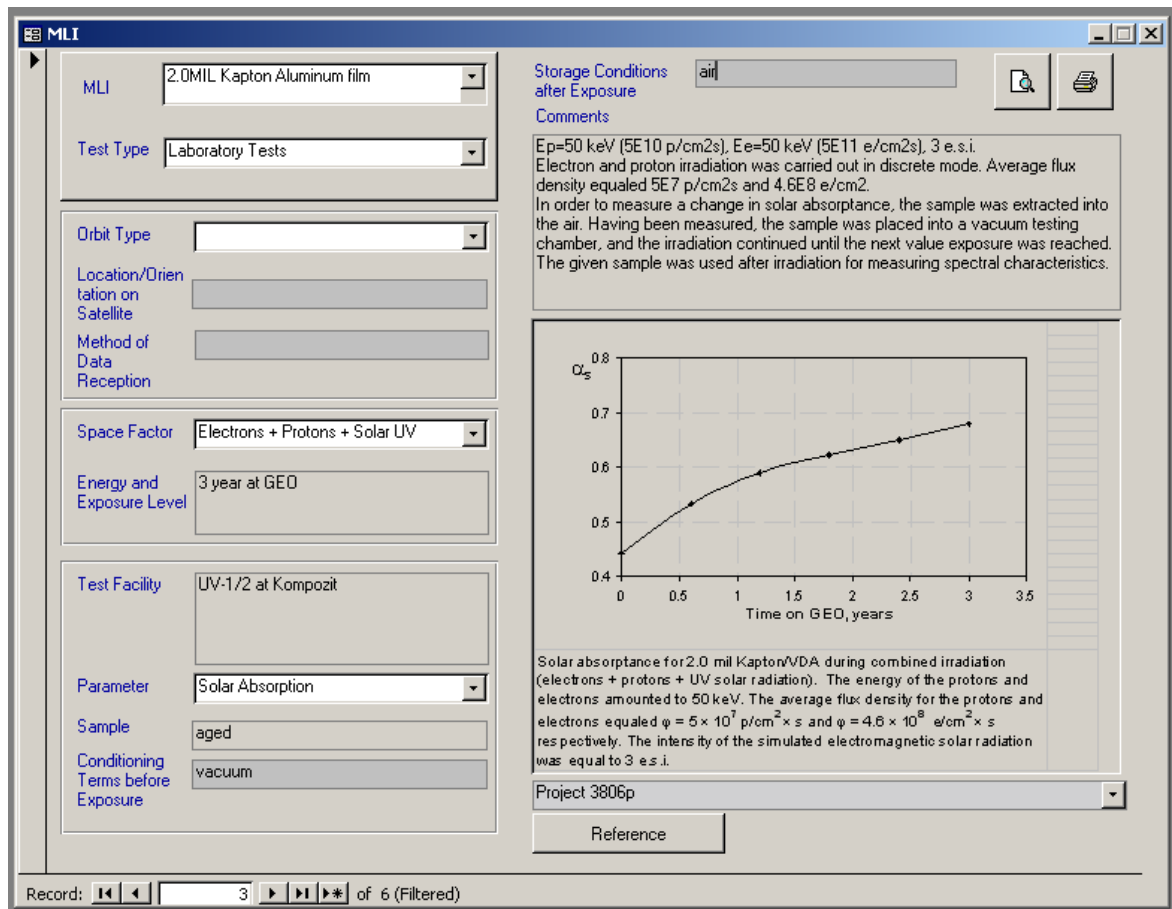


Figure 11. Dependence of solar absorbance A_s of samples of Sheldahl films on time of a complex irradiation (electrons + protons + UV Sun radiation)
 Curve 1 (top) - sample 2.0 mil Kapton/ VDA №7,
 Curve 2 (bottom) - sample 2.0 mil Kapton/ VDA №8



MLI																	
MLI	2.0MIL Kapton Aluminum film																
Test Type	Laboratory Tests																
Orbit Type																	
Location/Orientation on Satellite																	
Method of Data Reception																	
Space Factor	Electrons + Protons + Solar UV																
Energy and Exposure Level	3 year at GEO																
Test Facility	UV-1/2 at Komposit																
Parameter	Solar Absorption																
Sample	aged																
Conditioning Terms before Exposure	vacuum																
Storage Conditions after Exposure	inert gas (argon)																
Comments	<p>Ep=50 keV (5E10 p/cm2s), Ee=50 keV (5E11 e/cm2s), 3 e.s.i. Electron and proton irradiation was carried out in discrete mode. Average flux density equaled 5E7 p/cm2s and 4.6E8 e/cm2. In order to measure a change in solar absorptance, the sample was extracted into the air. Having been measured, the sample was placed into a vacuum testing chamber, and the irradiation continued until the next value exposure was reached. After irradiation the given sample was delivered to the partner.</p>																
<table border="1"><caption>Data points for Solar absorptance vs Time on GEO</caption><thead><tr><th>Time on GEO, years</th><th>Solar absorptance (α_s)</th></tr></thead><tbody><tr><td>0</td><td>0.45</td></tr><tr><td>0.5</td><td>0.55</td></tr><tr><td>1.0</td><td>0.62</td></tr><tr><td>1.5</td><td>0.65</td></tr><tr><td>2.0</td><td>0.67</td></tr><tr><td>2.5</td><td>0.68</td></tr><tr><td>3.0</td><td>0.70</td></tr></tbody></table>		Time on GEO, years	Solar absorptance (α_s)	0	0.45	0.5	0.55	1.0	0.62	1.5	0.65	2.0	0.67	2.5	0.68	3.0	0.70
Time on GEO, years	Solar absorptance (α_s)																
0	0.45																
0.5	0.55																
1.0	0.62																
1.5	0.65																
2.0	0.67																
2.5	0.68																
3.0	0.70																
<p>Solar absorptance for 2.0 mil Kapton/VDA during combined irradiation (electrons + protons + UV solar radiation). The energy of the protons and electrons amounted to 50 keV. The average flux density for the protons and electrons equaled $\phi = 5 \times 10^7$ p/cm² × s and $\phi = 4.6 \times 10^8$ e/cm² × s respectively. The intensity of the simulated electromagnetic solar radiation was equal to 3 e.s.i.</p>																	
Project 3806p																	
Reference																	

Record: 4 of 6 (Filtered)

Changes in optical properties of MAP paints due to proton irradiation with energy of 50 keV

Table 1

Values of the solar radiation reflectance of MAP paints before and after exposure to protons (R_{s1} and R_{s2} are the reflectance values for the final and the intermediate values of the proton fluence).

No. of sample	Composition	R_{s0}	R_{s1} measured taking into account contamination	R_{s2} measured taking into account contamination
83	PUK Black Conductive Polyurethane Paint	0,040	0,085	0,099
84		0,039	0,090	0,102
3	PUI – Black Polyurethane Paint	0,045	0,078	0,089
4		0,045	0,083	0,094
261	SG121FD (White Paint)	0,789	0,658	0,565
262		0,793	0,645	0,540
183	PCBE (Conductive White Paint)	0,765	0,630	0,520
184		0,763	0,598	0,492

Dependence of the solar radiation absorptance α_s of the MAP samples on the fluence of proton irradiation (50 KeV) is shown in Figures 12-15. The corresponding Database records are shown also.

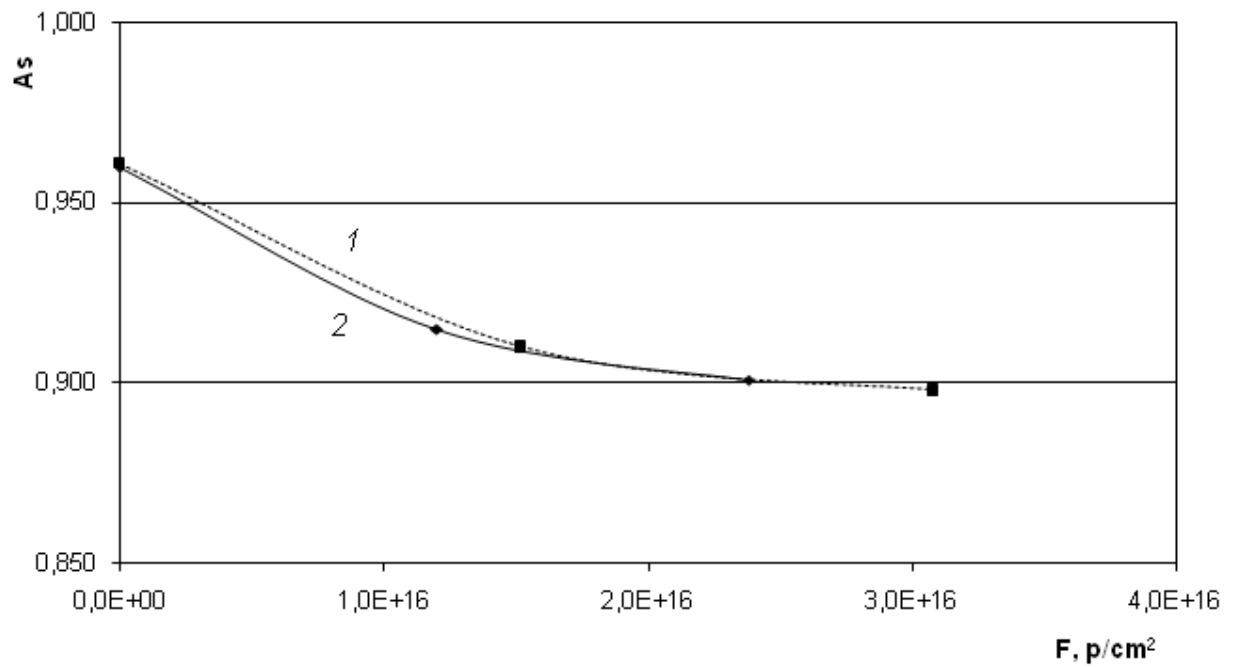
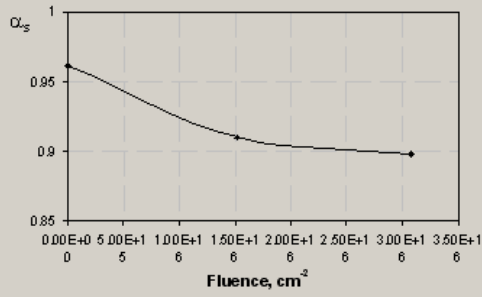


Figure 12. Dependence of the solar radiation absorptance A_s on the fluence of proton irradiation. Curve 1 (upper) and Curve 2 (lower) correspond to samples of a MAP coating (PUK Black Conductive Polyurethane Paint) No. 84 and No. 83 respectively

TCC									
TCC:	PUK Black Conductive Polyurethane Paint								
TCC Type	Enamel								
Test Type	Laboratory Tests								
Orbit Type									
Location/Orientation on Satellite									
Method of Data Reception									
Space Factor	Protons								
Energy and Exposure Level	50 keV, 1E12 p/cm2s								
Test Facility	UV-1/2 at Kompozit								
Parameter	Solar Absorption								
Sample	aged								
Conditioning Terms before Exposure	vacuum								
Storage Conditions after Exposure	inert gas (argon)								
Comments	In order to measure a change in solar absorptance, the sample was extracted into the air. Having been measured, the sample was placed into a vacuum testing chamber, and the irradiation continued until the next value exposure was reached. After irradiation the given sample was delivered to the partner								
 <table border="1"><caption>Data points from the graph</caption><thead><tr><th>Fluence, cm⁻²</th><th>α_s</th></tr></thead><tbody><tr><td>0.00E+0</td><td>0.97</td></tr><tr><td>1.50E+1</td><td>0.92</td></tr><tr><td>3.00E+1</td><td>0.90</td></tr></tbody></table>		Fluence, cm ⁻²	α_s	0.00E+0	0.97	1.50E+1	0.92	3.00E+1	0.90
Fluence, cm ⁻²	α_s								
0.00E+0	0.97								
1.50E+1	0.92								
3.00E+1	0.90								
Change in solar absorptance for enamel PUK (Black Conductive Polyurethane Paint) during proton irradiation. E=50 keV, flux - 10 ¹² p/cm ² s									
Project 3806p									
Reference >>									

Record: 1 of 5 (Filtered)

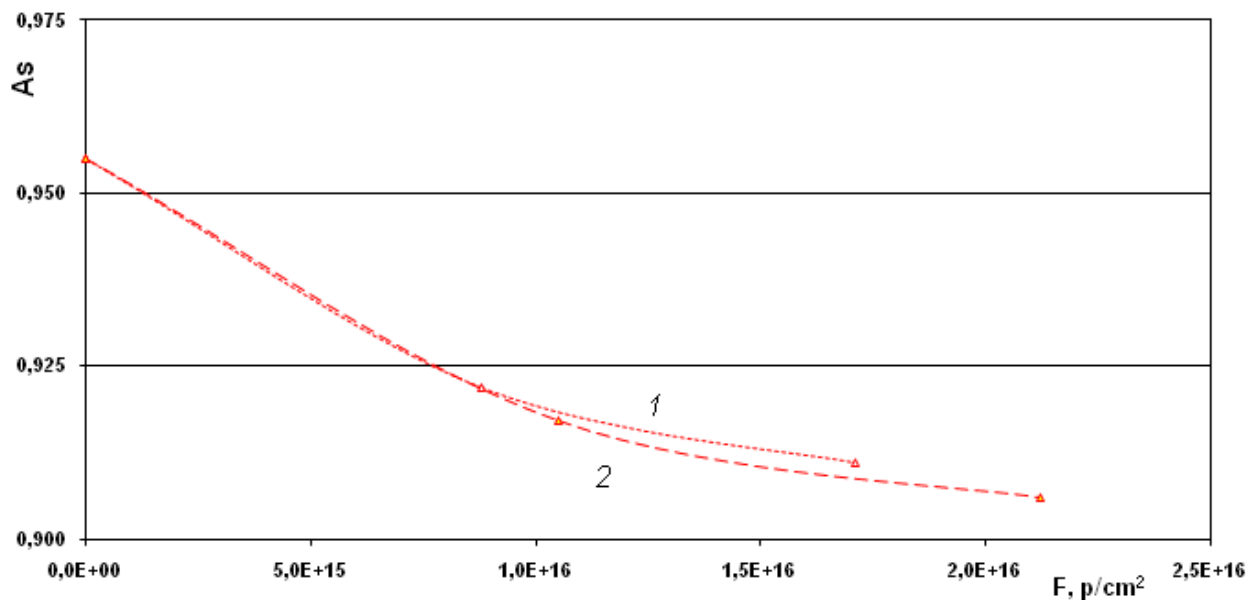
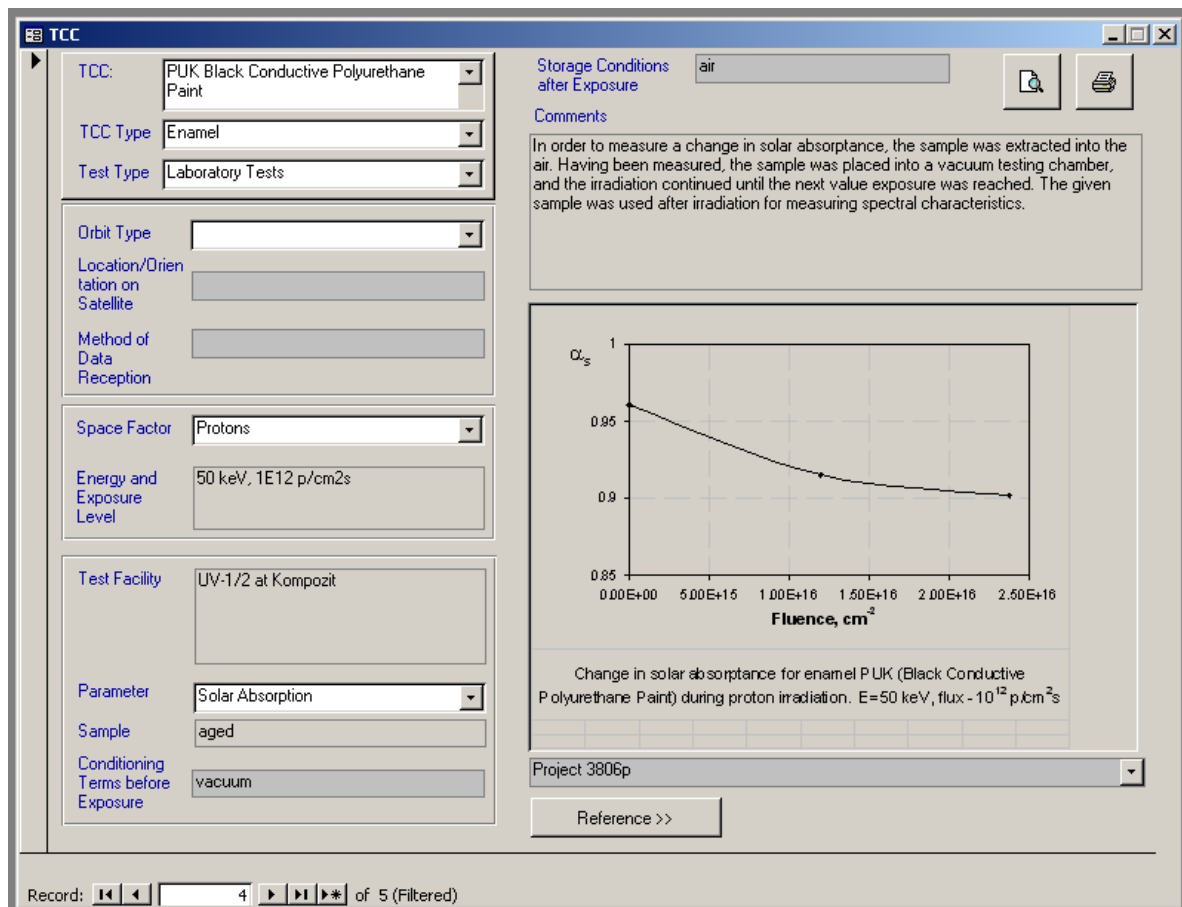


Figure 13. Dependence of the solar radiation absorptance A_s on the fluence of proton irradiation.

Curve 1 (upper) and Curve 2 (lower) correspond to samples of a MAP coating (PUI – Black Polyurethane Paint) No. 3 and No. 4 respectively.

TCC

TCC: PUI Black Polyurethane Paint

TCC Type: Enamel

Test Type: Laboratory Tests

Orbit Type:

Location/Orientation on Satellite:

Method of Data Reception:

Space Factor: Protons

Energy and Exposure Level: 50 keV, 1E12 p/cm2s

Test Facility: UV-1/2 at Kompozit

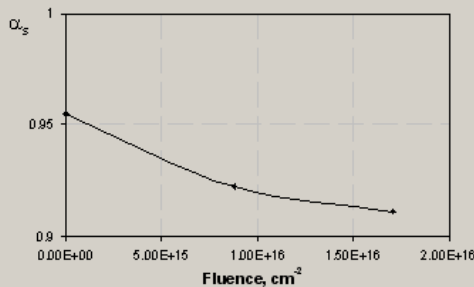
Parameter: Solar Absorption

Sample: aged

Conditioning Terms before Exposure: vacuum

Storage Conditions after Exposure: air

Comments: In order to measure a change in solar absorptance, the sample was extracted into the air. Having been measured, the sample was placed into a vacuum testing chamber, and the irradiation continued until the next value exposure was reached. The given sample was used after irradiation for measuring spectral characteristics.



Change in solar absorptance for enamel PUI (Black Polyurethane Paint) during proton irradiation. E=50 keV, flux - 10^{12} p/cm²s

Project 3806p

Reference >>

Record: 3 of 5 (Filtered)

TCC

TCC: PUI Black Polyurethane Paint

TCC Type: Enamel

Test Type: Laboratory Tests

Orbit Type:

Location/Orientation on Satellite:

Method of Data Reception:

Space Factor: Protons

Energy and Exposure Level: 50 keV, 1E12 p/cm2s

Test Facility: UV-1/2 at Kompozit

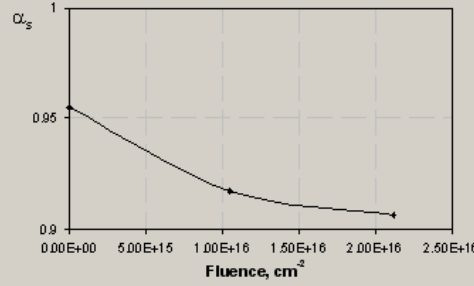
Parameter: Solar Absorption

Sample: aged

Conditioning Terms before Exposure: vacuum

Storage Conditions after Exposure: inert gas (argon)

Comments: In order to measure a change in solar absorptance, the sample was extracted into the air. Having been measured, the sample was placed into a vacuum testing chamber, and the irradiation continued until the next value exposure was reached. After irradiation the given sample was delivered to the partner



Change in solar absorptance for enamel PUI (Black Polyurethane Paint) during proton irradiation. E=50 keV, flux - 10^{12} p/cm²s

Project 3806p

Reference >>

Record: 4 of 5 (Filtered)

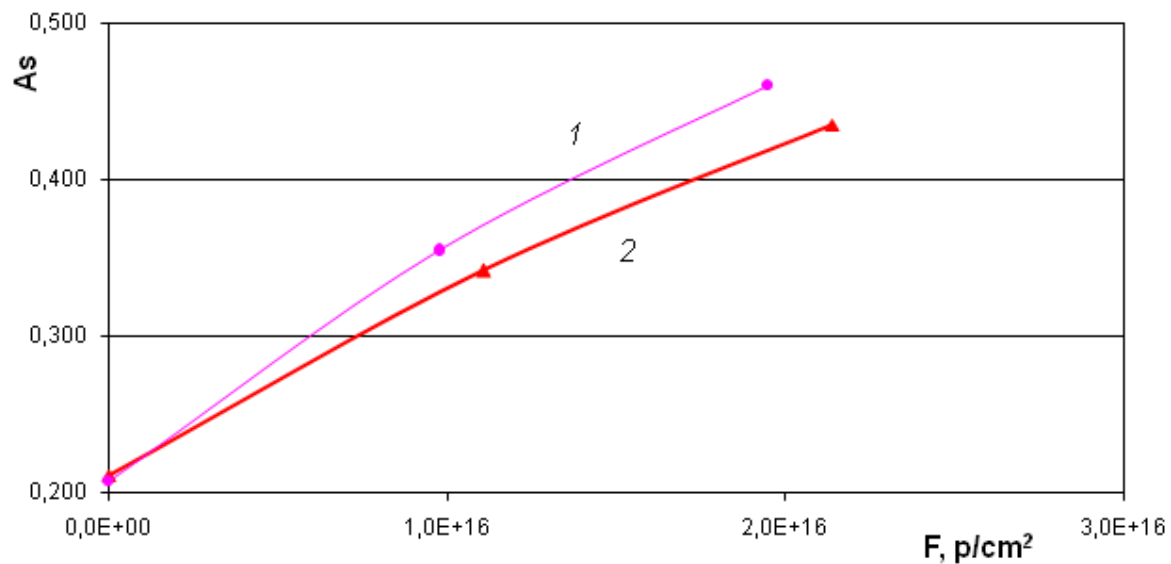
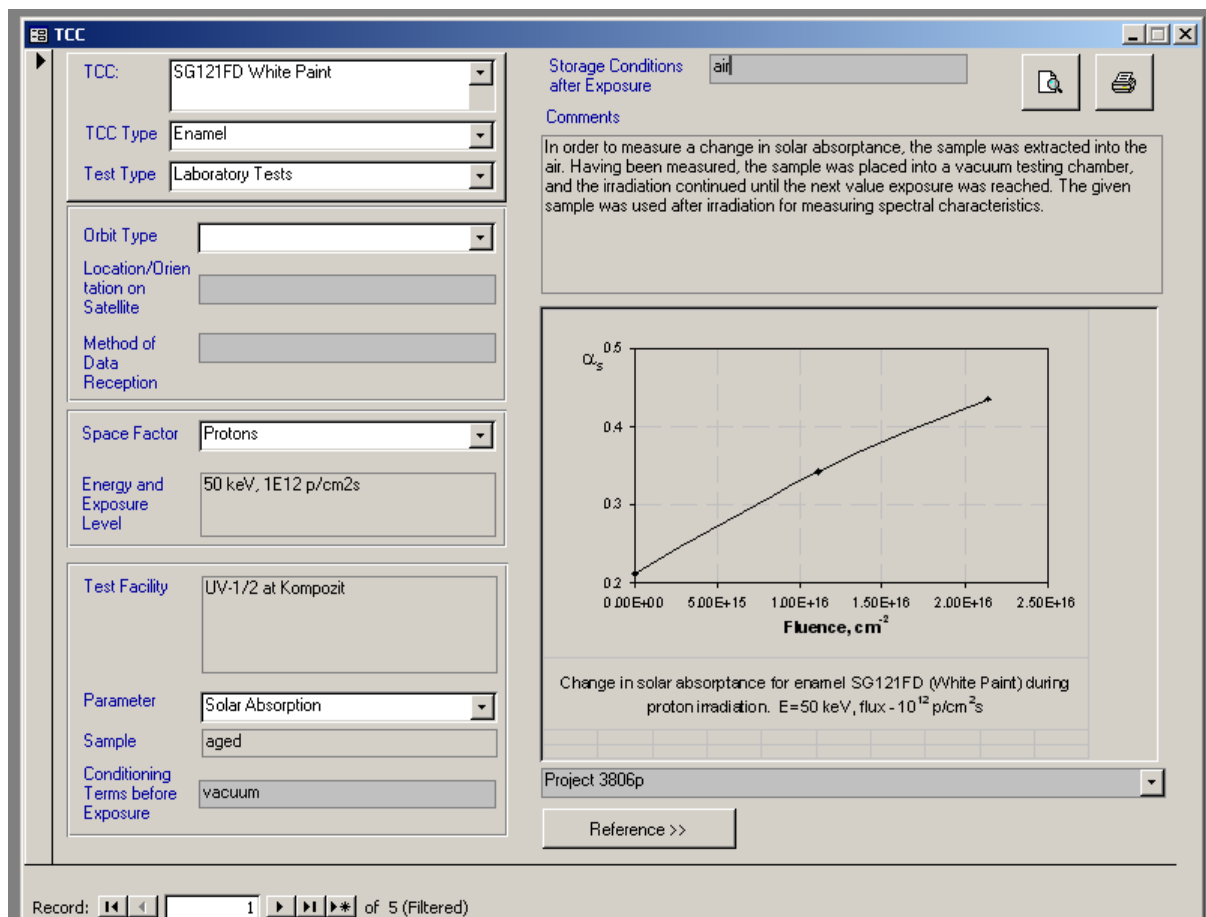


Figure 14. Dependence of the solar radiation absorptance A_s on the fluence of proton irradiation. Curve 1 (upper) and Curve 2 (lower) correspond to samples of a MAP coating (SG121FD (White Paint)) No. 262 and No. 261 respectively



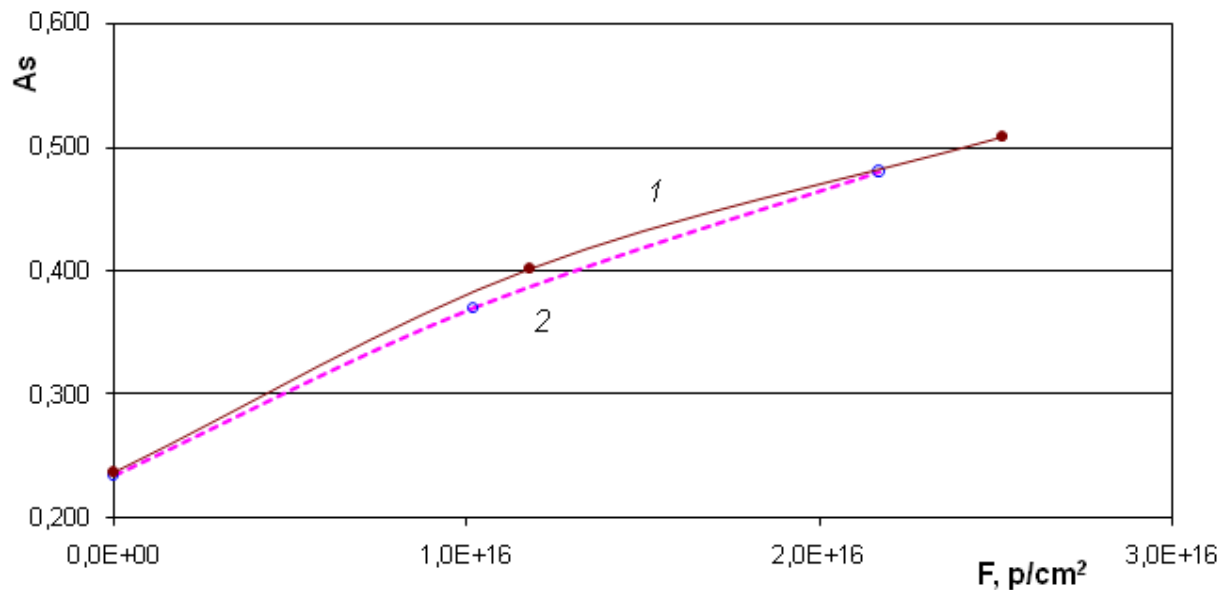
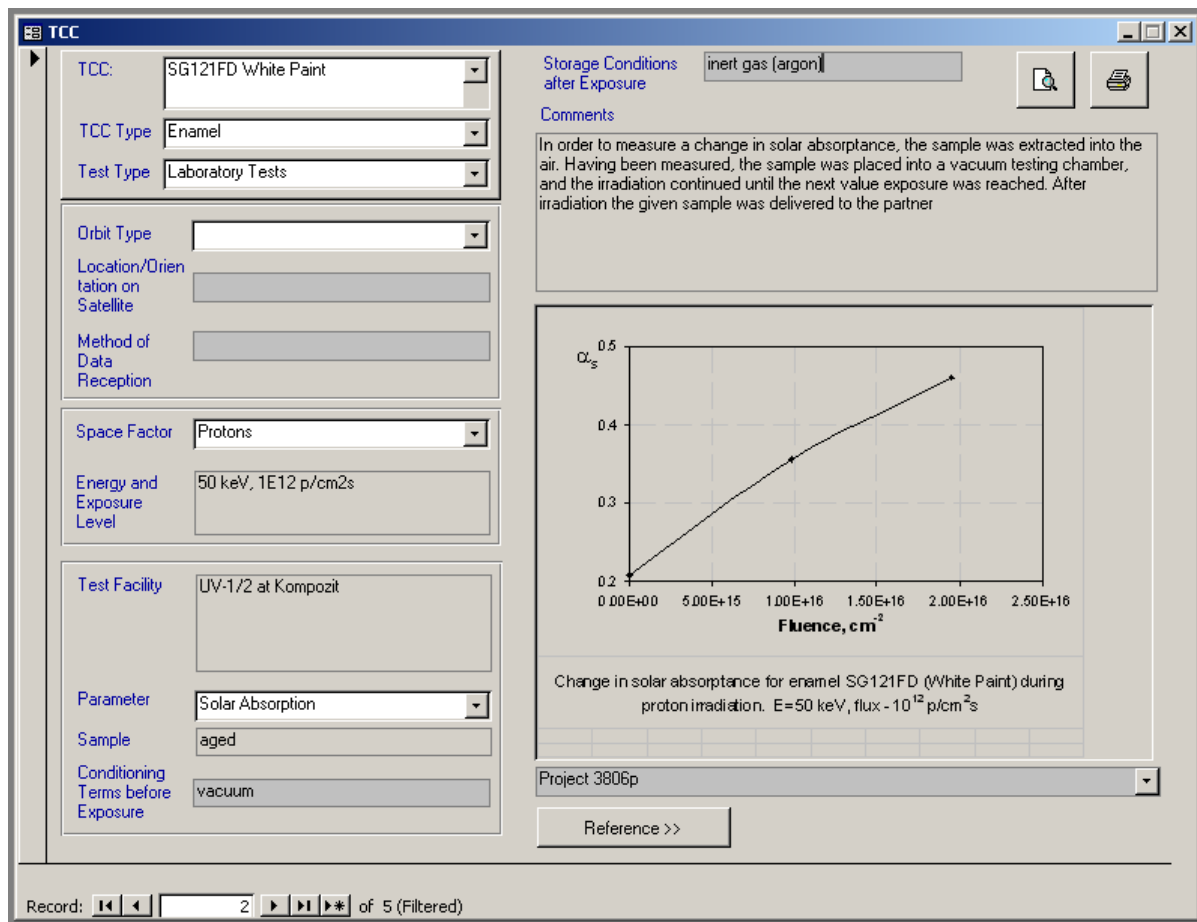


Figure 15. Dependence of the solar radiation absorptance A_s on the fluence of proton irradiation. Curve 1 (upper) and Curve 2 (lower) correspond to samples of a MAP coating (PCBE (Conductive White Paint)) No. 184 and No. 183 respectively

TCC

TCC: PCBE Conductive White Paint

TCC Type: Enamel

Test Type: Laboratory Tests

Orbit Type:

Location/Orientation on Satellite:

Method of Data Reception:

Space Factor: Protons

Energy and Exposure Level: 50 keV, 1E12 p/cm²s

Test Facility: UV-1/2 at Kompozit

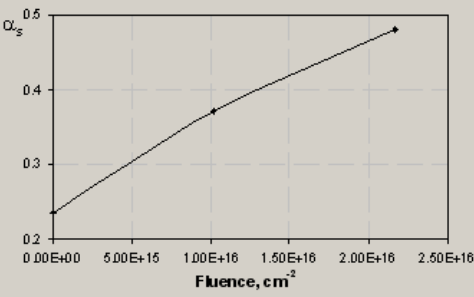
Parameter: Solar Absorption

Sample: aged

Conditioning Terms before Exposure: vacuum

Storage Conditions after Exposure: air

Comments: In order to measure a change in solar absorptance, the sample was extracted into the air. Having been measured, the sample was placed into a vacuum testing chamber, and the irradiation continued until the next value exposure was reached. The given sample was used after irradiation for measuring spectral characteristics.



Change in solar absorptance for enamel PCBE (Conductive White Paint) during proton irradiation. E=50 keV, flux = 10^{12} p/cm²s

Project 3806p

Record: 3 of 5 (Filtered)

TCC

TCC: PCBE Conductive White Paint

TCC Type: Enamel

Test Type: Laboratory Tests

Orbit Type:

Location/Orientation on Satellite:

Method of Data Reception:

Space Factor: Protons

Energy and Exposure Level: 50 keV, 1E12 p/cm²s

Test Facility: UV-1/2 at Kompozit

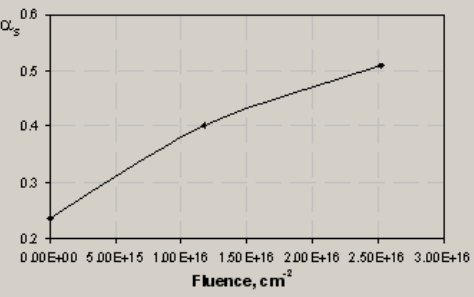
Parameter: Solar Absorption

Sample: aged

Conditioning Terms before Exposure: vacuum

Storage Conditions after Exposure: inert gas (argon)

Comments: In order to measure a change in solar absorptance, the sample was extracted into the air. Having been measured, the sample was placed into a vacuum testing chamber, and the irradiation continued until the next value exposure was reached. After irradiation the given sample was delivered to the partner



Change in solar absorptance for enamel PCBE (Conductive White Paint) during proton irradiation. E=50 keV, flux = 10^{12} p/cm²s

Project 3806p

Record: 4 of 5 (Filtered)

Changes in optical properties of of Sheldahl films due to proton irradiation with energy of 50 keV

In Fig. 16-17 dependence of solar absorbance A_s for samples of Sheldahl films on electron radiation fluence with energy of 50 keV is presented. The corresponding Database records are shown also.

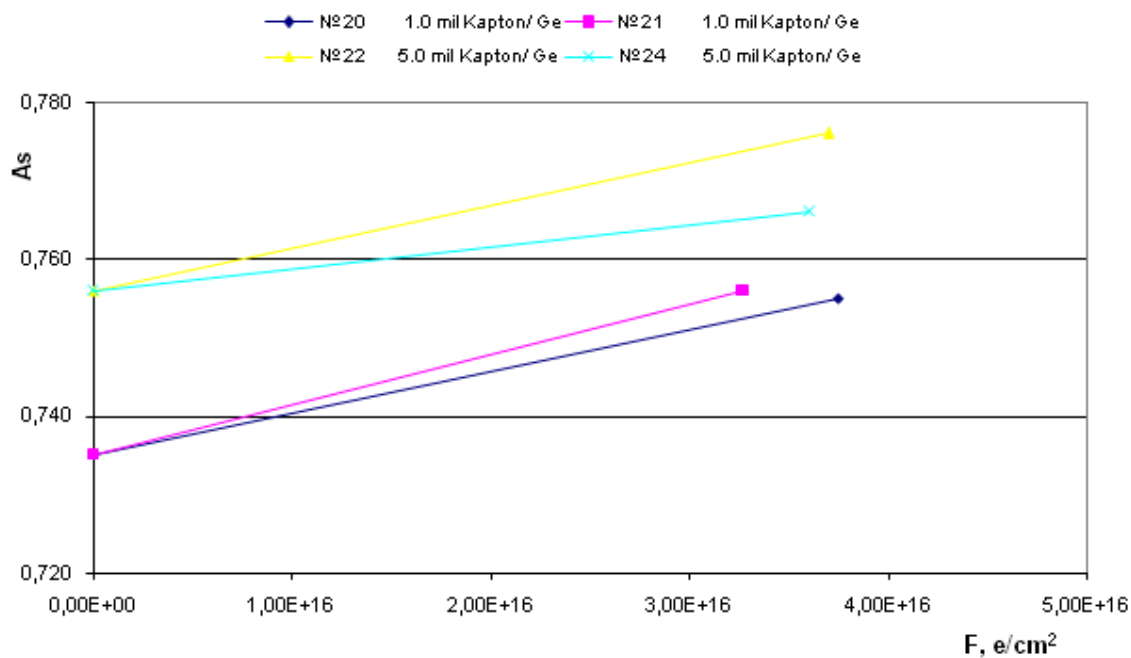


Figure 16. Dependence of solar radiation absorbance A_s for samples of Sheldahl films on electron radiation fluence with energy of 50 keV

MLI 1.000A GE 1.0MIL Kapton film

Test Type Laboratory Tests

Orbit Type

Location/Orientation on Satellite

Method of Data Reception

Space Factor Electrons

Energy and Exposure Level 50 keV, 2E12 e/cm2s

Test Facility UV-1/2 at Komposit

Parameter Solar Absorption

Sample aged

Conditioning Terms before Exposure vacuum

Storage Conditions after Exposure air

Comments

In order to measure a change in solar absorptance, the sample was extracted into the air. Having been measured, the sample was placed into a vacuum testing chamber, and the irradiation continued until the next value exposure was reached. The given sample was used after irradiation for measuring spectral characteristics.

Change in solar absorptance for 1.0 mil Kapton/Ge during electron irradiation. E=50 keV, flux - 2×10^{12} e/cm²s

Project 3806p

Reference

Record: 7 of 8 (Filtered)

MLI 1.000A GE 1.0MIL Kapton film

Test Type Laboratory Tests

Orbit Type

Location/Orientation on Satellite

Method of Data Reception

Space Factor Electrons

Energy and Exposure Level 50 keV, 2E12 e/cm2s

Test Facility UV-1/2 at Komposit

Parameter Solar Absorption

Sample aged

Conditioning Terms before Exposure vacuum

Storage Conditions after Exposure inert gas (argon)

Comments

In order to measure a change in solar absorptance, the sample was extracted into the air. Having been measured, the sample was placed into a vacuum testing chamber, and the irradiation continued until the next value exposure was reached. After irradiation the given sample was delivered to the partner

Change in solar absorptance for 1.0 mil Kapton/Ge during electron irradiation. E=50 keV, flux - 2×10^{12} e/cm²s

Project 3806p

Reference

Record: 8 of 8 (Filtered)

MLI 1.000A GE 5.0MIL Kapton film

Test Type Laboratory Tests

Orbit Type

Location/Orientation on Satellite

Method of Data Reception

Space Factor Electrons

Energy and Exposure Level 50 keV, 2E12 e/cm2s

Test Facility UV-1/2 at Kompozit

Parameter Solar Absorption

Sample aged

Conditioning Terms before Exposure vacuum

Storage Conditions after Exposure air

Comments

In order to measure a change in solar absorptance, the sample was extracted into the air. Having been measured, the sample was placed into a vacuum testing chamber, and the irradiation continued until the next value exposure was reached. The given sample was used after irradiation for measuring spectral characteristics.

Change in solar absorptance for 5.0 mil Kapton/Ge during electron irradiation. E=50 keV, flux - 2×10^{12} e/cm²s

Project 3806p

Reference

Record: 7 of 8 (Filtered)

MLI 1.000A GE 5.0MIL Kapton film

Test Type Laboratory Tests

Orbit Type

Location/Orientation on Satellite

Method of Data Reception

Space Factor Electrons

Energy and Exposure Level 50 keV, 2E12 e/cm2s

Test Facility UV-1/2 at Kompozit

Parameter Solar Absorption

Sample aged

Conditioning Terms before Exposure vacuum

Storage Conditions after Exposure inert gas (argon)

Comments

In order to measure a change in solar absorptance, the sample was extracted into the air. Having been measured, the sample was placed into a vacuum testing chamber, and the irradiation continued until the next value exposure was reached. After irradiation the given sample was delivered to the partner

Change in solar absorptance for 5.0 mil Kapton/Ge during electron irradiation. E=50 keV, flux - 2×10^{12} e/cm²s

Project 3806p

Reference

Record: 8 of 8 (Filtered)

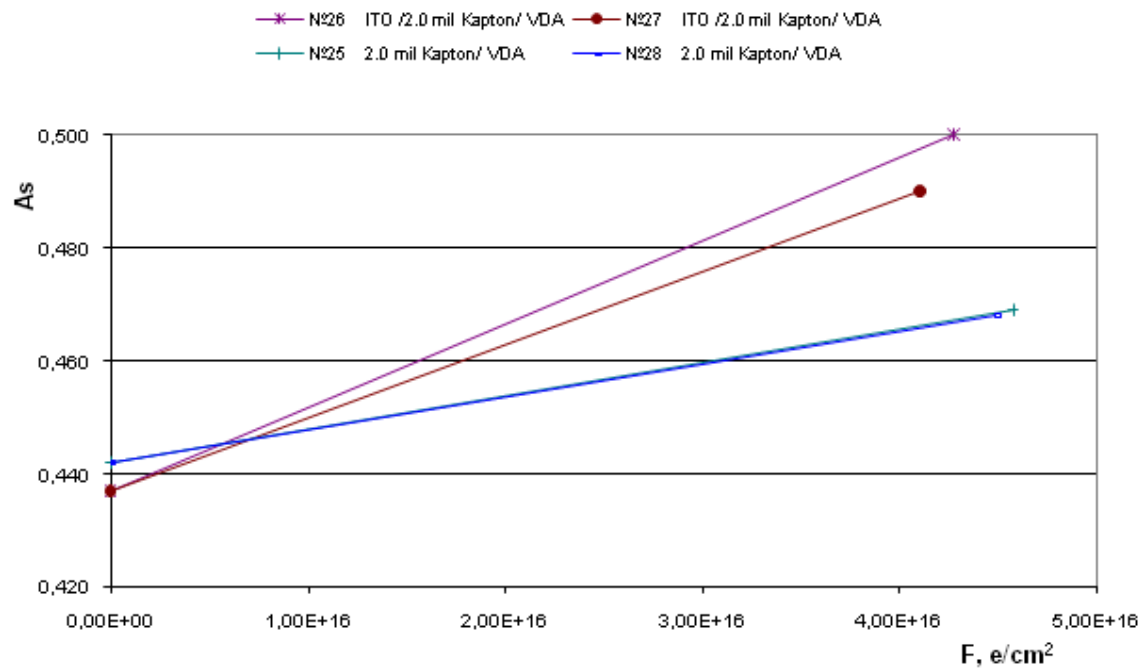
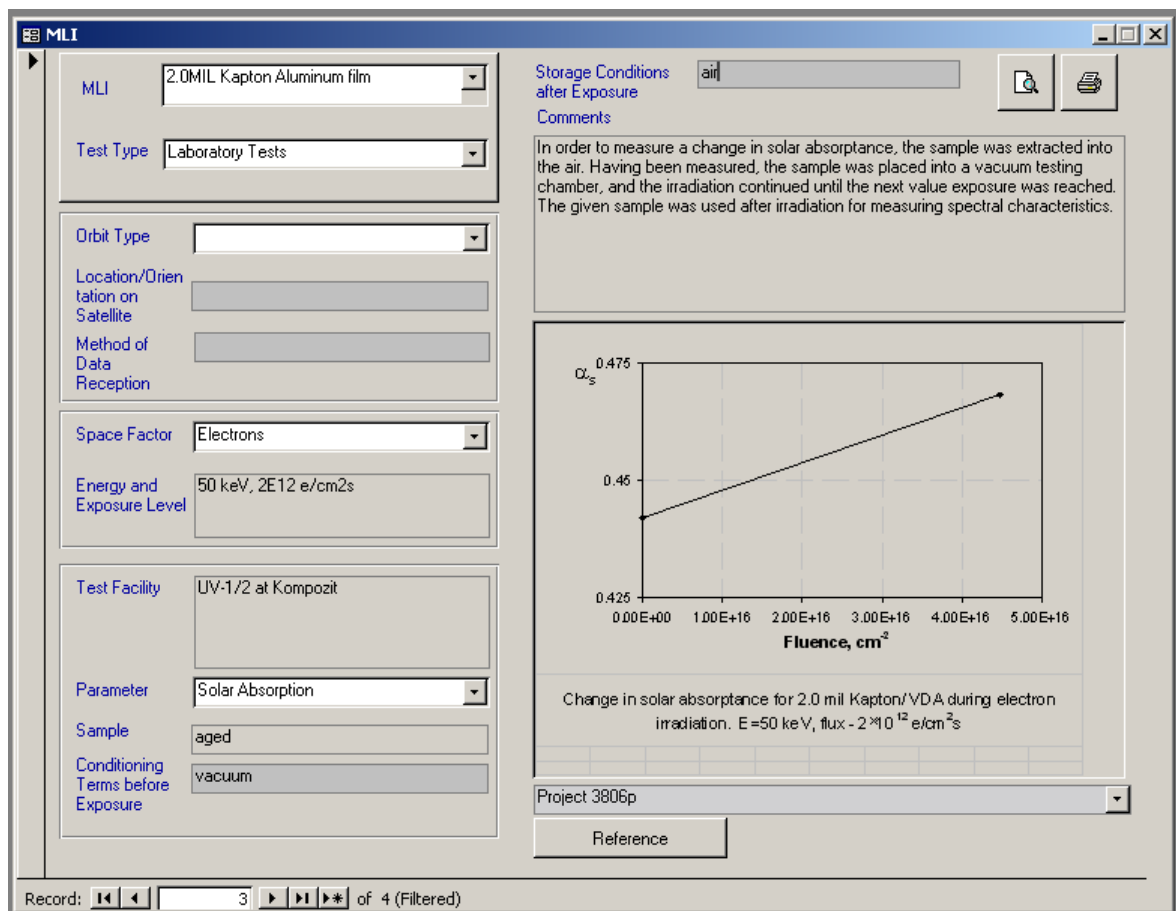
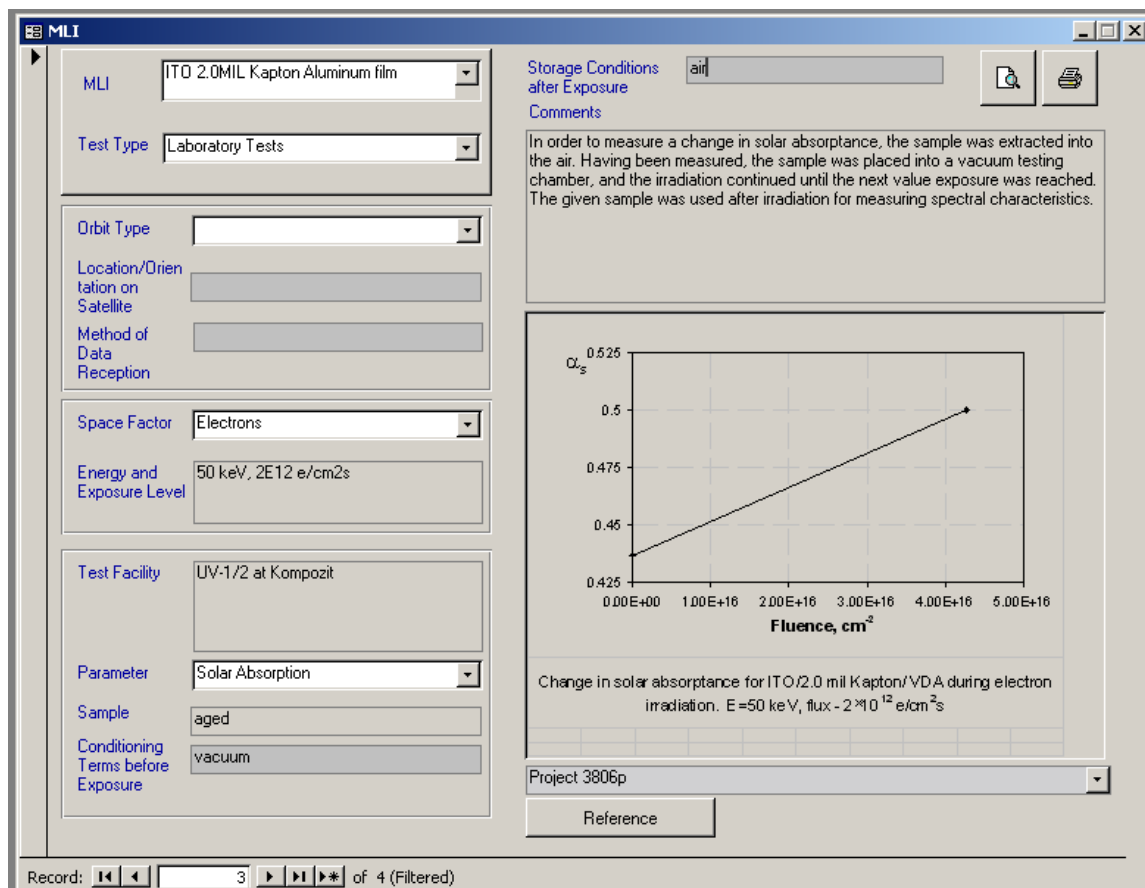
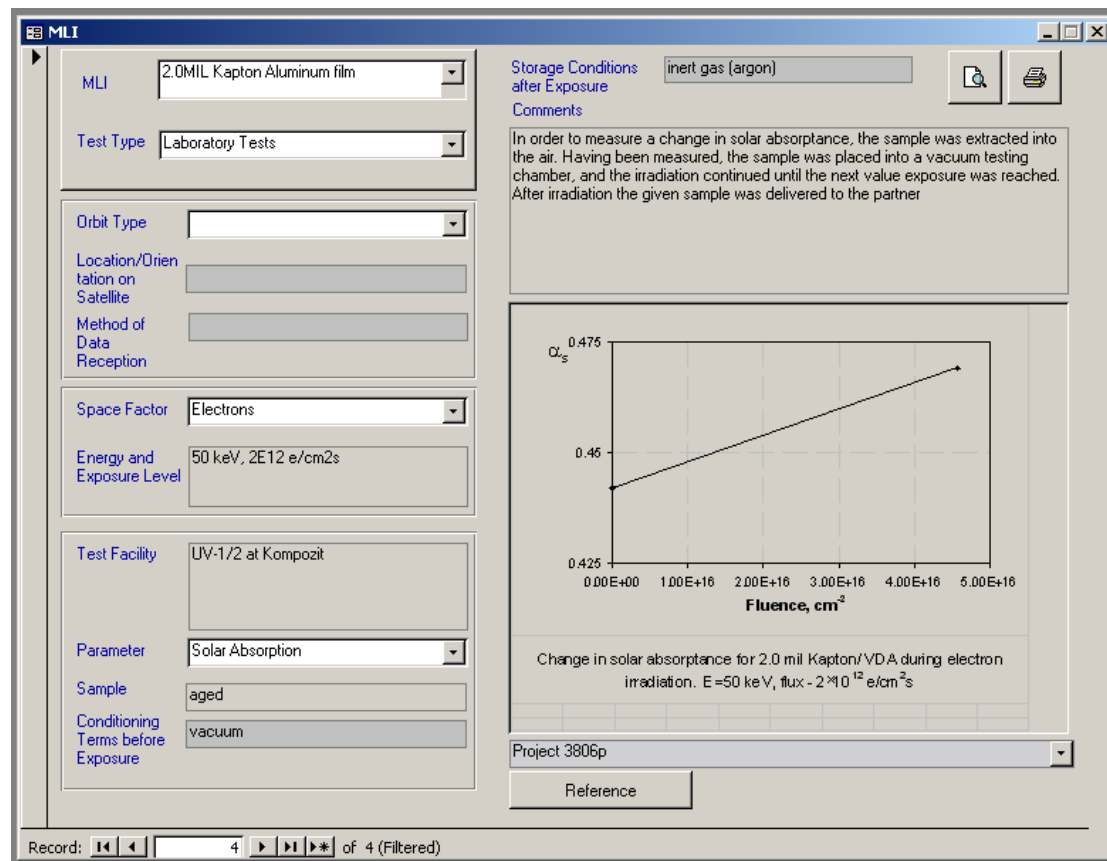


Figure 17. Dependence of solar radiation absorbance A_s for samples of Sheldahl films on electron radiation fluence with energy of 50 keV





MLI

ITO 2.0MIL Kapton Aluminum film

Test Type

Laboratory Tests

Orbit Type

Location/Orientation on Satellite

Method of Data Reception

Space Factor

Electrons

Energy and Exposure Level

50 keV, 2E12 e/cm2s

Test Facility

UV-1/2 at Komposit

Parameter

Solar Absorption

Sample

aged

Conditioning Terms before Exposure

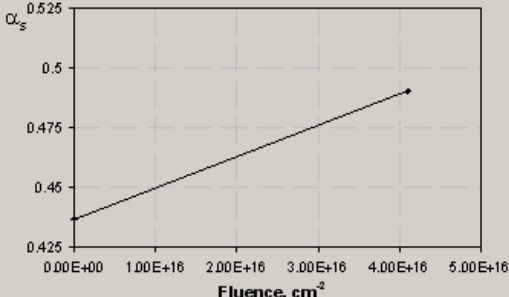
vacuum

Storage Conditions after Exposure

inert gas (argon)

Comments

In order to measure a change in solar absorptance, the sample was extracted into the air. Having been measured, the sample was placed into a vacuum testing chamber, and the irradiation continued until the next value exposure was reached. After irradiation the given sample was delivered to the partner



Change in solar absorptance for ITO/2.0 mil Kapton/VDA during electron irradiation. E=50 keV, flux = 2×10^{12} e/cm²s

Project 3806p

Reference

Record: 4 of 4 (Filtered)

Influence of factors of the space environment on the integral emission ability for different materials

In Table 2 values of factor of radiation of the irradiated samples are specified.

Table 2

Sample number	Name	ϵ	Exposure
2	FP-BSFR-100-208	0,86	complex exposure
4	FP-BSFR-200-208	0,87	complex exposure
10	EKOM-1	0,85	complex exposure
165	EKOM-2	0,88	complex exposure
5	MAP-PUI – Black Polyurethane Paint	0,87	complex exposure
85	MAP-PUK Black Conductive Polyurethane Paint	0,90	complex exposure
185	MAP-PCBE (Conductive White Paint)	0,87	complex exposure
263	MAP-SG121FD (White Paint)	0,87	complex exposure
5	ITO /2.0 mil Kapton/ VDA	0,77	complex exposure
7	2.0 mil Kapton/ VDA №7	0,77	complex exposure
3	MAP-PUI – Black Polyurethane Paint	0,89	$E_p=50 \text{ keV } \Phi=2*10^{16} \text{ cm}^{-2}$
83	MAP-PUK Black Conductive Polyurethane Paint	0,87	$E_p=50 \text{ keV } \Phi=2*10^{16} \text{ cm}^{-2}$
183	MAP-PCBE (Conductive White Paint)	0,87	$E_p=50 \text{ keV } \Phi=2*10^{16} \text{ cm}^{-2}$
261	MAP-SG121FD (White Paint)	0,87	$E_p=50 \text{ keV } \Phi=2*10^{16} \text{ cm}^{-2}$
187	MAP-PCBE (Conductive White Paint)	0,90	$E_p=50 \text{ keV } \Phi=2*10^{16} \text{ cm}^{-2}$
265	MAP-SG121FD (White Paint)	0,89	$E_p=50 \text{ keV } \Phi=2*10^{16} \text{ cm}^{-2}$
7	MAP-PUI – Black Polyurethane Paint	0,90	$E_p=50 \text{ keV } \Phi=2*10^{16} \text{ cm}^{-2}$
99	MAP-PUK Black Conductive Polyurethane Paint	0,89	$E_p=50 \text{ keV } \Phi=2*10^{16} \text{ cm}^{-2}$
21	1,0 Kapton 1000A° Ge	0,79	$E_p=50 \text{ keV } \Phi=2*10^{16} \text{ cm}^{-2}$
22	5,0 Kapton 1000A° Ge	0,87	$E_p=50 \text{ keV } \Phi=2*10^{16} \text{ cm}^{-2}$
26	ITO 2,0 Kapton Al VDA	0,78	$E_p=50 \text{ keV } \Phi=2*10^{16} \text{ cm}^{-2}$

Sample number	Name	ϵ	Exposure
28	2,0 Kapton Al VDA	0,78	$E_p=50 \text{ keV } \Phi=2*10^{16} \text{ cm}^{-2}$
-	peinture PUI	0,89	$E_e=50 \text{ keV } \Phi=2*10^{16} \text{ cm}^{-2}$
-	peinture PUK	0,90	$E_e=50 \text{ keV } \Phi=2*10^{16} \text{ cm}^{-2}$
-	ITO 5,0 Teflon Ag Inc.	0,82	$E_e=50 \text{ keV } \Phi=2*10^{16} \text{ cm}^{-2}$
-	10,0 Teflon Ag Inc.	0,88	$E_e=50 \text{ keV } \Phi=2*10^{16} \text{ cm}^{-2}$
-	peinture SG.121.FD	0,90	$E_e=50 \text{ keV } \Phi=2*10^{16} \text{ cm}^{-2}$
-	peinture PCBE	0,90	$E_e=50 \text{ keV } \Phi=2*10^{16} \text{ cm}^{-2}$
-	5,0 Teflon Ag Inc.	0,82	$E_e=50 \text{ keV } \Phi=2*10^{16} \text{ cm}^{-2}$
-	1000 Ge 1,0 Kapton	0,72	$E_e=50 \text{ keV } \Phi=2*10^{16} \text{ cm}^{-2}$
-	ITO 3,0 Kapton Al	0,83	$E_e=50 \text{ keV } \Phi=2*10^{16} \text{ cm}^{-2}$
-	3,0 Kapton Al	0,82	$E_e=50 \text{ keV } \Phi=2*10^{16} \text{ cm}^{-2}$
-	2,0 Kapton Al	0,77	$E_e=50 \text{ keV } \Phi=2*10^{16} \text{ cm}^{-2}$
-	ITO 1,0 Kapton Al	0,66	$E_e=50 \text{ keV } \Phi=2*10^{16} \text{ cm}^{-2}$
-	ITO 2,0 Kapton Al	0,76	$E_e=50 \text{ keV } \Phi=2*10^{16} \text{ cm}^{-2}$
-	1,0 Kapton Al	0,67	$E_e=50 \text{ keV } \Phi=2*10^{16} \text{ cm}^{-2}$
-	1000 Ge 5,0 Kapton	0,75	$E_e=50 \text{ keV } \Phi=2*10^{16} \text{ cm}^{-2}$
-	ITO 10,0 Teflon Ag Inc.	0,86	$E_e=50 \text{ keV } \Phi=2*10^{16} \text{ cm}^{-2}$
-	2,0 Teflon Ag Inc.	0,68	$E_e=50 \text{ keV } \Phi=2*10^{16} \text{ cm}^{-2}$